Multiscale Analysis of Clay-Polymer Composites for Geoenvironmental Applications

Dissertation

as a requirement for the degree of
Doktor-Ingenieur (Dr.-Ing.)

at the
Faculty of Civil and Environmental Engineering
Ruhr-Universität Bochum

by
Hanna Haase

Reviewers
Prof. Dr.-Ing. habil. Tom Schanz
Prof. Asuri Sridharan, PhD, D.Sc.
Dr. Snehasis Tripathy

Bochum, July 2017

Vorwort des Herausgebers

Die vorliegende Promotion von Frau Haase ist im Bereich der Grundlagenforschung in der Bodenmechanik angesiedelt. Sie entstammt aus einem erfolgreich eingeworbenen DFG-Antrag im Normalverfahren, den Frau Haase maßgeblich selbst entwickelt und geschrieben hat. Ton und Polymer Komposite haben bereits heute zahlreiche Anwendungen im Spezialtiefbau (Suspensionen für Schlitzwände), dem Tunnelbau (Ortsbrustkonditionierung) und der Umweltgeotechnik (Abwasser- und Schlammbehandlung). Beim Design dieser Komposite lässt sich jedoch leider feststellen, dass gemachte Erfahrungen bzw. Ergebnisse von Studien nicht verallgemeinerbar sind bzw. sich nicht, weder quantitativ noch qualitativ, auf andere Mischungen übertragen lassen.

An dieser Stelle setzt die Promotion von Frau Haase an: sie beinhaltet eine rational begründete und systematische Studie zu den Materialeigenschaften von Ton-Polymer Kompositen. Untersucht werden nicht einzelne ausgewählte natürliche Materialien oder spezielle technische Produkte, sondern gezielt Mischungen dreier unterschiedlicher Polymertypen mit zwei Bentoniten (Na und Ca belegt) und Kaolin. Bei Kenntnis der dominierenden Tonmineralogie weiterer "natürlicher Tone" lässt sich mit den Ergebnissen von Frau Haase so das geeignetste Polymer entsprechend der jeweiligen Anforderung auswählen.

Das Materialverhalten von gesättigten und teilgesättigten Tonen (bezüglich der hydraulischen und mechanischen Eigenschaften und der damit einhergehende Zusammenhang mit der Mikrostruktur) ist wohl verstanden. Es existieren theoretische physikalisch-chemische Konzepte, die, bei aller notwendigen Idealisierung, die Wirkung der relevanten interpartikulären Kräfte berücksichtigen. Die herausragende Leistung von Frau Haase besteht nun darin, die zusätzliche Gegenwart von unterschiedlichen Klassen von Polymeren in derartigen Ton-Wasser-Systemen zu berücksichtigen. Dazu betrachtet sie ausschließlich Pasten der Komposite, mit einem initialen Wassergehalt in der Nähe der Fließgrenze der Materialien. Die theoretische Modellbildung geht dabei von der Tatsache aus, dass die Mikrostruktur über die Existenz oder die Abwesenheit der diffusen Doppelschicht maßgeb-

lich beeinflusst wird. Frau Haase entwickelt originäre Konzepte, wo, bei der entsprechenden Mischung, sich das Polymer an den Ton anlagert, bzw. welche Auswirkungen die Präsenz der unterschiedlichen Polymerklassen auf die diffuse Doppelschicht hat. Basierend auf der erweiterten DDL-Theorie beschäftigt sich Frau Haase theoretisch mit Kompositen nichtionischer Polymere mit unterschiedlichen Tonen. Mit dem von Frau Haase vorgeschlagenen theoretischen Modell können die experimentellen Ergebnisse zum Quellen und der Permeabilität sehr gut beschrieben werden. Diese Arbeiten sind nach Kenntnis des Herausgebers international erstmalig auch quantitativ belastbar dargestellt. Das Verständnis beider Prozesse ist u.a. für verschiedene Anwendungen derartiger Komposite in der Umweltgeotechnik von entscheidender Bedeutung. Die experimentellen Arbeiten sind sehr umfangreich und in ihrer Systematik nach Kenntnis des Unterzeichners erstmalig. An den unterschiedlichen Kompositen bestimmt Frau Haase deren Plastizität, Adsorptionscharakteristiken, die Wasserretention, das Quellverhalten und die Permeabilität. Besonders eindrücklich ist z.B. der Zusammenhang zwischen Änderung der Permeabilität und Änderung der Mikrostruktur, letztere basierend auf ESEM Untersuchungen. Die generellen Ergebnisse ihrer Arbeit verifiziert Frau Haase an einer umweltgeotechnischen Fragestellung. Dazu werden die hydraulischen Eigenschaften von reinem bzw. polymermodifiziertem Na-Bentonit unter Berücksichtigung unterschiedlicher Herstellungsverfahren der Komposite untersucht. Die erzielten Ergebnisse zur Permeabilität der Komposite gegenüber Wasser und Calcium-Chlorid lassen sich auf Grund des von Frau Haase erstellten Konzepts schlüssig erklären. Mit dem von Frau Haase erarbeiteten Konzept lässt sich für Ton-Polymer Komposite erstmals quantitativ nicht nur die Frage nach dem "Was" sondern vor allem auch die Frage nach dem "Warum" beantworten.

Die Arbeit von Frau Haase bewegt sich international auf höchstem Niveau der theoretischen, analytischen und experimentellen Bodenmechanik. Die von ihr vorgelegten Untersuchungen zum Konstitutivverhalten von Ton-Polymer Kompositen sind in dieser strengen Systematik, dem damit verbundenen Umfang und in dieser Qualität einzigartig und wegweisend. Im Gegensatz zum heute üblichen "trial-and-error"-Konzept der Polymerberatung, entwickelt und verifiziert Frau Haase ein rationales und systematisches Konzept zur Bewertung von Ton-Polymer Kompositen. Die Abbildungen der Mikrostruktur sind aus meiner persönlichen Sicht besonders hervorzuheben und finden früher oder später sicherlich ihren Weg in die Lehrbücher.

Bochum, Juli 2017 Tom Schanz

Acknowledgement

The research work was performed at the Chair of Foundation Engineering, Soil and Rock Mechanics of Ruhr-Universität Bochum. It was funded by the German Research Foundation and represents one part of a collaborative research work with Karlsruhe Institute of Technology. First of all, I thank my supervisor Prof. Dr.-Ing. habil. Tom Schanz for giving me the opportunity to work on the novel and interdisciplinary research topic of clay-polymer composites. His helpful advices and inspiring ideas contributed significantly to the success of the research work. Further, I wish to thank the reviewers of my thesis Prof. Asuri Sridharan and Dr. Snehasis Tripathy. Their internationally reputable understanding of clay behaviour greatly influenced my work.

Special thanks to the head of the soil mechanical laboratory Michael Skubisch. His unlimited support and outstanding technical skills significantly promoted the success of the experimental part of the work. Further, I thank Werner Müller, Andreas Langolf and Reinhard Mosinski for their technical support.

The technical cooperation with the Center for Electrochemical Sciences of Ruhr-Universität Bochum for performing the microscopic analyses is gratefully acknowledged.

I really appreciate the scientific discussions with Dr.-Ing. Wiebke Baille and Dr. Frank Friedrich. I thank Dr. Yang Yang for sharing his expertise in fields of mathematics promoting the success of the theoretical part of the research work.

Finally, I wish to thank my student co-workers for their commitment in performing experiments in the laboratory: Hanna Dehn, M.Sc., Mira Salomon, M.Sc., Maximilian Schoen, B.Sc., Silas Kaufmann, B.Sc., Wolfgang Lieske, M.Sc. and Sebastian Beck, B.Sc..

Bochum, July 2017 Hanna Haase

Abstract

Based on their great success in providing enhanced material properties in fields of polymeric science, clay-polymer composites have faced considerable attention in fields of geotechnical and geoenvironmental engineering in recent years. Thereby, one of the most promising focuses is on the stabilization of bentonite hydraulic barrier performance even when permeated with chemically aggressive solutions. To date, several specific composites have been developed and investigated and were found to deviate significantly in terms of their hydro-mechanical behaviour. However, detailed analysis of the governing mechanisms and thus, understanding of clay-polymer composite multiscale behaviour is lacking. The present research aims to overcome this limitation in order to promote the precise development of clay-polymer composites having beneficial and reliable hydro-mechanical properties. Therefore, in a first approach composites were prepared by varying clay and polymer constitutive characteristics systematically, i.e., the clay mineralogy, the polymer charge as well as the polymer-to-clay ratio. Experimental micro- and macro-scale analyses including the determination of adsorption characteristics, the microscopic investigation of composite fabric as well as the determination of composite plasticity, volumetric behaviour, hydraulic permeability and water retention were conducted. The multiscale coupling phenomena were analyzed theoretically by (i) the development of new sets of equations based on diffuse double-layer theory accounting for composite volumetric behaviour and (ii) the adoption of cluster model accounting for composite hydraulic permeability. Experimental and theoretical findings were interpreted in order to identify general relationships between clay and polymer constitutive characteristics as well as composite micro- and macro-scale (coupling) behaviour. In a second approach, the hydraulic barrier performance of bentonite-polymer composites was addressed. Hydro-mechanical tests were performed by taking into account the practical demands in terms of composite preparation as well as the initial loading and chemical boundary conditions. Finally, conclusions were drawn regarding the governing mechanisms in polymer based bentonite barrier enhancement.

Zusammenfassung

Aufgrund ihrer sehr vorteilhaften Materialeigenschaften sind Ton-Polymer Komposite innerhalb der Polymerwissenschaften weit verbreitet. Auch auf dem Gebiet der (Umwelt-)-Geotechnik ist das Interesse an diesen Kompositen in der Vergangenheit deutlich gewachsen, wobei die Stabilisierung von Bentonit-Barrieren unter chemischer Beanspruchung einen großen Stellenwert einnimmt. Die bislang entwickelten Komposite weisen allerdings sehr unterschiedliche hydro-mechanische Eigenschaften auf und ein fundiertes Verständnis über die maßgebenden Mechanismen ist nicht vorhanden. Ziel der vorliegenden Arbeit ist es daher, diese Einschränkung zu überwinden und die Entwicklung von Ton-Polymer Kompositen mit vorteilhaften und zuverlässigen hydro-mechanischen Eigenschaften voranzubringen. Dazu wurden in einem ersten Ansatz Komposite hergestellt, deren Komponenten Ton und Polymer in ihren konstitutiven Eigenschaften systematisch variieren. Dies betrifft die Ton-Mineralogie, die Polymer-Ladung sowie das Mischungsverhältnis von Ton und Polymer. Die Komposite wurden experimentell untersucht, wobei die Bestimmung des Adsorptionsverhaltens und der Struktur auf mikroskopischer Ebene sowie der Plastizität, des volumetrischen Verhaltens, der hydraulischen Durchlässigkeit und des Wasserrückhaltevermögens auf der makroskopischen Ebene durchgeführt wurden. Die Ergebnisse wurden auf Grundlage theoretischer Ansätze zum mehrskaligen Materialverhalten analysiert, indem (i) die 'diffuse double-layer theory' weiterentwickelt sowie (ii) der 'cluster model' Ansatz verwendet wurde. Die experimentellen und theoretischen Ergebnisse wurden schließlich mit dem Fokus interpretiert, allgemeingültige Zusammenhänge zwischen den konstitutiven Eigenschaften der Komponenten sowie den mikro- und makroskopischen Eigenschaften der Komposite abzuleiten. In einem zweiten Ansatz wurde die hydraulische Barriere-Wirkung von Bentonit-Polymer Kompositen unter Berücksichtigung der praxisrelevanten Anforderungen hinsichtlich der Komposit-Herstellung sowie der Initial- und Randbedingungen untersucht. Die Ergebnisse wurden schließlich hinsichtlich der maßgebenden Mechanismen bei der polymerbasierten Modifikation von Bentonit-Barrieren analysiert.

Contents

List of Figures

List of Tables

Nomenclature

RH	relative humidity (-)
A	cross sectional area of soil sample (m^2)
a	fitting parameter for the SWCC (-)
$C(\Psi)$	correction function for the SWCC (-)
C_1, C_2	integration constant (-)
C_c	compression index (-)
C_s	decompression index (-)
c_v	coefficient of consolidation (m^2/s)
c_{PEG}	PEG concentration (g/g)
c_{eq}	concentration of polymer in solution (mg/l)
d	half the distance between two charged surfaces (m)
d_p	thickness of the adsorbed polymer layer (m)
$d_{p,0}$	thickness of the adsorbed polymer layer in its initial state (m)
$d_{p,res}$	thickness of the adsorbed polymer layer in its residual state (m)
e	void ratio (-)

e'	elementary charge (C)
e_c	intra-cluster void ratio according to cluster model (-)
e_p	inter-cluster void ratio according to cluster model (-)
e_t	total void ratio according to cluster model (-)
$e_{c,0}$	initial intra-cluster void ratio according to cluster model (-)
e_{clay}	modified void ratio (-)
$e_{t,0}$	initial total void ratio according to cluster model (-)
G	specific gravity (-)
g	gravity acceleration (m/s^2)
Δh	difference between inflow and outflow pressure head (m)
I^+	ionicity of cationic polyacrylamide polymer (mol-%)
K	Langmuir adsorption coefficient (-)
k	hydraulic permeability (m/s)
k'	Boltzmann's constant (J/K)
k_0	pore shape factor according to Kozeny-Carman equation (-)
k_{CM}	hydraulic permeability calculated according to cluster model (m/s)
k_{KC}	hydraulic permeability calculated according to Kozeny-Carman approach (m/s)
Δl	length of permeated soil sample (m)
M	molar mass of water (g/mol)

m fitting parameter for the SWCC (-)

M^+ molar mass of methylated dimethylaminoethylacrylate (g/mol)

M^o molar mass of acrylamide (g/mol)

m_c mass of clay (g)

m_v coefficient of volume compressibility (m^2/kN)

m_w mass of water (g)

N number of particles per cluster according to cluster model (-)

n fitting parameter for the SWCC (-)

n^+, n^- local cation/anion concentration ($1/m^3$)

n_0^+, n_0^- bulk cation/anion concentration ($1/m^3$)

n_0 bulk ion concentration ($1/m^3$)

p repulsive pressure (N/m^2)

p' applied vertical load (kPa)

p_s swelling pressure (kPa)

p_{atm} atmospheric pressure (kPa)

Q flow rate permeating soil sample (m^3/s)

q mass of adsorbed polymer per gram clay (mg/g)

q_{max} maximum adsorption capacity (mg/g)

$q_{max}*$ maximum adsorption capacity (meq/g)

R	ideal gas constant (J mol/K)
S	specific surface area of the clay (m^2/g)
S_0	specific surface area of solids according to Kozeny-Carman equation (1/m)
S_r	degree of saturation (-)
T	absolute temperature (K)
t	tortuosity factor according to Kozeny-Carman equation (-)
u	nondimensional midplane potential function (-)
u_a	pore air pressure (MPa)
u_w	pore water pressure (MPa)
V_c	volume of clay (cm^3)
V_p	volume of polymer (cm^3)
V_v	volume of voids (cm^3)
w^*	modified water content (%)
w_l^*	modified liquid limit (%)
w_p^*	modified plastic limit (%)
w_s^*	modified shrinkage limit (%)
w_l	liquid limit (%)
w_p	plastic limit (%)
w_s	shrinkage limit (%)

w_{opt} optimum water content according to standard proctor compaction (%)

x distance to charged surface (m)

y nondimensional potential function (-)

y_1, y_2 nondimensional potential function in region 1/2 (-)

z nondimensional surface potential function (-)

β polymer-electrolyte interaction parameter (-)

β_{res} polymer-electrolyte interaction parameter in its residual state (-)

χ_{ip} interaction parameter between dissociated ions and polymer (-)

χ_{si} interaction parameter between solvent and dissociated ions (-)

χ_{sp} interaction parameter between solvent and polymer (-)

δ thickness of Stern-layer (m)

ϵ static permittivity (C^2/Jm)

η viscosity of fluid according to Kozeny-Carman equation (Ns/m^2)

γ specific gravity of fluid according to Kozeny-Carman equation (N/m^3)

κ double-layer parameter (1/m)

ν valency of ions (-)

ν^+, ν^- valency of cations/anions (-)

ϕ_p volume fraction occupied by polymer (-)

ϕ_{pb} volume fraction occupied by polymer in the bulk phase (-)

Ψ soil suction (MPa)

Ψ' electric potential (V)

Ψ'_0 electric surface potential (V)

Ψ'_1, Ψ'_2 electric potential in region 1/2 (V)

Ψ'_d electric midplane potential between two interacting diffuse double-layers separated by distance $2d$ (V)

Ψ'_δ electric potential at the Stern-plane (V)

$\Psi'_{x=d}$ electric potential of a single diffuse double-layer at distance d to charged surface (V)

Ψ_m matric suction (MPa)

Ψ_{AEV} air entry value (MPa)

Ψ_o osmotic suction (MPa)

Ψ_{tot} total suction (MPa)

ρ_w density of water (g/cm^3)

ρ_{opt} optimum dry density according to standard proctor compaction (g/cm^3)

σ total charge of the diffuse double-layer (C/m^2)

ξ nondimensional distance function (-)

ξ_{d_p} nondimensional distance function at distance d_p to charged surface (-)

1 Introduction

1.1 Motivation

In recent years, clay-polymer composites have faced considerable attention in fields of geotechnical engineering. With respect to various applications, e.g., landfill lining, tunnelling and expansive soil stabilization, their beneficial hydro-mechanical properties compared to pure clays have been demonstrated, i.e., stabilization of bentonite barrier performance even when permeated with chemically aggressive solutions (Scalia et al. 2014), reduction of adhesion on steel surfaces and improvement of shear strength of clay pastes (Zumsteg et al. 2013*b*) and reduction of montmorillonite swelling for expansive soil stabilization (Inyang et al. 2007). On the other hand, also limitations with respect to the target composite properties have been observed, e.g., by Ashmawy et al. (2002), Razakamanantsoa et al. (2012) and Zumsteg et al. (2013*a*). Since the studies conducted show great variabilities in composite composition, especially concerning the type and amount of polymer, as well as in composite preparation condition general relationships between composite constitutive properties and its macro-scale engineering behaviour have not yet been deduced. For this reason, the benefits of their high potential performance are strongly limited to single specific compositions and applications that have been developed to date.

In geotechnical engineering, the macro-scale hydro-mechanical behaviour of soils is of primary interest in research and practice. However, it is established since decades that the macro-scale properties can be related to the soils micro-scale characteristics, i.e., the microstructure, which is in turn determined by small scale interparticle forces as well as the external loading conditions. Since interparticle forces play a major role in the formation of clay micro-structure, multiscale analysis on the hydro-mechanical behaviour of clays, e.g., the hydraulic permeability (Olsen 1962) and the swelling behaviour (Sridharan & Jayadeva 1982), is well established in literature. Thus, based on clay constitutive prop-

erties, i.e., mineralogy, environmental conditions as well as initial preparation and hydraulic/mechanical boundary conditions, the engineering behaviour of clays can be estimated by theoretical approaches. However, the findings on clay multiscale coupling have not yet been transferred to the understanding of composite hydro-mechanical behaviour, although clay-polymer composites have been comprehensively studied with respect to their formation and micro-scale characteristics. Thereby, their physico-chemical and microstructural features have primarily been investigated in the fields of material and colloid chemical sciences and several general relationships and sensitivities regarding clay and polymer constitutive properties as well as the environmental conditions have been exposed in literature, e.g., by Deng et al. (2006), Heller & Keren (2003) and Greenland (1963).

1.2 Objectives

The present research aims to overcome the above termed limitations with respect to the targeted and reliable preparation and application of clay-polymer composites in fields of geotechnical engineering. It is aimed to derive fundamental understanding on the effect of polymer adsorption on clay mineral surfaces by focusing composite properties on various scales. Composite characterization is based on the state of the art clay research and involves the adsorption characteristics as well as the micro-structural and hydro-mechanical properties. Characterization is conducted on composites differing systematically in their composition. Therefore, the components clay and polymer as well as their ratio in the composite are categorized by means of their constitutive characteristics, i.e., the electrostatic properties of the polymer, the predominant clay mineralogy as well as the polymer-to-clay ratio related to its maximum adsorbing rate. Doing so, it is aimed to bridge the gap in scientific literature of relating general compositional characteristics to the resulting properties of the composite material on various scales. In addition to the phenomenological multiscale characterization of clay-polymer composites it is aimed to attribute micro- and macro-scale observations to their origin with respect to the physico-chemical polymer layered clay mineral surface characteristics as well as the resulting micro-fabric. Therefore, classical theoretical approaches on the micro- and macro-scale coupling in clays, i.e., diffuse double-layer (DDL) theory and cluster model, are used and advanced in order to understand clay-polymer composite multiscale behaviour. Further, one of the most promising fields of application is addressed, i.e., bentonite-polymer composites as hydraulic barrier

materials in geoenvironmental engineering, in order to account for the inconsistent performances observed in literature. Therefore, the relevant findings of clay-polymer composite multiscale analysis are considered as well as the practical demands with respect to composite preparation as well as the initial loading and chemical boundary conditions. In detail, the main objectives of the study are:

- Identification of general relationships between clay and polymer constitutive properties and clay-polymer composite micro-scale characteristics in terms of complex formation (adsorption) and composite micro-fabric.
- Identification of general relationships between clay and polymer constitutive properties and clay-polymer composite macro-scale characteristics in terms of the hydro-mechanical behaviour.
- Identification of multiscale coupling phenomena accounting for clay-polymer composite engineering performance.
- Development of theoretical approaches to describe clay-polymer composite multiscale behaviour.
- Identification of the governing mechanisms determining bentonite-polymer composite hydraulic barrier performance in geoenvironmental practice.

1.3 Layout of the thesis

The thesis is composed of eight chapters. The first chapter (this chapter) introduces to the topic of clay-polymer composites for application in geotechnical engineering. The motivation for the research is given by highlighting the deficits in scientific knowledge based on the existing literature. On this basis, the objectives of the present work are given.

The second chapter covers the state of the art knowledge with respect to the relevant fields of this study. Therefore, basic clay mineralogical as well as physical polymer characteristics are given and the governing mechanisms determining complex formation between clay minerals and polymers are summarized. Further, the fundamentals of clay micro- and macro-scale properties in terms of the structure and the hydro-mechanical behaviour are outlined and phenomenological multiscale coupling phenomena are summarized. In addi-

tion, introduction is given to classical theoretical approaches on clay multiscale behaviour, i.e., DDL theory accounting for the volumetric behaviour and cluster model accounting for the hydraulic permeability. Finally, the current status with respect to the hydraulic barrier performance of bentonite-polymer composites for application in geoenvironmental engineering is outlined.

In the third chapter the experimental and theoretical concept of this research is introduced. Subsequently, the main properties of the materials used are given, i.e., the mineralogical and soil mechanical classification of clays, the physical and chemical characteristics of polymers as well as the preparation conditions of their respective composites. Further, the experimental methods for the determination of micro- and macro-scale clay-polymer composite behaviour as well as of bentonite-polymer composite hydraulic barrier performance are outlined. Finally, the individual procedures and parameter sets used for the theoretical analysis of clay-polymer composite multiscale behaviour are summarized.

The fourth chapter summarizes the main outcome of micro-scale analysis. This involves the determination of polymer adsorption characteristics on clay mineral surfaces as well as the resulting composite micro-structure.

The fifth chapter summarizes the main outcome of macro-scale analysis. This involves soil mechanical classification tests with respect to clay-polymer composite plastic properties as well as hydro-mechanical testing with respect to composite volumetric behaviour, hydraulic permeability and water retention.

In the sixth chapter clay-polymer composite multiscale behaviour in terms of its volumetric behaviour and hydraulic permeability is analyzed theoretically. Therefore, in the first part of the chapter new equations expressing the micro- and macro-scale coupling phenomenon with respect to composite volumetric behaviour are introduced on the basis of DDL theory. Subsequently, theoretical e-$\log(p)$ relationships of composites are compared to the experimental test results presented in chapter five. Further, by use of cluster model clay-polymer composite hydraulic permeabilities are analyzed theoretically. Thereby, composite micro-scale properties, i.e., the fabric, derived from theoretical consideration in order to reproduce its macro-scale behaviour, i.e., the hydraulic permeability, are compared to the experimental test results presented in chapter four.

The seventh chapter covers the topic of bentonite-polymer composites for geoenvironmental applications. The experimental test results on composite hydraulic permeability as

well as classical (index) properties for the estimation of hydraulic barrier performance, i.e., the liquid limit and the swelling behaviour, are presented. Test results are analyzed with respect to (i) the governing mechanisms potentially enhancing bentonite barrier performance and (ii) the validity of classical relations between material index properties and the hydraulic permeability.

In the eighth chapter a summary of the main conclusions drawn from the outcome of the foregoing chapters, i.e., the experimental and theoretical analysis of clay-polymer composite hydro-mechanical behaviour, is given. The fundamental findings on composite multiscale behaviour and an evaluation of the proposed theoretical models is given. Further, potentials and perspectives with respect to the application of clay-polymer composites in various fields of geotechnical engineering are addressed.

2 State of the art

2.1 General

In the following chapter, the basics of clay, polymer and clay-polymer composite properties are presented with respect to the micro- and macro-scale including the phenomenological and theoretical multiscale coupling behaviour. Clay mineralogical as well as physical polymer characteristics are summarized briefly and the governing mechanisms determining complex formation between clay minerals and polymers are outlined. Further, the fundamentals with respect to clay fabric as well as clay hydro-mechanical behaviour relevant to this study are presented and phenomenological multiscale coupling phenomena are discussed. In addition, introduction is given to classical theoretical approaches on clay multiscale behaviour, i.e., DDL theory accounting for the volumetric behaviour and cluster model accounting for the hydraulic permeability. Finally, the current status with respect to the hydraulic barrier performance of bentonite-polymer composites for application in geoenvironmental engineering is outlined.

2.2 Formation and structure of clay-polymer composites

2.2.1 Clays

2.2.1.1 Basics of clay mineralogy

The clay mineralogical structure is built up by the two basic units, tetrahedron and octahedron, each consisting of a cation, which is coordinated to four and six oxygen atoms,

respectively (Figure 2.1a & 2.2a). Typical cations that can be found in the basic units of clay minerals are Si^{4+}, Al^{3+} and Fe^{3+} in the tetrahedra as well as Al^{3+}, Fe^{3+}, Fe^{2+} and Mg^{2+} in the octahedra (Bergaya & Lagaly 2013). Therefore, the terms 'silicon-tetrahedra' as well as 'aluminum-octahedra' are widely used. With these basic units, sheets of either tetrahedra or octahedra are formed by sharing oxygen atoms between units. As a result, corner-connected tetrahedral sheets as well as edge-connected octahedral sheets are formed with large lateral dimension (Figure 2.1b & 2.2b). In tetrahedral sheets, one sheet side is built up of the tetrahedral bases connected to each other, whereas the other sheet side is built up of tetrahedral tops. Octahedral sheets, on the other hand, have identical sheet sides. Tetrahedral and octahedral sheets are additionally connected with each other to form 2-sheet and 3-sheet layers by sharing non-saturated oxygen atoms of tetrahedral tops and octahedra, respectively. 2-sheet layers are built up by one octahedral as well as one tetrahedral sheet (1:1 layers), whereas 3-sheet layers are built up by one octahedral sheet sandwiched between two opposed tetrahedral sheets (2:1 layers). In Figure 2.3a & 2.3b sheet associations including oxygen sharing as well as locations of remaining non-saturated oxygens forming hydroxyls are shown schematically for both, 1:1 and 2:1 layers.

1:1 and 2:1 layer silicates are electrically neutral for different cation occupancies, e.g., Si^{4+} in each tetrahedron, Al^{3+} in two of three octahedra (di-octahedral sheet) as well as Mg^{2+} in each octahedron (tri-octahedral sheet). Generally, cation occupancy differs from these conditions due to either isomorphous substitution by lower charged cations or vacancies of cations in basic units. This results in a net-negative layer charge expressed by the negative charge per unit formula. The layer charge of 1:1 layer silicates is generally close to zero, whereas the layer charge of 2:1 layer silicates ranges from approximately zero to 2. The negative layer charges are compensated by mainly inorganic cations, which are located close to the layer surface and are generally exchangeable by other cationic species. Thereby, due to the increased electrostatic attraction multivalent and small sized cations are preferred following the sequence (Eggloffstein 2000):

$$Al^{3+} > Ca^{2+} > Mg^{2+} > K^{+} > Na^{+}$$

In case of so called 1:2:(1) layer silicates, the net-negative charge is compensated by a positively charged octahedral sheet. In consequence of these imperfections in the clay mineral lattice, the general unit formulae of 1:1 and 2:1 layer silicates can be written as

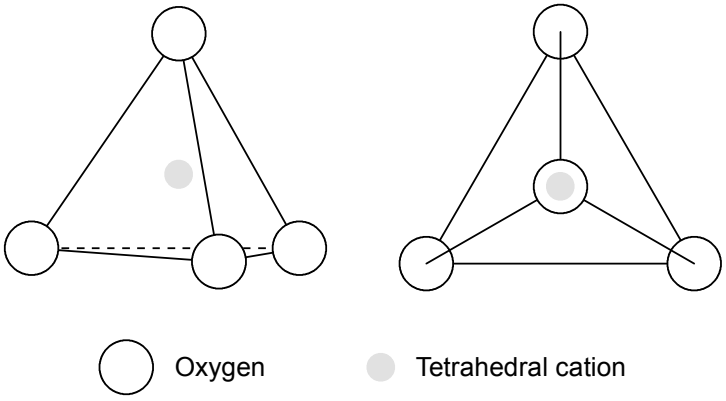

(a)

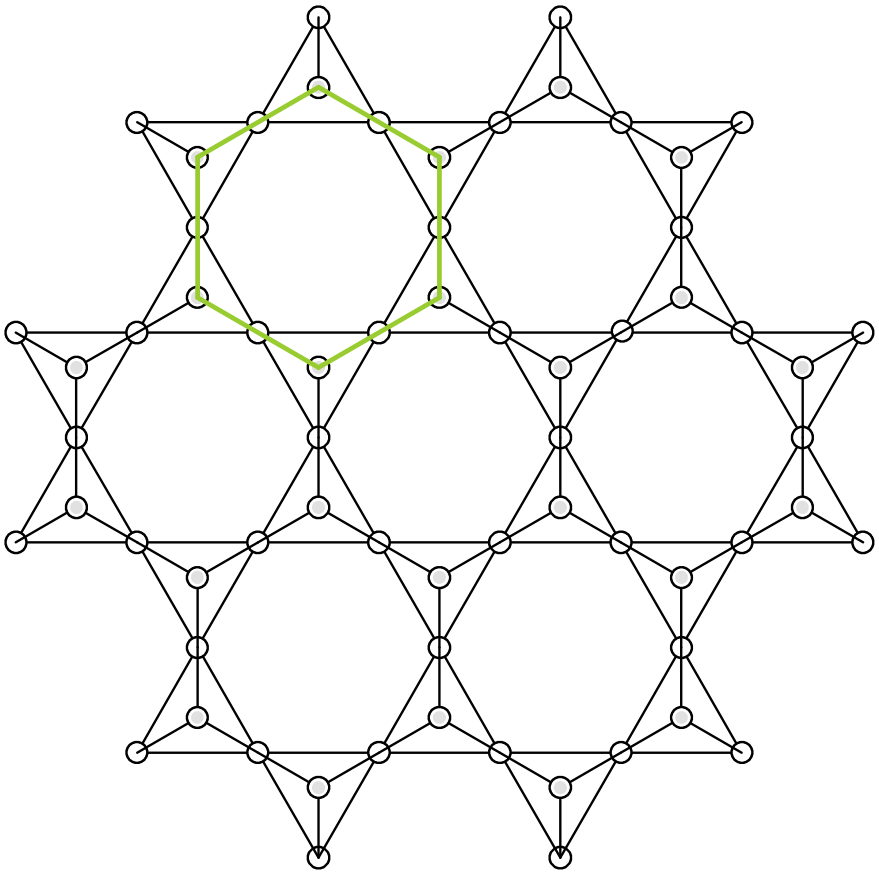

(b)

Figure 2.1: General sketch of clay mineralogy: front view and top view of tetrahedron (a); top view of tetrahedral sheet (b).

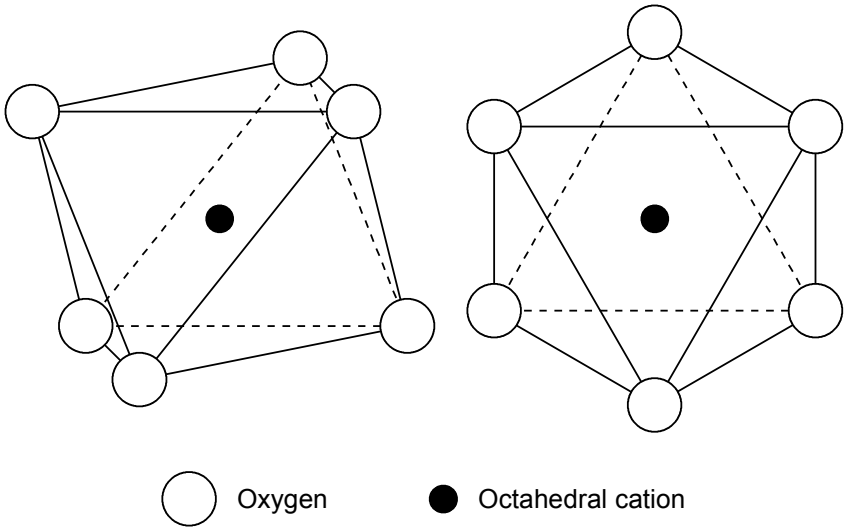

(a)

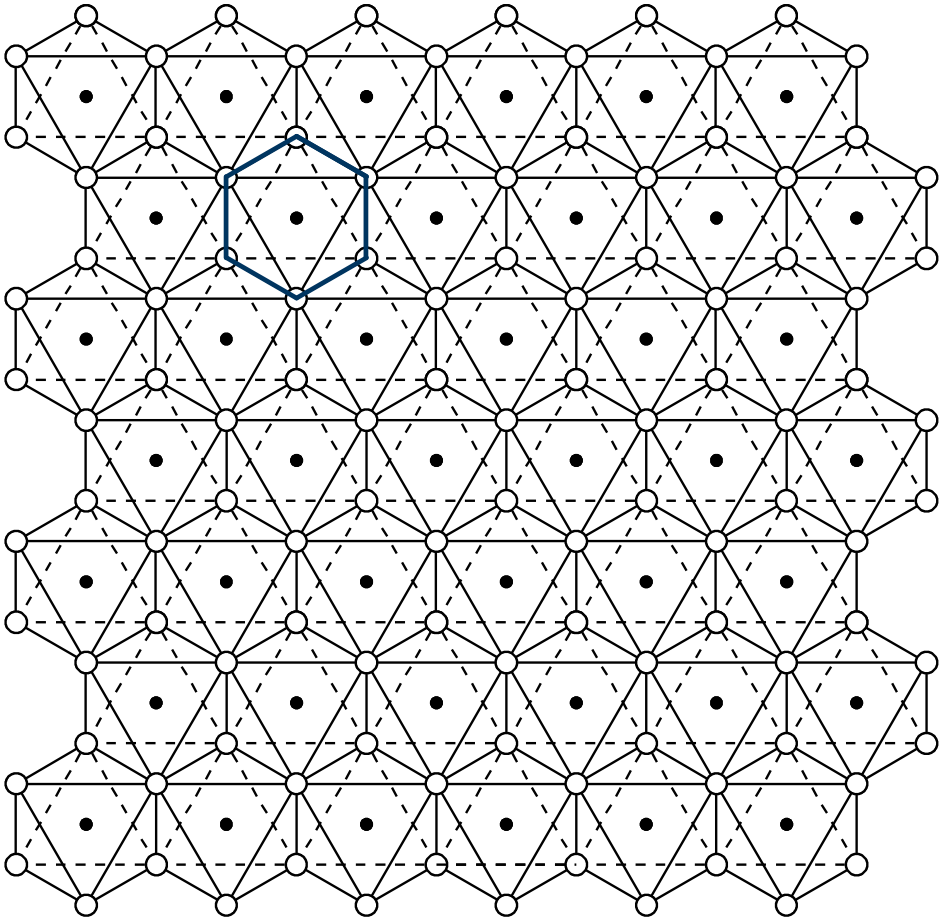

(b)

Figure 2.2: General sketch of clay mineralogy: front view and top view of octahedron (a); top view octahedral sheet (b).

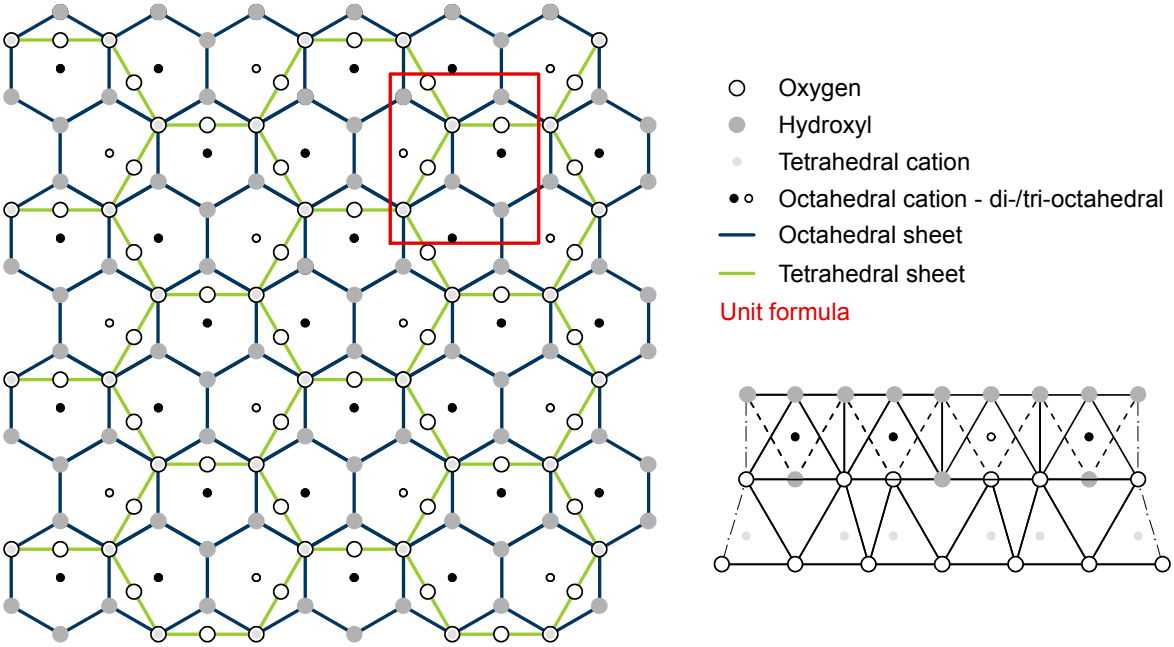

(a)

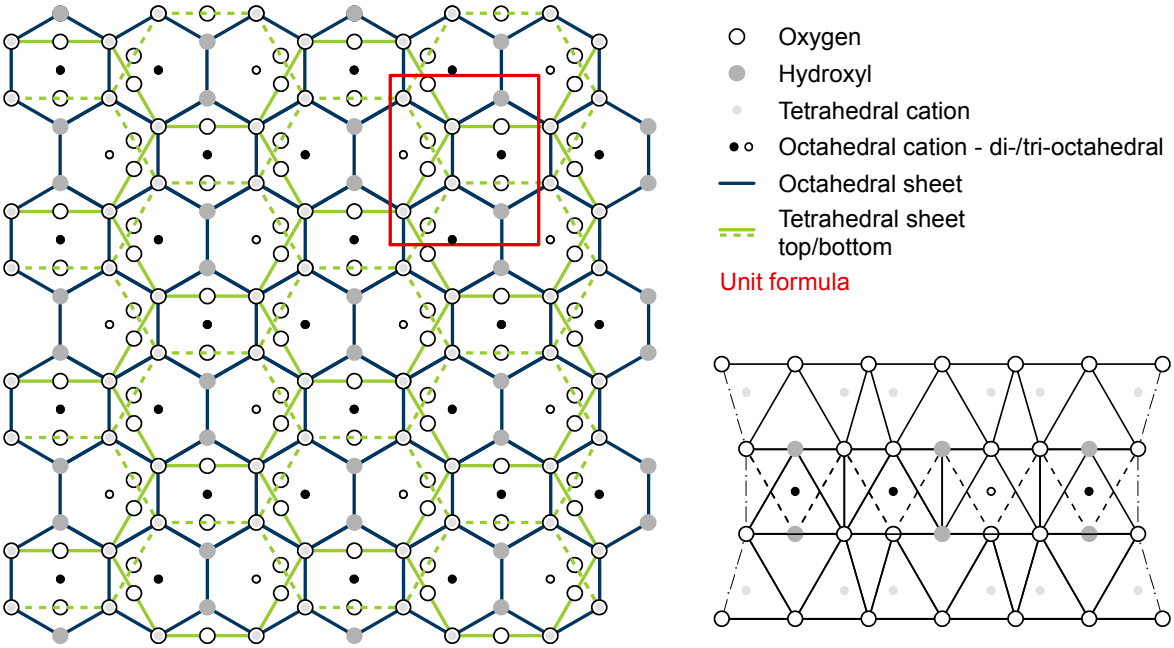

(b)

Figure 2.3: General sketch of clay mineralogy: top view and cross section of 1:1 layer (a); top view and cross section of 2:1 layer (b).

follows:

$$
\begin{aligned}
Si_2Al_2O_5(OH)_4 \quad & \text{(di-octahedral 1:1 layer)} \\
Si_2Mg_3O_5(OH)_4 \quad & \text{(tri-octahedral 1:1 layer)} \\
(Si_{4-x}Me_x^{3+})(Al_{2-y}Me_y^{2+})O_{10}(OH)_2, (x+y)M^+ \quad & \text{(di-octahedral 2:1 layer)} \\
(Si_{4-x}Me_x^{3+})(Mg_{3-y}Me_y^{+})O_{10}(OH)_2, (x+y)M^+ \quad & \text{(tri-octahedral 2:1 layer)}
\end{aligned}
$$

where x and y are the numbers of substituted silicium, aluminum and magnesium ions in the tetrahedra and octahedra, respectively, Me is a variable metal ion and M refers to the exchangeable cations. The cation exchange capacity, CEC (meq/g), represents one of the main clay mineralogical characteristics.

In addition to permanent negative charges due to isomorphous substitution and vacancies in the clay mineral lattice, also variable charges, which are controlled by environmental pH conditions, contribute to the total layer charge. The variable charges are originated by protonation and deprotonation of hydroxyls located at the broken bonds of mineral layer edges as well as at the octahedral basal surfaces of 1:1 layer silicates (Ma & Eggleton 1999) following the reactions:

$$
\begin{aligned}
Si/Al - OH + OH^- &\longrightarrow Si/Al - O^- + H_2O \\
Si/Al - OH + H^+ &\longrightarrow Si/Al - OH_2^+
\end{aligned}
$$

Therefore, hydroxylic clay mineral surfaces carry positive charges in acidic environment and negative charges in alkaline environment. The point of zero edge charges can be found at slightly acidic conditions, i.e., at values around pH 5 (Bergaya & Lagaly 2013). Exchangeable cations and also anions are therefore also located at the edges of mineral layers.

Silicate layers tend to arrange parallel to each other, which is mainly induced by attractive van der Waals forces acting numerously between layers as well as ion-ion attraction between layers and cations. In 1:1 layer silicates, parallel layer arrangement is additionally strengthen by hydrogen bonding between octahedral hydroxyls and tetrahedral oxygens leading to a fixed interlayer distance, i.e., the thickness of one layer plus one interlayer space, of 0.7 nm. 2:1 layer silicates, on the other hand, are characterized by various in-

terlayer distances depending on the type and thus, size of exchangeable cations, i.e., from 0.9 nm in case of non-charged 2:1 layer silicates to 1.4 nm in case of 1:2:(1) layer silicates. Since parallel layer stacking is limited by a finite amount of layers, clays are characterized by having 'inner', i.e., interlayer, and 'outer surfaces'. Generally, the amount and thus, area of inner surfaces is in a distinctly higher order of magnitude compared to the outer surfaces. The resulting unit, which is composed of several parallelly stacked clay mineral layers, is considered as a clay particle (Bergaya & Lagaly 2013).

2.2.1.2 Clay mineral-water interaction

Silicate layers interact with water by two general mechanisms, (i) electrostatic attraction and (ii) osmosis. The intensity of both mechanisms strongly depends on the mineralogical characteristics of layers as well as on the environmental conditions of the clay-water system and may overcome the attractive van der Waals forces between parallelly ordered mineral layers. Generally, in 1:1 and 2:1:(1) layer silicates interlayer bonding mechanisms are too strong to be overcome by the interaction of clay mineral surfaces with water, whereas in case of 2:1 layer silicates clay mineral-water interaction is capable to dominate interlayer attraction. In consequence, interlayer distances of 2:1 layer silicates may increase stepwise from 10 Å to 20 Å as well as towards total clay mineral layer separation due to water adsorption in the interlayer space.

According to Mitchell & Soga (2005), electrostatic interaction is based on ion-dipole and dipole-dipole attraction acting between the clay mineral surface, water molecules and exchangeable cations, respectively. The term 'hydration' of clay minerals is often used when referring to this type of interaction. Thereby, water-molecule dipoles form hydration shells around cations by ion-dipole attraction. Interaction strongly depends on the size and valence of cations and can be expressed by the cation specific hydration energy. In general, the hydration energy and thus, the amount of water molecules in the hydration shell increases with decreasing size and increasing valence of cations (Xiang & Czurda 1995). In addition to ion-dipole attraction, dipole-dipole interaction between water-molecules located in different layers of the hydration shell strengthen its structure by forming hydrogen-bonds. Taking into account the pH dependent variable charges in clay mineral layers, ion hydration, i.e., either cation or anion hydration, also occurs at the layer edges. Another type of dipole-dipole attraction occurs between water-molecules and the clay mineral surface. Thereby,

the water-molecule dipole interacts with either octahedral hydroxyls or tetrahedral oxygens, which carry positive and negative partial charges, respectively. Tetrahedral oxygens are relatively weak electron donors (Bergaya & Lagaly 2013), whereas octahedral hydroxyls strongly interact with the water-molecule dipole. On the other hand, with increasing amount of isomorphous substitution in the tetrahedral sheet, tetrahedral oxygens increase their electron-donating capacity, for which reason dipole-dipole interaction between water-molecules and clay mineral surfaces is important for both, 1:1 and 2:1 layer silicates. As a result of electrostatically induced clay mineral-water interaction, water-molecule dipoles in the interacting water layers are oriented with respect to the clay mineral surface and exchangeable cations as it is illustrated in Figure 2.4 - 2.6 for basal surfaces of 1:1 and 2:1 clay mineral layers.

It is obvious, that hydration of 1:1 layer silicates occurs exclusively at their outer surfaces since hydrogen bonding between layers is strong and prevents inner surface, i.e., interlayer, hydration (Figure 2.4). 2:1 layer silicates, on the other hand, may also hydrate in the interlayer space (Figure 2.6), provided that hydration forces overcome van der Waals and ion-ion attraction between layers. This condition is fulfilled in case of (i) moderate layer charges as well as (ii) small and multivalent exchangeable cations. Generally, hydrogen-atoms, i.e., the positive part of water-molecule dipoles, are oriented towards tetrahedral basal surfaces of clay mineral layers, whereas oxygen atoms, i.e., the negative part of water-molecule dipoles, are oriented towards octahedral basal surfaces, which are only present in 1:1 layer silicates. Additionally, with respect to ion hydration, water-molecule oxygens tend to orient towards cations. Since isomorphous substitution in 1:1 layer silicates mainly occurs in the tetrahedral sheets and 2:1 layer silicate surfaces are exclusively built up by tetrahedral sheets, water-molecule orientation with respect to the clay mineral surface and exchangeable cations is consistent and also corresponds to the theory proposed by Mitchell & Soga (2005) considering clay mineral layers as negative condenser plates.

In case of the second mechanism, i.e., osmosis, the driving force for water adsorption in the near-field of clay mineral surfaces is given by concentration gradients arising from the high amount of exchangeable ions. Thereby, two opposing mechanisms, i.e., electrostatic attraction tending to keep them near to the negatively charged clay mineral surface and diffusion tending to repel them in order to reach equilibrated ion concentrations, act simultaneously (van Olphen 1963). As a result of the two mechanisms a characteristic distribution of ion concentration, which decreases with increasing distance to the clay mineral surface, ad-

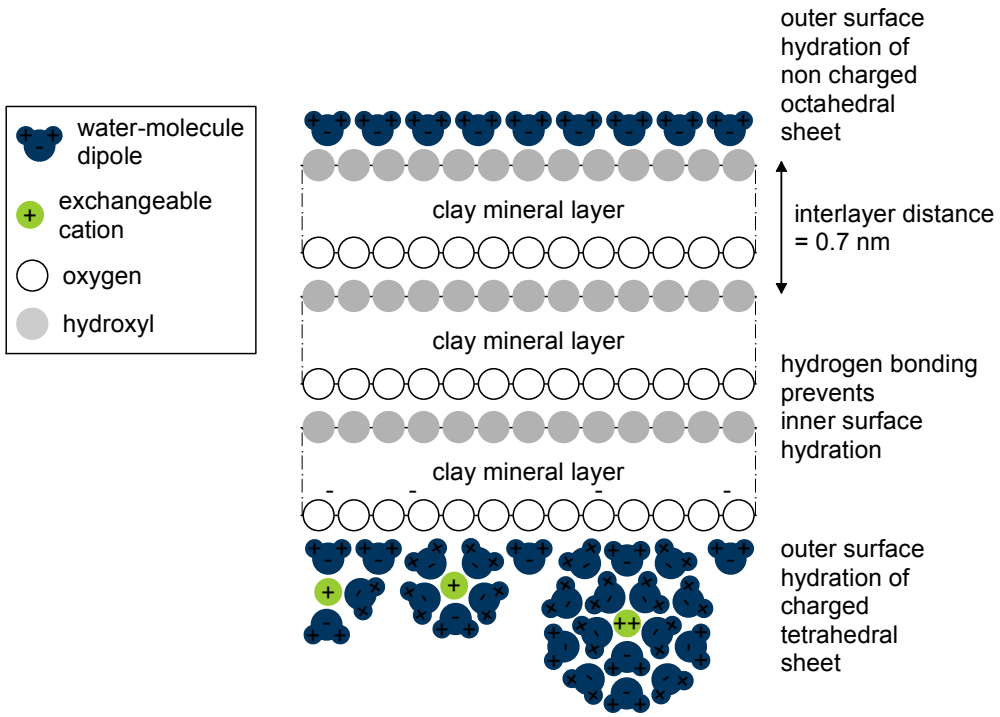

Figure 2.4: General sketch of 1:1 clay mineral layer hydration.

justs. Consequently, the clay mineral surface acts as a semipermeable membrane located at a certain distance, where exchangeable ions are not able to pass through since attraction dominates repulsion in this region. The combined effect of electrostatic and diffusive driving forces therefore induces osmotic conditions, under which the movement of water is permitted, whereas the movement of ions is prevented between two regions having different concentrations, i.e., the near-field of clay mineral surfaces and bulk solution. Generally, osmotic driving forces increase with (i) increasing concentration gradient, i.e., increasing diffusive repulsion, as well as (ii) increasing size of hydrated ions and (iii) decreasing valence of ions, i.e., decreasing electrostatic attraction. The resulting distribution of ions and water adsorbed to the clay mineral surface due to osmosis is illustrated in Figure 2.7. In this region, ions and water exist in a diffuse manner, i.e., individually, they have no fixed position, whereas ion concentration distribution with respect to the distance to the clay mineral surface is constant and characteristic for the clay mineral-water system. In this state, the negatively charged clay mineral surface in combination with adsorbed cations and water is termed the 'diffuse double-layer' (Mitchell & Soga 2005).

Water adsorption due to osmosis requires a continuous liquid water phase between the

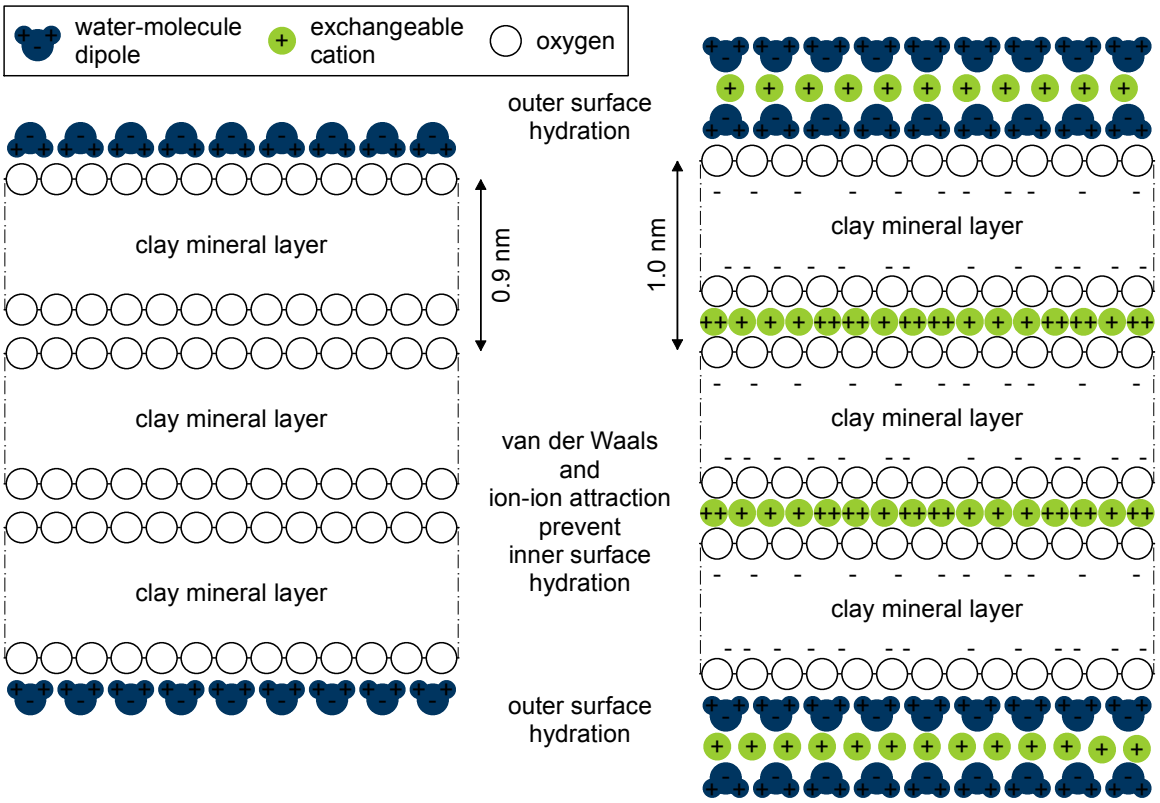

Figure 2.5: General sketch of 2:1 clay mineral layer hydration: non-charged clay mineral layers (left); highly charged clay mineral layers (right).

highly concentrated near-field of clay mineral surfaces and low concentrated bulk solution. Clay hydration, on the other hand, occurs from the dry state when coming into contact with the liquid as well as vapour water phase, even at low water vapour pressures. For this reason, electrostatic and osmotic driving forces dominate water adsorption on clay mineral surfaces successively, i.e., clay mineral surface hydration precedes osmotic water adsorption.

Since the inner surface area of clay minerals significantly exceeds their outer surface area, hydration and osmotic water adsorption in the interlayer space significantly contributes to total water adsorption. Clay mineralogies allowing for interlayer water adsorption have therefore attained great attention when studying clay mineral-water interaction processes. The interlayer distances expand from 10 Å to 20 Å due to hydration as well as to total layer separation due to osmotic water adsorption (e.g., Norrish 1954, Norrish & Quirk 1954). Consequently, the macroscopic clay volume increases significantly, for which reason the

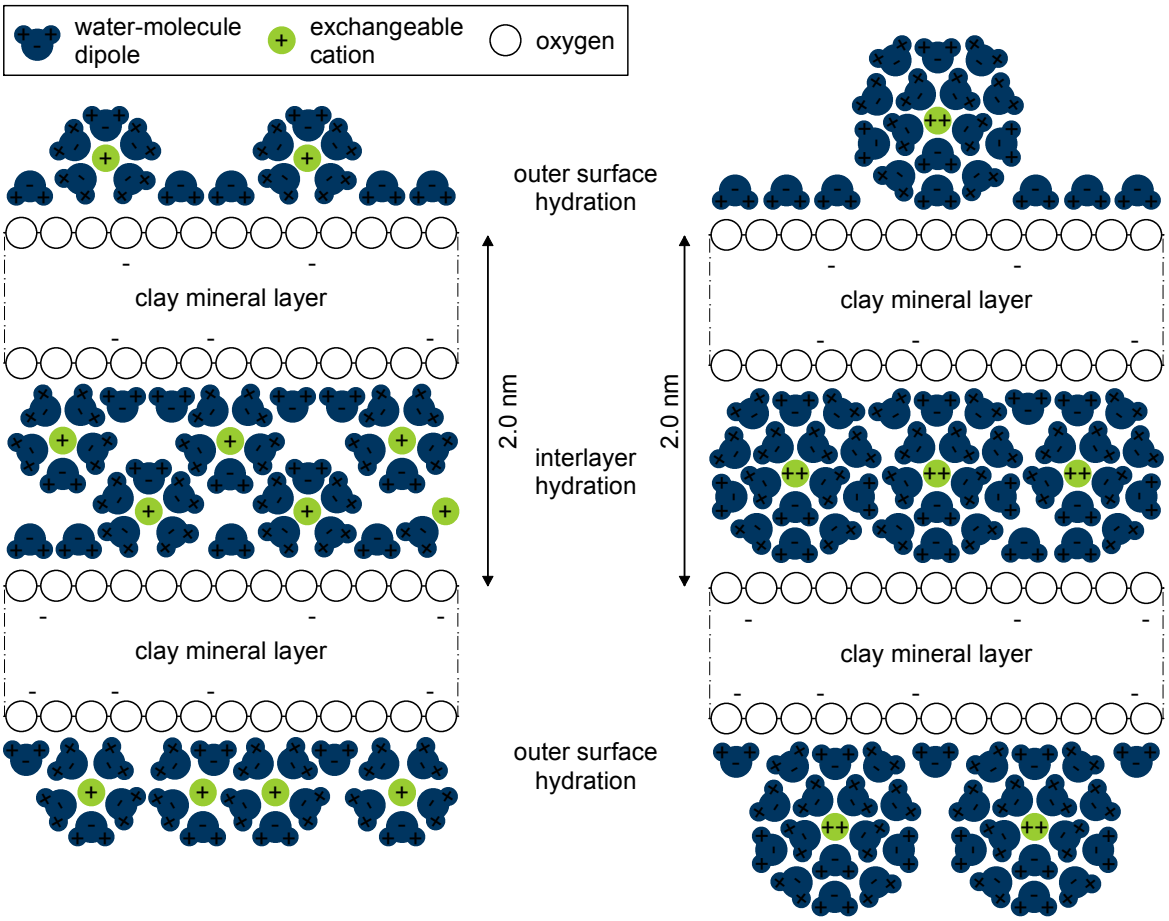

Figure 2.6: General sketch of 2:1 clay mineral layer hydration: monovalent (left) and divalent (right) exchangeable cations of moderately charged clay mineral layers.

term 'clay swelling' is used in the engineering context. Thereby, it can be distinguished between 'innercrystalline swelling' and 'osmotic swelling' referring to water adsorption due to hydration and osmosis, respectively (Madsen & Müller-Vonmoos 1989).

2.2.1.3 Structure in clays - terms, definitions and formation conditions

The structure in soils is characterized by the geometrical arrangement of soil particles, i.e., the fabric, and the bonding mechanisms between them (Mitchell & Soga 2005). Since in clays, soil particle geometry is strongly anisotropic, i.e., they have a platy shape, and surface forces are capable to overcome the influence of gravity, their variations in fabric are quite complex compared to silt or sand particle dominated soils. Generally, the terms 'ag-

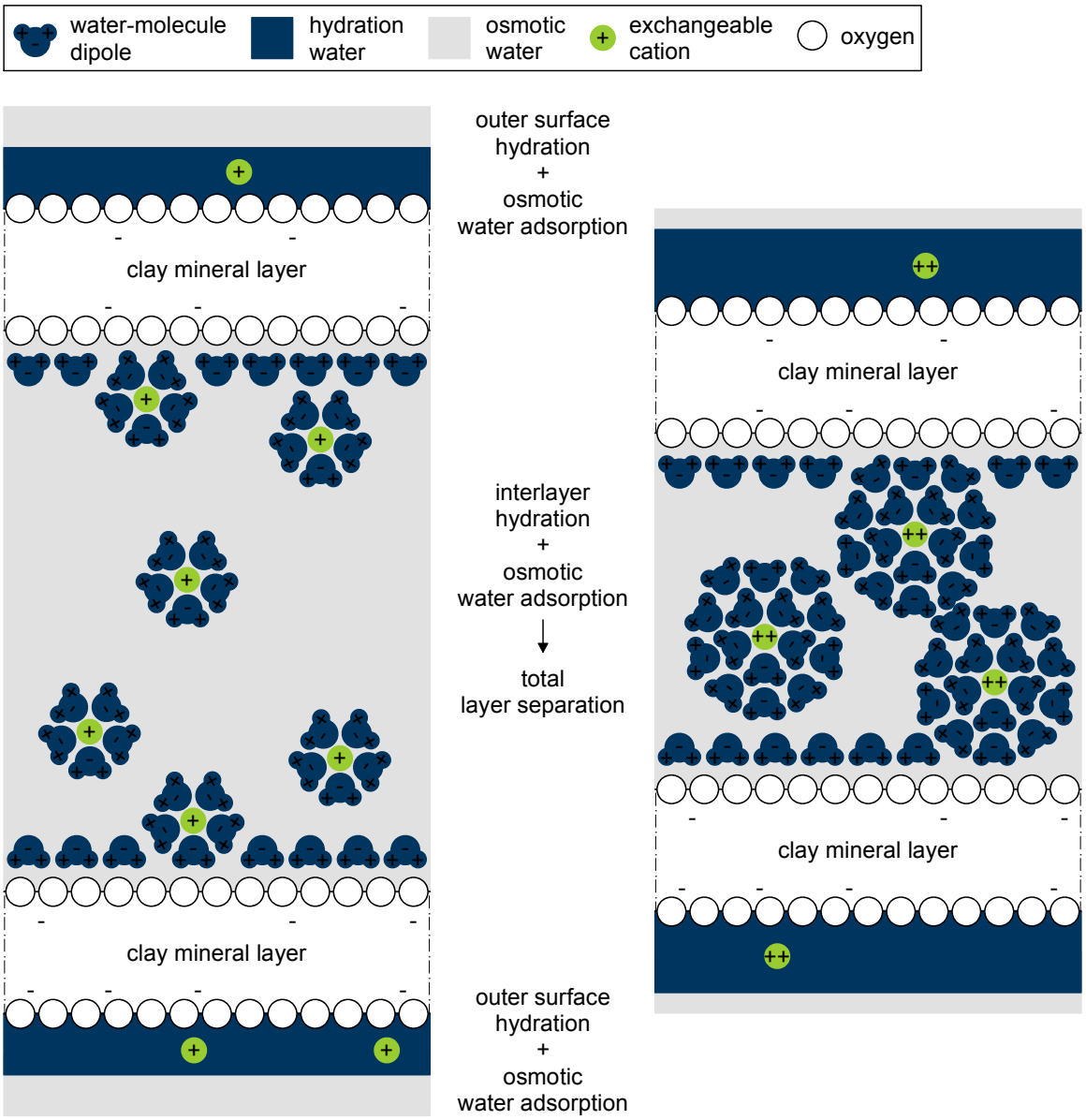

Figure 2.7: General sketch of 2:1 clay mineral layer osmotic water adsorption: monovalent (left) and divalent (right) exchangeable cations of moderately charged clay mineral layers.

gregated' and 'dispersed' are used when referring to face-to-face (F-F) particle associations, whereas the terms 'flocculated' and 'deflocculated' are used when referring to edge-to-face (E-F) and edge-to-edge (E-E) particle arrangement (van Olphen 1963). Thereby, particle faces correspond to surfaces, which are built up by layer bases and particle edges correspond to surfaces, which are built up layer edges. Since in case of interlayer swelling clay mineralogies, particles may consist of a very little amount of clay mineral layers or even single layers aggregated and dispersed as well as flocculated and deflocculated clay fabrics my also be observed between single layers. Various combinations of preferential particle arrangements are schematically illustrated in Figure 2.8.

Clay fabric, i.e., the arrangement of clay particles, mandatorily includes the voids between clay particles, for which reason additional differentiations regarding the clay fabric have to be considered. Generally, voids can be distinguished by their size, which is defined in (Rouquerol et al. 1994), leading to the terms 'micro-', 'meso-' and 'macropores'. On the other hand, they can be qualitatively distinguished by their relative position between clay particles. According to Nagaraj & Miura (2001), voids between particles, which are associated with each other, are termed 'intra-aggregate pores'. By this definition, aggregates are defined as being a group of several clay particles forming separate units. Thereby, the special type of clay particle association within units according to Figure 2.8, i.e., aggregation, E-E and E-F flocculation, respectively, is neglected when using the term 'aggregate'. In addition, 'inter-aggregate pores' exist, which include the larger pores between units. In consequence of this differentiation, the pore size distribution (PSD) in clays may be characterized by having two dominant fractions of pore sizes referring to inter- and intra-aggregate pores, respectively, i.e., they have a bimodal PSD. Dispersed and deflocculated fabrics, on the other hand, are characterized by having only one dominant fraction of pore sizes since no clay particle units exist, i.e., they have an unimodal PSD. Figure 2.9 schematically illustrates the fabric differentiations considering inter- and intra-aggregate pores.

The clay fabric develops as a result of various factors, which can be distinguished by having their origin in (i) interparticle forces and (ii) external loading. The former was comprehensively discussed by Santamarina et al. (2002), where the concept of preferred minimal energy configuration of clay particles was introduced. At zero external loading conditions, clay fabric was suggested to be directly related to environmental pH and ionic concentration since they control interparticle attractive and repulsive forces. Thereby, environmental pH

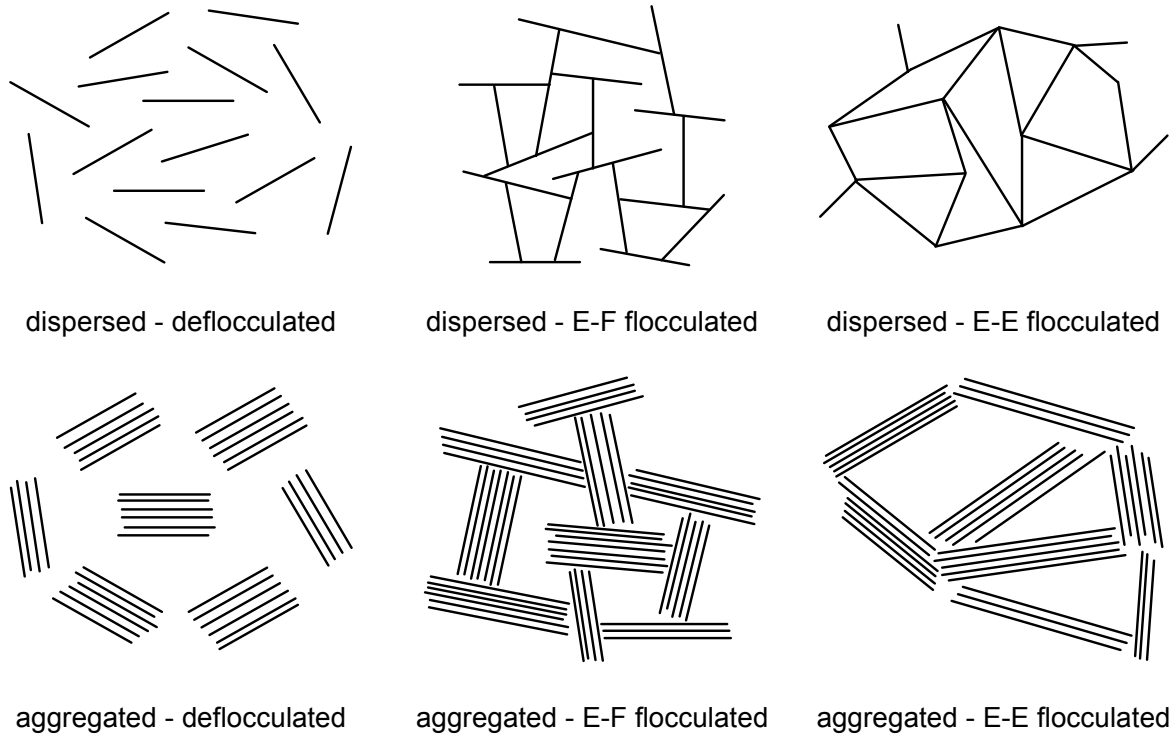

Figure 2.8: Definition of clay fabric according to van Olphen (1963).

controls edge surface charges of clay particles and thus, electrostatic particle attraction and repulsion between edges and base surfaces, whereas ion concentration controls the thickness of the diffuse double-layer and thus, electrostatic repulsion between base surfaces by double-layer overlapping. Dispersed and deflocculated clay fabrics follow from dominating repulsion, i.e., from low ionic concentrations, by which double-layer repulsion is increased, as well as from alkaline pH conditions, by which electrostatic repulsion between negatively charged clay particle bases and equally charged clay particle edges is induced. E-F flocculation, on the other hand, simply requires positive edge charges, i.e., acidic pH conditions, by maintaining low ionic concentrations to prevent F-F aggregation. By increasing ionic concentrations and thus, decreasing the thickness of the diffuse double-layer, interparticle base surface repulsion decreases just as well, until attractive van der Waals forces prevail at small distances and finally cause F-F aggregation. E-E flocculation is proposed to occur as an intermediate state at moderate ionic concentrations and alkaline pH conditions with van der Waals attraction already dominating E-E surface interaction, but not yet overcoming F-F surface double-layer repulsion.

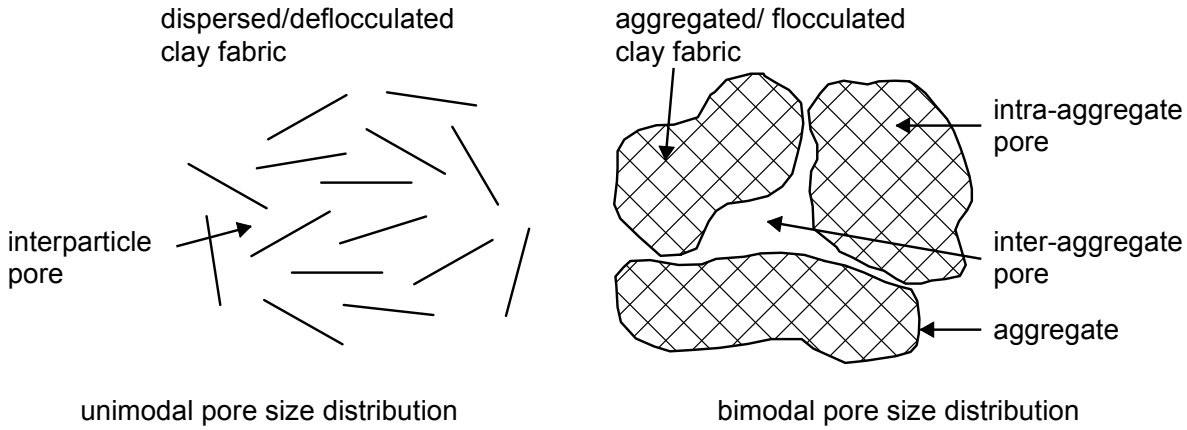

Figure 2.9: Definition of voids related to clay fabric according to Nagaraj & Miura (2001).

Interparticle forces dominate the formation of clay particle fabric in several naturally occurring systems, e.g., in soil deposits formed by sedimentation, whereas with respect to geotechnical systems, forces originated by external loading conditions have to be additionally taken into account and may dominate the clay fabric. Generally, it can be distinguished between mechanical and suction loading conditions since they were found to dominate clay fabric on different scales. It was stated by several researchers that suction loading affects intra-aggregate pores straightforward, whereas it affects inter-aggregate pores indirectly (e.g., Thom et al. 2007, Romero 2013). Mechanical loading, on the other hand, affects clay fabric dominantly with respect to inter-aggregate pores (e.g., Delage & Lefebvre 1984, Burton et al. 2014). However, special boundary conditions, which are discussed in the following, also allow for changes in intra-aggregate pores.

With respect to suction loading, intra-aggregate pores tend to increase with decreasing suction, whereas they tend to decrease with increasing suction, which is caused by water adsorption and desorption processes on associated clay particle surfaces promoting clay particle separation and approaching, respectively. This behaviour was found to be almost completely reversible (Romero et al. 2011), which accounts for the conclusion that preferential F-F, E-F and E-E associations remain unaffected by drying and wetting cycles. In consequence of water adsorption and desorption processes, units expand and shrink, which indirectly affects inter-aggregate pores, i.e., they decrease when units expand and thus, when suction decreases, whereas they shrink as well when units shrink and thus, when suction increases. The decrease in indirectly affected inter-aggregate pores caused by decreasing suction is therefore irreversible. Since the clay fabric at low suctions is dominated

by interparticle forces according to Santamarina et al. (2002), the expansion and shrinkage behaviour of units due to suction loading and unloading is different for varying clay mineralogies, pH conditions and ion concentrations. Additionally, when relating expansion behaviour to the space of inter-aggregate pores to be filled, the resulting distribution of inter- and intra-aggregate pores due to suction loading and unloading may be different. When units expand completely into inter-aggregate pores, clay PSDs change from bimodal to completely unimodal states with decreasing suctions, whereas with increasing suctions unimodal PSDs are preserved by clay shrinking (e.g., Romero et al. 2011, Burton et al. 2014). On the other hand, when unit expansion is reduced, an appreciable fraction of remaining inter-aggregate pores and thus, bimodal PSDs, can be observed at both states, after decreasing as well as subsequent increasing suction (Thom et al. 2007).

With respect to mechanical loading, main effects were found on inter-aggregate pores by decreasing them irreversibly with increasing loading. In doing so, the largest available pores become reduced since they have the lowest resistance against deformation. Intra-aggregate pores, on the other hand, remain approximately unchanged (Delage & Lefebvre 1984, Romero 2013). It was shown by Thom et al. (2007) that this phenomenon can be best observed under isotropic loading conditions since particle rearrangement within units is limited. Under anisotropic oedometric conditions, on the other hand, also reductions in intra-aggregate pores have been detected and can be attributed to partial restructuring of clay fabrics within units. Since flocculated clay fabrics have generally looser densities compared to aggregated clay fabrics, observations on restructuring due to mechanical loading refer to clay fabrics within units, which are initially flocculated. In addition, direct effects of mechanical loading on intra-aggregate pores can also be observed in case of preferentially F-F associated clay particles, whose interparticle distances are subjected to great variabilities and are controlled by double-layer repulsion at zero external loading conditions, i.e., in case of osmotically interlayer swelling clay mineralogies (Gens & Alonso 1992). Thereby, deformations due to external mechanical loading are controlled by reduction and expansion of interparticle/-layer basal distances, i.e., intra-aggregate pores, corresponding to the equilibrium of double-layer repulsion and external mechanical loading (Sridharan 2002). Generally, these changes are supposed to be completely reversible (Bolt 1956). Provided that complete dispersion and deflocculation corresponds to the preferential clay fabric under zero external loading conditions, actually no units and thus, differentiations between inter- and intra-aggregate pores exist. In such cases, deformations due to mechanical (un)loading are exclusively related to interparticle/-layer distances.

2.2.2 Polymers

Polymers are macro-molecules composed of numerous repeating units, i.e., monomers, forming chains. Due to their (potentially) synthetic nature, the variety of polymers is enormous. For this reason, polymer characteristics addressed in the present study are limited to the constitutive properties governing the interaction with clay mineral surfaces, i.e., the electrostatic characteristics. Thereby, cationic, anionic, non-ionic and polar as well as non-ionic and non-polar polymers can be distinguished. The polarity varies in dependence on the individual electric dipole moment of the monomers, whereas the cationicity and anionicity vary in dependence on the ratio of charged monomers within the polymer chain. Since the interaction of non-ionic and non-polar polymers with both, clay mineral surfaces as well as water molecules, is significantly reduced as compared to polar and/or ionic polymers this type of polymer is not considered in the following of this study. In general, one main feature of polymers refers to their flexibility, which is in contrast to the rigid nature of clay mineral layers (Theng 2012).

2.2.3 Interaction of clay minerals and polymers in aqueous solution

2.2.3.1 Driving forces of polymer adsorption and bonding mechanisms between clay mineral surfaces and polymers

Clay minerals and polymers were found to have high affinity to form strongly connected composites. This behaviour is promoted by two governing mechanisms, i.e., electrostatic attraction and entropy gain (Theng 2012). The first mechanism arises from the electrostatic surface characteristics of clay minerals, i.e., the layer charge of basal surfaces and edges and the polar characteristics of oxygen- and hydroxyl-terminations, as well as of polymers, i.e., the monomer charges and polar characteristics of various terminations. The second mechanism arises from the desorption of numerous water molecules, which are replaced by the adsorption of only one polymer chain (Theng 1982).

The electrostatic interaction mechanisms between non-ionic polymers and 2:1 clay mineral layer surfaces were found by Deng et al. (2006) to be dominated by ion-dipole attraction between exchangeable ions of the clay mineral and polar parts of the polymer chain as well as dipole-dipole attraction between water-molecules of the hydrated clay mineral and polar

parts of the polymer chain. In the case of 1:1 layer silicates, also the octahedral hydrogens were found to form hydrogen-bonds with polymers by dipole-dipole attraction (Mpofu et al. 2003). Other mechanisms have been suggested, e.g., by Laird (1997) and Stutzmann & Siffert (1977), referring to hydrophobic bonding, e.g., between the polymer backbone and the tetrahedral oxygens of clay mineral surfaces, as well as to protonation of polymers in the near-field of clay mineral surfaces, by which they become positively charged and are attracted to the negatively charged basal clay mineral surface. However, since the bonding strength of adsorbed water molecules on the clay mineral surface by ion-dipole and dipole-dipole attraction is very high, their replacement by non-ionic polymer adsorption results in a very small or even positive value of enthalpy change. The second governing mechanism in clay-polymer composite formation, i.e., entropy gain, is therefore considered to be the major driving force in case of non-ionic polymer adsorption (Theng 1982). Quantitatively, this was shown, e.g., by Parfitt & Greenland (1970), calculating the changes in enthalpy and entropy due to polymer adsorption of various molecular weights on the basis of measured values of adsorbed polymer volumes and desorbed water molecule volumes, respectively.

In case of charged polymers, their interaction with the clay mineral surface is dominated by the type (cationic/anionic) of charge as well as their degree of ionicity, i.e., the ratio of charged monomers in the polymer chain. Thereby, ion exchange by polymer adsorption plays a major role since exchangeable ions at the clay mineral surface are replaced by ionic segments of the polymer chain. Ueda & Harada (1968) proved this kind of mechanism by demonstrating that clay CEC decreases with increasing amount of adsorbed cationic polymer. The main bonding mechanisms are therefore Coulombian in nature, i.e., ion-ion attraction. However, the mechanisms detected in case of non-ionic polymers, i.e., ion-dipole and dipole-dipole interaction, were found to be also relevant for ionic polymer adsorption (Deng et al. 2006), i.e., polar parts of the ionic polymer chain additionally bond to hydration water and exchangeable ions at the clay mineral surface. In case of anionic polymers, cation-bridging is additionally proposed to significantly contribute to clay-polymer composite formation, (e.g., Laird 1997, Güngör & Karaoglan 2001). By this mechanism, it is implied that due to the adsorption of exchangeable cations for layer charge equilibration positive charges prevail locally at the clay mineral surface, which gives rise to local ion-ion attraction between exchangeable cations and anionic polymers. Therefore, cation-bridging phenomena are relevant in case of multivalent exchangeable cations, when the local excess in positive surface charge is increased. In case of anion bridging between adsorbed multivalent anions on the positively charged clay mineral edges and cationic

polymers, this effect has not yet been proposed to be of significance for the formation characteristics of clay-polymer composites.

The particular bonding mechanisms dominating non-ionic, cationic and anionic polymer adsorption on clay minerals surfaces are summarized in Figure 2.10 - 2.12.

2.2.3.2 Polymer shape in solution and in the adsorbed state on clay mineral surfaces

Depending on their specific charge characteristics, polymers in aqueous solution are characterized by various preferential shapes. Thereby, non-ionic polymers can be described by randomly coiled chains, whereas ionic polymers have rather stretched geometries (Theng 2012). The latter can be attributed to intra-chain ionic repulsion arising from equally charged monomers. Its degree depends on the ionicity, i.e., the distance between monomer-charges, as well as environmental pH and electrolyte concentration, by which monomer charges become equilibrated due to (de)protonation and counterion adsorption, respectively. When coming into contact with the clay mineral surface, in case of non-ionic polymers the theory of adsorption in terms of trains (polymer segments tightly adsorbed to the clay mineral surface), loops (polymer segments in solution bounded to trains at both sides) and tails (polymer segments in solution bounded to trains at one side), which has been theoretically derived by Scheutjens & Fleer (1990), is widely accepted (Figure 2.10). This behaviour is consistent with the theory of preferential polymer shape in solution, i.e., randomly coiled, as well as statistical considerations on segment adsorption in the near-field of clay mineral surfaces. Thereby, with varying amount of polymer adsorption, the ratio of train, loop and tail segments varies significantly, i.e., when the amount of adsorbed polymer is low, train segments are dominant, whereas with increasing amount of adsorption, loops and tails enlarge and become dominant (e.g., Cohen Stuart 1991). Similar changes in the ratio of train, loop and tail segments occur when the polymer chain length increases.

In contrast, the shape of ionic polymers in the near-field of clay mineral surfaces is still dominated by intra-chain repulsion of equally charged monomers, i.e., they have stretched geometries (Figure 2.11 - 2.12). In case of cationic polymers, by which exchangeable cations at the basal clay mineral layer surface are replaced due to adsorption, intra-chain repulsion results in predominating train segments since the polymer collapses almost completely to the clay mineral surface. However, some small loops and tails develop when the amount

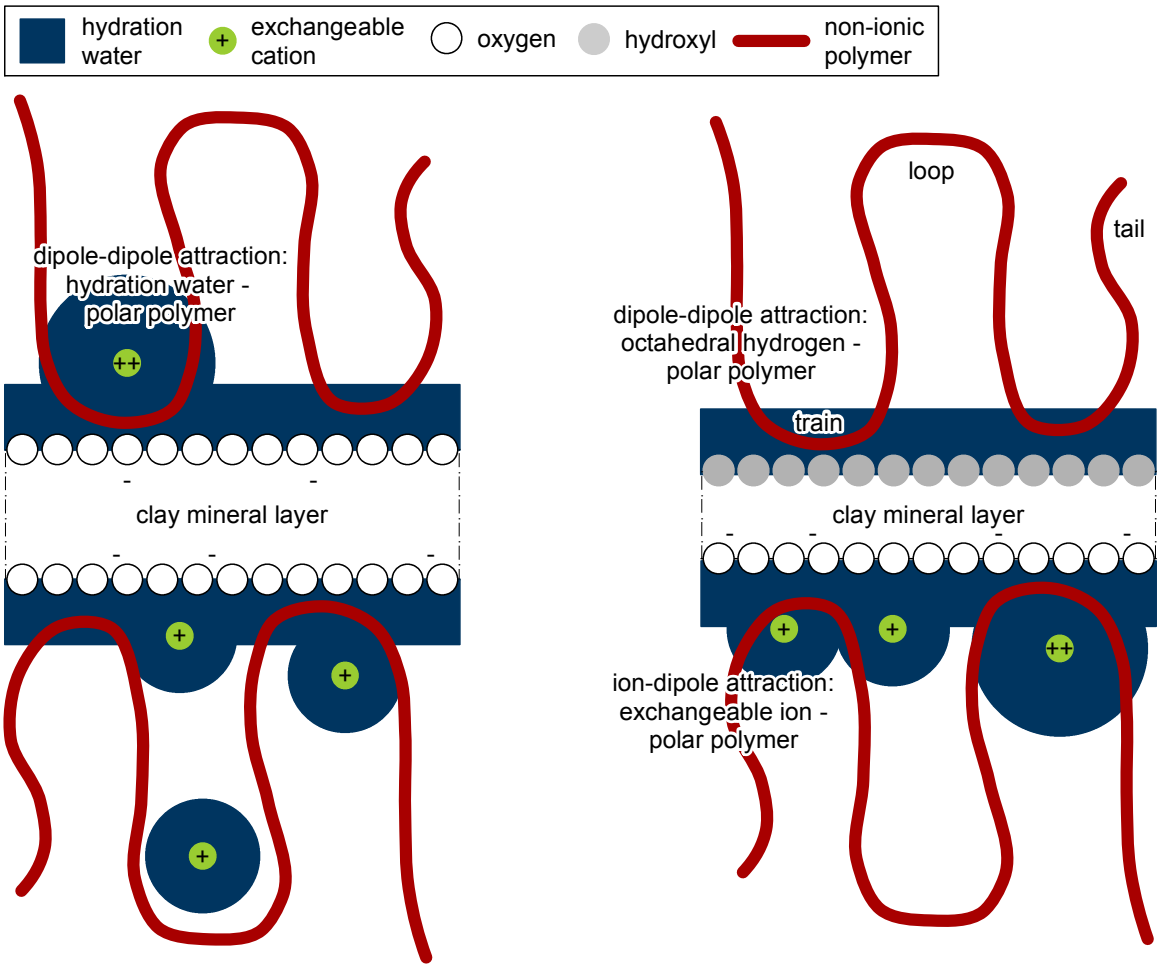

Figure 2.10: General sketch of non-ionic polymer adsorption: interlayer swelling 2:1 clay mineral layers (left); 1:1 clay mineral layers (right).

of adsorbed polymer exceeds total surface coverage (Ueda & Harada 1968). Additionally, in case of higher charge densities of the polymer chain compared to the clay mineral layer, cationic polymer adsorption in the adsorbed state is characterized by an appropriate increase in loop and tail segments and the clay mineral surface is electrostatically equilibrated by train segments only (Breen 1999). Anionic polymers, on the other hand, are characterized by only few adsorption spots on the clay mineral surface since they are generally repelled from the predominantly negatively charged clay mineral surface (Theng 2012). Adsorption by anion exchange on positively charged clay mineral edges as well as by multivalent cation bridging, respectively, causes therefore single train segments with large tails and no loops. Since due to intra-chain repulsion the polymer chain is still stretched, tails

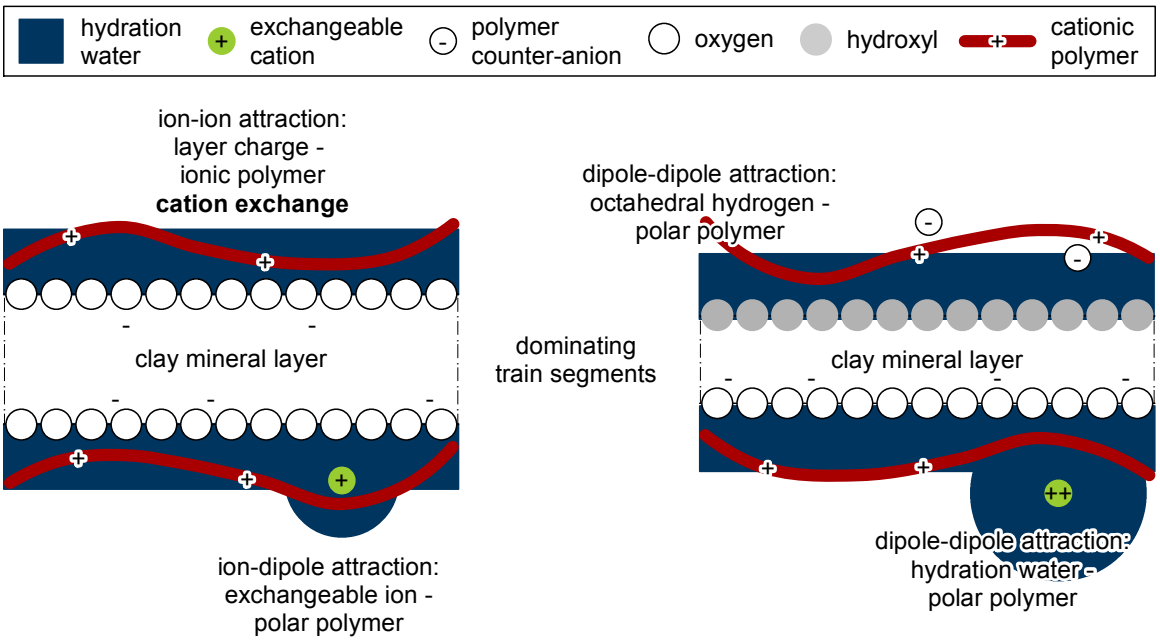

Figure 2.11: General sketch of cationic polymer adsorption: interlayer swelling 2:1 clay mineral layers (left); 1:1 clay mineral layers (right).

significantly extend into the aqueous solution. Similar to ionic polymer behaviour in solution, the shape of adsorbed ionic polymers varies in dependence on the environmental conditions, i.e., with decreasing (anionic polymers) and increasing (cationic polymers) environmental pH as well as increasing electrolyte concentration polymer charges become equilibrated resulting in classical train, loop and tail segment adsorption as proposed for non-ionic polymers.

2.2.3.3 Adsorption capacity of polymers on clay mineral surfaces

Most of the studies conducted on the topic of clay-polymer composite formation have focused on the investigation of adsorption isotherms. In doing so, the mass of adsorbed polymer in equilibrium is determined in dependence on polymer concentration in solution. For clay-polymer-water systems, the resulting curves were found to approximately follow the 'Langmuir'-type adsorption (e.g., Schamp & Huylebroeck 1973, Espinasse & Siffert 1979, Inyang & Bae 2005), which is characterized by a steep increase in adsorbed mass at low polymer concentrations in solution followed by a sudden reach of a defined

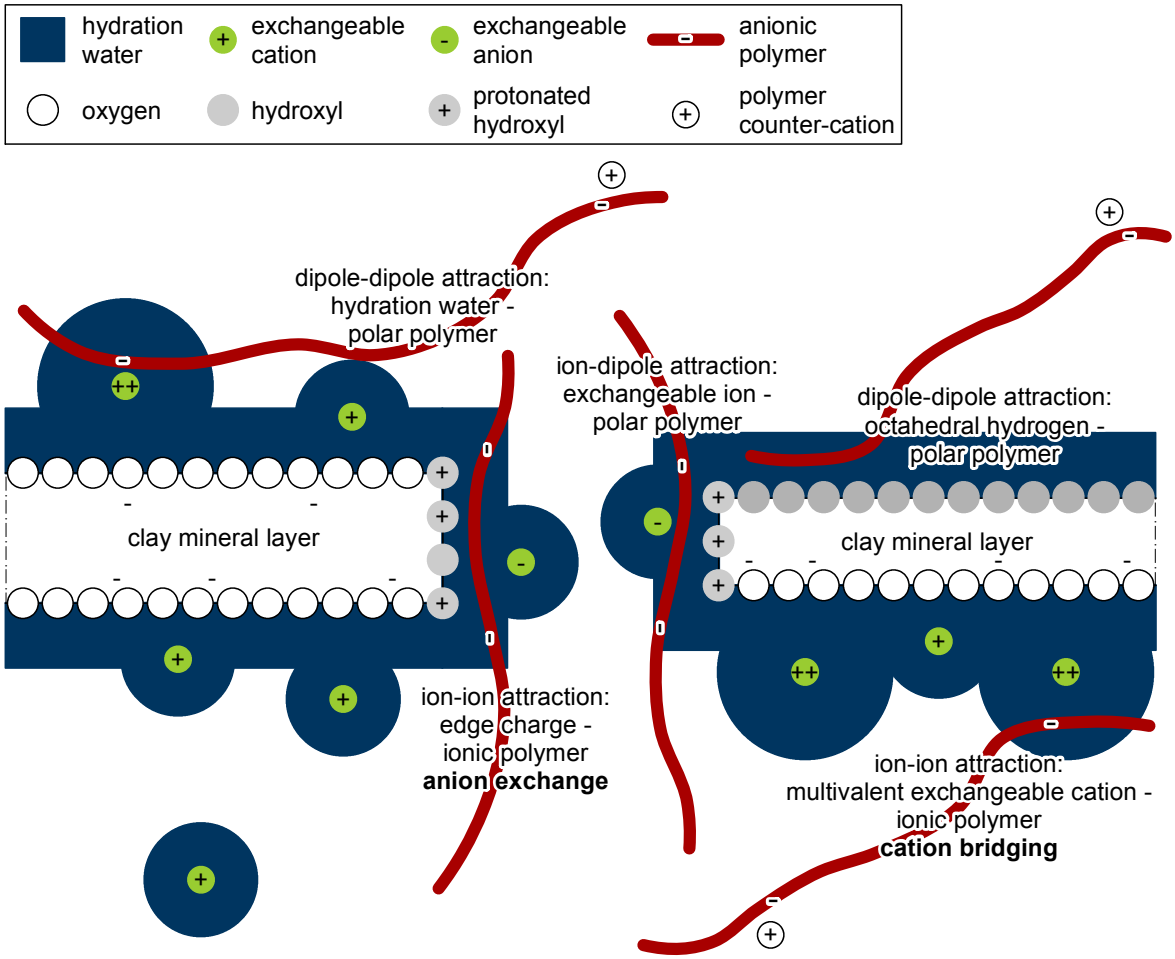

Figure 2.12: General sketch of anionic polymer adsorption: interlayer swelling 2:1 clay mineral layers (left); 1:1 clay mineral layers (right).

plateau value, which equals the maximum adsorption capacity. On the other hand, it is suggested that at very low polymer concentrations the equilibrium concentration in solution is practically zero (Cohen Stuart 1991, Theng 2012). Therefore, in this region adsorption may be characterized by the 'high-affinity'-type, which differs from the 'Langmuir'-type by having adsorbed polymer masses > 0 even when the equilibrium concentration in solution is $= 0$. In Figure 2.13 the types of adsorption isotherms proposed are illustrated.

In literature, many individual adsorption isotherms for various clays, polymers as well as boundary and environmental conditions have been derived and led to comprehensive knowledge on several general relationships. As a result, the polymer- as well as the clay

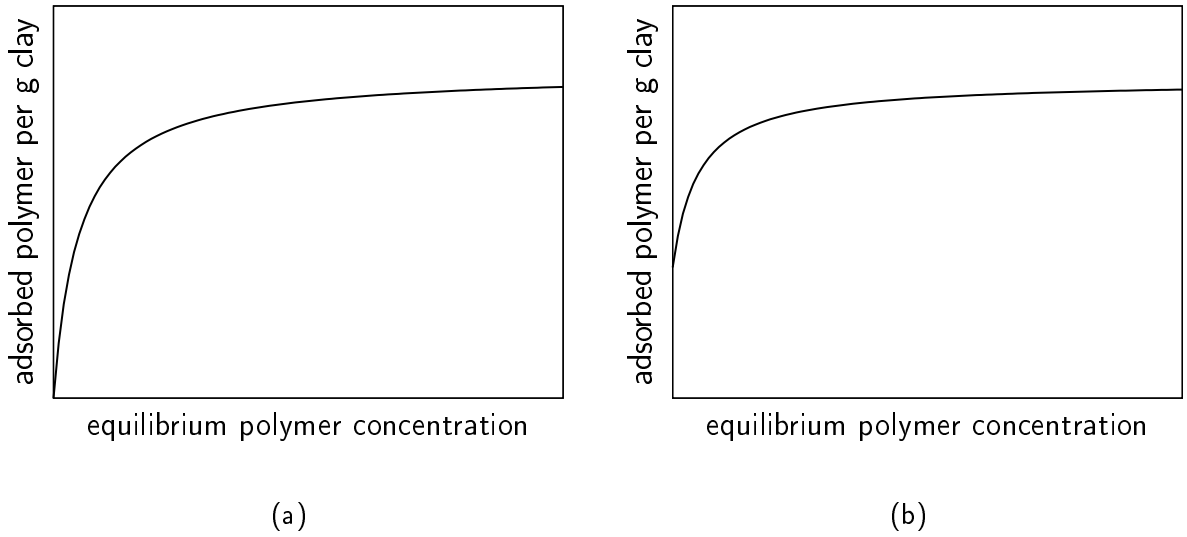

Figure 2.13: Shapes of adsorption isotherms proposed for clay-polymer-water systems: Langmuir-type (a); high-affinity-type (b).

mineralogy-specific affinity for interaction as discussed in subsubsection 2.2.3.1 as well as geometrical factors of the clay-polymer-water system controlling clay mineral surface accessibility have been found to be of great significance (Theng 2012). With respect to the former, non-ionic and cationic polymers have generally higher affinity to interact with the clay mineral surface as compared to anionic polymers. This can be attributed to their overall attraction to the (mainly) negatively charged clay mineral surface, whereas anionic polymers are widely repelled, especially from the basal surfaces. The maximum adsorption capacity of non-ionic and cationic polymers is therefore distinctly higher as compared to anionic polymers since the amount of adsorption spots is increased. However, the latter can be increased by acidic pH conditions (Heller & Keren 2003) as well as the presence of multivalent exchangeable cations (Güngör & Karaoglan 2001), by which the amount of adsorption spots due to anion exchange and cation bridging, respectively, is increased. Also, with increasing electrolyte concentration in solution charge neutralization of the anionic polymer is promoted and thus, its repulsion from the clay mineral surface is reduced giving rise to the dominance of attractive forces (Heller & Keren 2003). In addition to the charge characteristics of clay minerals and polymers, entropy gain plays a major role, especially for non-ionic polymer adsorption. Thereby, the maximum adsorption capacity increases with increasing polymer molecular weight (e.g., Greenland 1963, Parfitt & Greenland 1970). However, this property acts oppositional when referring to the second factor determining

polymer adsorption capacity, i.e., clay mineral surface accessibility. It was shown, e.g., by Greenland (1963) and Schamp & Huylebroeck (1973), that an increase in polymer molecular weight may hinder the polymer to enter the interlayer and interparticle space due to steric effects. Adsorption therefore, may take place only on the outer surfaces of clay particles and aggregates, respectively. In consequence, the resulting amount of polymer adsorption is decreased. Similarly, in case of interlayer swelling clay mineralogies, the type of exchangeable cation as well as the electrolyte concentration in solution controls surface accessibility in the interlayer space. Greenland (1963) for instance found that the maximum amount of adsorbed non-ionic polymer is almost three times higher in case of exchangeable sodium cations as compared to calcium. Also, an adsorption limiting effect by about 85% due to increased electrolyte concentrations from 0 to 1.0 mol/l in solution was demonstrated. Furthermore, with increasing clay concentration in solution from 0.25% to 4.0% clay mineral surface accessibility and thus, polymer adsorption was restricted by about 60% due to mutual interaction of clay mineral layers.

2.2.4 Structure of clay-polymer composites

In accordance to the clay structure, clay-polymer composite structure is characterized by the geometrical arrangement of clay particles, i.e., the fabric, and the bonding mechanisms between them, which are significantly determined by polymer adsorption on clay particle surfaces. Characteristics of the latter have been discussed in detail in subsection 2.2.3, on which basis the formation of composite fabric will be examined in the following.

Generally, polymer adsorption on clay mineral surfaces in aqueous solutions, i.e, at zero external loading conditions, affects the initial clay fabric by either promoting aggregation and flocculation or stabilizing dispersion and deflocculation, respectively. The former effect implies that polymers bridge between two adjacent clay particles by adsorbing simultaneously on both of them, whereas the latter mechanism implies that polymer adsorption keeps clay particles separated from each others attraction sphere. With respect to particle aggregation and flocculation, the effect of interparticle bridging by polymers is promoted by (i) polymer shapes overcoming the equilibrium interparticle distance as well as by (ii) charge-neutralization of the clay mineral surface due to polymer adsorption reducing interparticle repulsion and thus, the interparticle distance. Both mechanisms are related to ionic polymer adsorption since they have stretched geometries and are capable to neutral-

ize electric surface charges. Thereby, Laird (1997) found that anionic polymers mainly operate by overcoming the equilibrium interparticle distance, whereas cationic polymers mainly operate by charge neutralization of the clay mineral base surfaces. However, it was shown by Yu et al. (2006) that in case of cationic polymers the dominance of charge neutralization decreases and bridging by overcoming the equilibrium interparticle distances increases when the polymer ionicity is reduced and the polymer molecular weight is increased. Non-ionic polymers, on the other hand, are less effective in promoting aggregated and flocculated clay fabrics, respectively. This can be attributed to their randomly coiled geometry, by which their bridging capacity along large interparticle distances is limited (Theng 2012).

In addition to the requirement of polymer geometries overcoming interparticle distances in order to effect clay particle aggregation and flocculation, which is promoted by ionic polymers and high molecular weights, the amount of polymer adsorbed to the clay mineral surface is of great significance in composite fabric formation. Thereby, aggregation and flocculation occurs in case of moderate polymer adsorption, i.e., when the clay mineral surface susceptible for polymer adsorption is partially occupied by polymers. Stabilization of dispersion and deflocculation, on the other hand, results in case of polymer adsorption close to the maximum adsorption capacity. In this state, polymer shapes have increased loop and tail segments preventing clay particle approaching into each others attraction sphere, which is referred to 'steric stabilization' (Theng 2012). Additionally, due to ionic polymer adsorption close to the maximum adsorption capacity, clay mineral surfaces may undergo charge reversal, whereas charge neutralization results from moderate ionic polymer adsorption. (e.g., Breen 1999, Ueda & Harada 1968). As a result, interparticle repulsive forces are increased and thus, dispersed and deflocculated clay fabrics are promoted, which is referred to 'charge stabilization' (Theng 2012). It has to be noted, that the effect of dispersion and deflocculation explicitly refers to the stabilization of an existing fabric, i.e., the degree of initial dispersion and deflocculation is preserved. Thereby, in case of initially aggregated or flocculated clay fabrics, further aggregation and flocculation of clay units is prevented by steric or charge stabilization between clay units. Also, the degree of aggregation and flocculation within clay units is preserved since they are stabilized by polymer adsorption like a 'coat of paint' enclosing units (Greenland 1963).

2.3 Multiscale coupling in clays

2.3.1 Definitions

Clay mineralogical properties and its resulting behaviour on particle level have been examined in subsection 2.2.1 by relating clay fabric to the underlying interparticle forces and external loading conditions. Thereby, when referring to the clay fabric, its behaviour is characterized on the *micro-scale*, whereas with respect to applications in geotechnical and geoenvironmental engineering, clay behaviour is characterized and valuated by its properties on the *macro-scale*, which include the deformation and strength characteristics as well as the hydro-mechanical behaviour by treating the clay as a continuum. However, it is established since decades that macro-scale soil properties can be attributed to the micro-scale soil characteristics giving rise to multiscale relationships, e.g., on clay behaviour (Mitchell & Soga 2005). In this section, the micro- and macro-scale coupling in clays with respect to their volumetric behaviour and hydraulic permeability will be discussed. Thereby, the focus is set on the main findings of classical conceptual work rather than the discussion of detailed experimental work.

2.3.2 Volumetric behaviour

The volumetric behaviour of clays refers to their macro-scale response aiming on an increase or decrease in the total volume caused by changes in external loading conditions. Thereby, various loading and boundary conditions, e.g., mechanical and suction loading conditions; isotropic and anisotropic loading conditions; confined and unconfined boundary conditions, can be distinguished. Depending on the boundary condition, different measures in terms of strain and stress can be determined. In order to account for the specific influence of clay mineralogy and environmental conditions on clay volumetric behaviour, various studies were conducted on samples prepared to initially zero suction and mechanical loading conditions, i.e., slurry conditions with water contents of the clay greater than the liquid limit. The main findings are summarized in the following:

Based on one-dimensional compression and rebound tests, Sridharan & Rao (1973) concluded that two governing mechanisms can be distinguished to control clay volumetric behaviour, i.e., interparticle shearing resistance, which dominate volume change of non-

swelling clays, as well as DDL repulsion, which dominate volume change of swelling clays. With respect to the former mechanism, test results on kaolinite-rich clays, whose clay mineralogical structure is composed of non-swelling 1:1 clay mineral layers, have shown that interparticle shearing resistance is directly related to the clay fabric. Thereby, flocculated clay fabrics with preferential E-F and E-E particle orientations, have higher resistance as compared to aggregated clay fabrics with preferential F-F particle orientations. Macro-scale volume change is therefore increased in case of micro-scale F-F aggregated fabrics and vice versa (Rao & Sridharan 1985). The second mechanism controlling volume change behaviour in swelling clays, i.e., DDL repulsion, has been examined by several researchers (e.g., Bolt 1956, Mesri & Olson 1971, Marcial et al. 2002, Di Maio et al. 2004). Thereby, exchangeable cations, electrolyte concentrations as well as the dielectric constant of the pore fluid have been varied systematically highlighting the micro- and macro-scale coupling between the thickness of DDLs at clay mineral surfaces and the volume of the clay continuum. On this basis, volume change of swelling clays can be expected to be completely reversible, but this has been experimentally clearly disproved. It has been concluded e.g., by Bolt (1956) and Nagaraj & Srinivasa Murthy (1983) that reduced clay volumes during unloading as compared to the corresponding clay volumes during loading at the same applied stress can be attributed to the dominance of attractive van der Waals forces at small interlayer distances overcoming repulsive double-layer forces and thus, preventing interlayer expansion. However, evidence of DDL formation during unloading controlling clay volume change, e.g., at the outer clay particle surfaces, has been given by Sridharan & Rao (1973) based on experimental results on the influence of varying pore fluid characteristics.

In addition to the dominance of DDL forces in volume change behaviour of swelling clays, some effects related to the clay fabric have also been suggested, e.g., by Bolt (1956). Thereby, clay fabric in the low stress range during one-dimensional compression is supposed to be characterized by randomly oriented clay particles as against base surface orientation parallel to the applied loading in the high stress range. In consequence, the dominance of DDL repulsion in clay volumetric behaviour increases with increasing loading during one-dimensional compression. The tendency of clay particle reorientation under anisotropic loading conditions, i.e., base surface orientation parallel to the applied loading, has also been suggested by Marcial et al. (2002) and Tripathy et al. (2010) comparing the volume change of swelling clays due to one-dimensional mechanical loading induced compression as well as suction loading induced unconfined shrinkage. Thereby, systematic deviations in the form of increased void ratios in case of isotropic suction loading as compared to anisotropic

mechanical loading have been observed. However, macro-scale deviations observed for differing loading conditions and related to the clay fabric in swelling clays are insignificant as against deviations occurring between swelling and non-swelling clays, which can be related to the clay fabric. This is indicated, e.g., by their great differences in shrinkage limit, i.e., by their residual fabric obtained under isotropic loading and unconfined boundary conditions. Since the significance of clay fabric in terms of its related interparticle shearing resistance during shrinking has been pointed out in (Sridharan & Prakash 1998) reduced shrinkage limits in case of swelling clays as compared to non-swelling clays can be attributed to their tendency of complete layer dispersion and deflocculation at the initial state, i.e., under zero suction and mechanical loading conditions, by which the interparticle shearing resistance is decreased. Further, the higher interparticle shearing resistance in case of non-swelling clays was found to limit clay particle reorientation under anisotropic loading conditions significantly, which is in contrast to the behaviour of swelling clays (Tripathy et al. 2010).

The importance of clay fabric with respect to the volumetric behaviour of swelling clays becomes more evident in case of compacted clays, which have been exposed to significant suction and mechanical loading conditions before testing. Consequently, the initial clay fabric corresponds to the particular stress history of the clay and may deviate significantly from idealized dispersed and deflocculated clay fabrics. Results of oedometer swelling tests under constant mechanical and decreasing suction loading conditions clearly demonstrate that with increasing initial suction conditions clay volume change due to swelling increases (Gens & Alonso 1992). Similar results have been obtained on the swelling pressure under confined volume and decreasing suction loading conditions (e.g., Kassiff & Ben Shalom 1971, Baille et al. 2010). The differences can be attributed to the existence of aggregated and flocculated clay units at the initial state. Since in this type of clay fabric, volume change due to DDL repulsion occurs predominantly in the intra-aggregate pores, units expand into inter-aggregate pores during testing (e.g., Romero et al. 2011). Thereby, clay particle redistribution to the point of minimum energy configuration, i.e., perfectly parallel base surface orientation, is facilitated with increasing degree of initial clay fabric homogeneity, i.e., with decreasing initial suction condition. Consequently, the total pore volume in case of oedometer swelling tests as well as the swelling pressure in case of isochoric swelling tests, increases with increasing initial suction condition caused by imperfect particle redistribution. Additionally, with increasing mechanical loading condition during testing, clay particle redistribution is promoted. This was stated e.g., by Gens & Alonso

(1992) based on oedometer compression test results on samples saturated under various mechanical loading conditions. Similarly, swelling pressure development under isochoric conditions indicates an increased tendency of particle redistribution with increasing dry density of the clay and thus, with increasing total stress state conditions during testing (e.g., Schanz & Tripathy 2009).

Generally, the macro-scale volume change behaviour of clays evoked by an increase or decrease in mechanical and suction loading, respectively, is directly correlated to their plastic properties (Mitchell & Soga 2005). The higher the liquid limit of the clay and thus, the lower its shrinkage limit in case of swelling clays as well as the greater its shrinkage limit in case of non-swelling clays, the greater its compressibility under one-dimensional mechanical loading conditions.

2.3.3 Hydraulic permeability

The hydraulic permeability of soils refers to the proportionality factor relating the macro-scale water flow rate through a soil to its corresponding driving force, i.e., the hydraulic gradient. For sandy soils, this relationship was found by Darcy (1856) to be linear for a wide range of hydraulic gradients provided that (i) laminar as well as (ii) steady state fluid flow prevail. Additionally, this relationship can be assumed for clays provided that (iii) constant fabric conditions throughout testing are preserved (Mitchell & Soga 2005). The latter condition has been the subject of great interest in order to account for its impact on clay hydraulic permeability, i.e., on the value of the proportionality factor. As an outcome of several research studies, the following relationships between clay micro-scale fabric and its macro-scale hydraulic permeability can be summarized:

Based on the time-compression behaviour during one-dimensional consolidation tests conducted on clay slurries Mesri & Olson (1971) and Rao & Mathew (1995) found that the hydraulic permeability for a given void ratio of the clay decreases with increasing degree of clay fabric dispersion and deflocculation, respectively. Thereby, clay fabric was controlled by the dielectric constant and electrolyte concentration of the pore fluid as well as the valency of exchangeable cations, i.e., by controlling the interparticle forces. The observed behaviour can be attributed to the corresponding difference in PSD, i.e., bimodal PSDs in aggregated and flocculated clay fabrics as against unimodal PSDs in dispersed and deflocculated clay fabrics. Since the flow rate through a clay is controlled by that flow path

having the lowest resistance, i.e., by the pore system having maximum size of pore radii and minimum length of flow paths, the existence of large inter-aggregate pores promotes the fluid flow and thus, increases the hydraulic permeability. Similar findings were made on compacted clays having various types of exchangeable cations (e.g., Ahn & Jo 2009), permeated with differently concentrated electrolyte solutions (e.g., Zhu et al. 2013, Ye et al. 2014) as well as fabricated under different initial suction loading conditions (e.g., Baille et al. 2010, Ören et al. 2014). Doing so, various clay fabrics developed during clay saturation and thus, are present under equilibrium testing conditions. Thereby, the development of unimodal PSDs causing decreased hydraulic permeabilities is promoted in case of monovalent exchangeable cations, low electrolyte concentrations as well as low initial suction loading conditions since particle redistribution from its initial state to the point of dispersed and deflocculated clay fabric is facilitated.

In addition to these findings, the influence of clay mineralogy on hydraulic permeability was discussed, e.g., by Mesri & Olson (1971) and Baille et al. (2010). It was pointed out that with increasing particle size and isotropy of particle shape pore radii increase and tortuosity of the pore system decreases leading to an increase in hydraulic permeability. Therefore, the hydraulic permeability of clays, which are predominantly composed of various clay mineralogies, was found to be in the following order: non-swelling 1:1 clay mineral layers (e.g., kaolinite) > non-swelling 2:1 clay mineral layers (e.g., illite) > swelling 2:1 clay mineral layers (e.g., montmorillonite) since basal dimensions of clay mineral layers as well as the amount of layers stacked to form particles decrease in the same order. Further, with respect to the tortuosity of the pore system, the significance of anisotropy in case of clay hydraulic permeability has been pointed out, e.g., by Olsen (1962).

According to Mesri & Olson (1971) the above named factors used in order to control clay hydraulic permeability can be categorized in mechanical and physico-chemical variables of the clay-water system. Thereby, mechanical variables determine directly the geometry of the pore system, e.g., by the clay particle size, whereas physico-chemical variables determine clay mineral surface-water interaction, e.g., by the electrolyte concentration. With respect to the physico-chemical variables, several researchers suggested that decreased hydraulic permeabilities result (in parts) from an increase in the inhibition of water mobility by bonding it to the clay mineral surface, i.e., hydration and formation of DDL, rather than from related modifications in mechanical variables, i.e., dispersed and deflocculated clay fabrics, as proposed by Mesri & Olson (1971). However, the latter conclusion, i.e.,

the dominance of changes in mechanical variables, is in accordance to findings by Olsen (1962) taking into account various factors quantitatively. Therefore, direct correlations between clay micro-scale fabric and its macro-scale hydraulic permeability are widely accepted (Mitchell & Soga 2005).

2.4 Theoretical approaches on multiscale coupling in clays

2.4.1 Physico-chemical approach

In case of interlayer swelling clay mineralogies, clay volumetric behaviour was found to be dominated by DDL repulsion between adjacent clay mineral layer basal surfaces (see subsection 2.3.2). Since from colloid-chemical point of view, this type of interaction can be quantified macro-scale clay volumetric behaviour can be calculated by use of the individual physico-chemical input parameters of the clay mineral-water system. The basic equations and limitations of the physico-chemical approach for determining clay volumetric behaviour are discussed in detail in the following:

Diffuse double-layer theory

In subsubsection 2.2.1.2 the adsorption mechanisms of water on clay mineral surfaces, i.e., hydration and osmosis, have been examined. The latter mechanism controls clay mineral layer surface separations > 1.0 nm ($\widehat{=}$ 2.0 nm interlayer distance) and thus, accounts for the macro-scale clay volumetric behaviour in the respective range. It is in turn determined by two governing mechanisms, i.e., electrostatic forces attracting cations and diffusion tending to repel them in the near-field of negatively charged and thus, clay mineral surfaces. The characteristic distribution of ions as a function of distance to a charged surface can be quantitatively described by the Gouy-Chapman diffuse double-layer theory, introduced by Gouy (1910) and Chapman (1913) and referred to clay mineral-water systmes first by Schofield (1946), Bolt (1956) and van Olphen (1963). The general equations are summarized in the following:

The fundamental differential equation expressing the electric potential, Ψ' (V), in the diffuse double-layer as a function of distance, x (m), to the charged surface is given by the

Poisson-Boltzmann equation:

$$\frac{d^2\Psi'}{dx^2} = \left(\frac{2n_0\nu e'}{\epsilon}\right)\sinh\left(\frac{\nu e'\Psi'}{k'T}\right) \tag{2.1}$$

where n_0 ($1/m^3$) is the bulk concentration of counterions, ν (-) is the valency of counterions, e' (C) is the elementary charge, ϵ (C^2/Jm) is the static permittivity, k' (J/K) is Boltzmann's constant and T (K) is the absolute temperature. For the sake of simplicity, Equation 2.1 assumes (i) $|\nu^+| = |\nu^-| = \nu$ and (ii) $n_0^+ = n_0^- = n_0$, i.e., the valency and bulk ion concentration of cations and anions are identical. Further, due to the negative surface charge of clay mineral layers Ψ' becomes negative in their near-field and thus, n_0 and ν refer to the species of counter-cations.

For simplicity, the following substitution are used:

$$y = \frac{\nu e'\Psi'}{k'T} \qquad z = \frac{\nu e'\Psi'_0}{k'T} \qquad \xi = \kappa x \qquad \kappa = \left(\frac{2n_0 e'^2\nu^2}{\epsilon k'T}\right)^{0.5} \tag{2.2}$$

and Equation 2.1 becomes:

$$\frac{d^2y}{d\xi^2} = \sinh(y) \tag{2.3}$$

Integration of Equation 2.3 with the boundary conditions that (1) for $\xi = \infty$ (i.e., at large distance to the charged surface), $dy/d\xi = 0$ and $y = 0$ and (2) for $\xi = 0$ (i.e., at distance zero to the charged surface), $y = z$ (i.e., $\Psi' = \Psi'_0$) gives the following equation expressing the electric potential as a function of distance to the charged surface for a single double-layer:

$$y = 2\ln\left(\frac{1 + e^{-\xi}\tanh\left(\frac{z}{4}\right)}{1 - e^{-\xi}\tanh\left(\frac{z}{4}\right)}\right) \tag{2.4}$$

Finally, Equation 2.4 can be solved by calculating z, i.e., the non-dimensional surface potential function. Therefore, the total charge of the double-layer, σ (C/m^2), is introduced, which equals the total surface charge and is directly proportional to the initial slope of the

potential function $(d\Psi'/dx)_{x=0}$:

$$\sigma = -\epsilon \left(\frac{d\Psi'}{dx}\right)_{x=0} = -\epsilon \left(\frac{dy}{d\xi}\right)_{\xi=0} \left(\frac{2n_0 k'T}{\epsilon}\right)^{0.5} = (2n_0 \epsilon k'T)^{0.5} \left(2\cosh(z) - 2\right)^{0.5} \quad (2.5)$$

For interacting double-layers, i.e., in case of moderate to small distances between charged surfaces, which is of great importance when dealing with clays in the context of geotechnical engineering rather than colloid chemistry, the boundary conditions change as follows: for $x = d$ (i.e., at the midplane between two charged surfaces), $dy/d\xi = 0$ and $y = u$, where d (m) is half the distance between two charged surfaces and $u = (\nu e' \Psi'_d)/(k'T)$, i.e., the non-dimensional midplane potential function. The resulting integral to be solved between the limits z and u for y as well as 0 and κd for ξ reads:

$$\int_z^u \left(2\cosh(y) - 2\cosh(u)\right)^{-0.5} dy = -\int_0^{\kappa d} d\xi = -\kappa d \quad (2.6)$$

Using Equation 2.6, the midplane potential expressed by u can be calculated for any given value of z, i.e., the surface potential, κ, i.e., the environmental conditions of the bulk solution, and d, i.e., the distance between surfaces. This procedure implies that the surface potential, which is determined by 'potential determining ions', is a constant parameter. For clay systems, however, another approach has been established in the past assuming the surface charge to be constant rather than the surface potential. In this case, the general relationship between the surface charge, which equals the total charge of the double layer, σ, and the inital slope of the potential function given in Equation 2.5 can be used again:

$$\begin{aligned} \sigma &= -\epsilon \left(\frac{d\Psi'}{dx}\right)_{x=0} = -\epsilon \left(\frac{dy}{d\xi}\right)_{\xi=0} \left(\frac{2n_0 k'T}{\epsilon}\right)^{0.5} \\ &= (2n_0 \epsilon k'T)^{0.5} \left(2\cosh(z) - 2\cosh(u)\right)^{0.5} \end{aligned} \quad (2.7)$$

By this approach, sets of values for z and u can be derived for a given value of σ (Equation 2.7) and related to d for a given value of κ (Equation 2.6). In both cases, i.e., the

constant-potential as well as the constant-charge approach, Equation 2.6 can be solved numerically for a specific set of input values. Consequently, no unique u-d-relationship exists in case of interacting double-layers, which is an essential drawback when using DDL theory for estimating clay volumetric behaviour. In case of weak surface interaction, i.e., at large surface separations or high concentrated bulk solution, van Olphen (1963) suggested to calculate the midplane potential by summation of the potentials of two single DDLs at the midplane, i.e., $u = 2y_{(x=d)}$. However, for conditions relevant in geotechnical engineering, this approach is invalid. To overcome this limitation, Tripathy et al. (2004) proposed to establish an empirical u-$\ln(\kappa d)$ relationship for the individual clay mineral-water system conditions on the basis of selectively conducted numerical calculations for various sets of values. More recently, Bharat et al. (2013) introduced an empirical relationship between the midplane potential calculated for interacting and single double-layers, respectively. Based on parameter variations of the clay mineral-water system conditions conducted in the same study, it was concluded that the following relationships are unique and apply independently on these conditions:

$$\Psi'_d = -6.24 \cdot 10^{-1}\Psi'^2_{x=d} + 1.205\Psi'_{x=d} + 8.582 \cdot 10^{-3} \tag{2.8}$$

$$\Psi'_{x=d} = 5.62 \cdot 10^{-1}\Psi'^2_d + 0.7934\Psi'_d - 6.1507 \cdot 10^{-3} \tag{2.9}$$

Where $\Psi'_{x=d}$ (V) is the electric potential of a single double-layer at distance d from the clay mineral surface and Ψ'_d (V) is the midplane potential between two interacting clay mineral surfaces separated by distance $2d$.

According to Bolt (1956), the repulsive pressure acting between two parallel clay mineral surfaces equals the difference between the osmotic pressure in the midplane and the bulk solution. He adopted the Van't Hoff equation in order calculate the difference in osmotic pressure by means of the local ion concentration in the midplane and bulk solution, respectively. Since by Boltzmann's equation the ratio of local and bulk ion concentration in the midplane is a function of the midplane potential, Ψ'_d, and thus, the midplane potential function, u, the following equation can be used to calculate the repulsive pressure, p (N/m^2), due to interacting double-layers (Sridharan & Jayadeva 1982):

$$p = 2n_0k'T(\cosh(u) - 1) \tag{2.10}$$

Limitations of diffuse double-layer theory

It was shown by several researchers that by use of the above equations macro-scale clay volumetric behaviour can be calculated quite accurately (e.g., Madsen & Müller-Vonmoos 1985, Sridharan & Jayadeva 1982, Bolt 1956). However, there are also several well known limitations when using this kind of multiscale approach with respect to both, theoretical as well as practical aspects:

Theoretically, the Gouy-Chapman relationship represents only one of the acting mechanisms between two charged surfaces. In addition, long-range attractive secondary valency forces, i.e., London-van der Waals forces, as well as Born's repulsion between surfaces have to be considered. With respect to the former mechanism, its nature can be explained by the mutual influence of temporary dipoles due to charge fluctuation, whereas the latter mechanism arises from the overlapping of electron shells. In consequence, dipole-dipole attraction as well as ionic repulsion between surfaces occur. With respect to their influence on clay volumetric behaviour, it was shown that London-van der Waals forces start to overcome repulsive forces by DDL overlapping first when surface separations become smaller than 1.25 Å (divalent exchangeable cations) and 0.75 Å (monovalent exchangeable cations), respectively. Also, Born's repulsion starts to become relevant when surface separations become smaller than 1.5 Å (Tripathy et al. 2006). Another aspect of importance refers to the fact, that in theory, ions are assumed to be point charges, whereas in fact, they have a finite dimension. Consequently, at a very small distance to the charged surface, calculated ion concentrations from DDL theory significantly exceed the maximum ion concentration, which is feasible with respect to their size ratio. To overcome this limitation, the 'Stern'-layer (Stern 1924) was introduced, in which a defined amount of counterions is tightly adsorbed to the charged surface. This layer is followed by the diffuse part of counterions corresponding to DDL theory. It was shown by Tripathy et al. (2013) that incorporation of the Stern-layer improves the agreement between theoretical and experimental data on clay volumetric behaviour in terms of both, underestimated repulsive pressure at small surface separations as well as overestimated repulsive pressure at medium surface separations as obtained by DDL theory alone. Thereby, it has to be noted that the approach of constant surface potential has been adopted. The approach of constant surface charge, on the other hand, was found to result in a permanent increase of the electric potential at any distance to the clay mineral surface (Sridharan & Satyamurty 1996). However, in Figure 2.14 typical distributions of ions and the electric potential as a function of distance to single clay mineral surfaces based on DDL theory and considering the Stern-layer are illustrated.

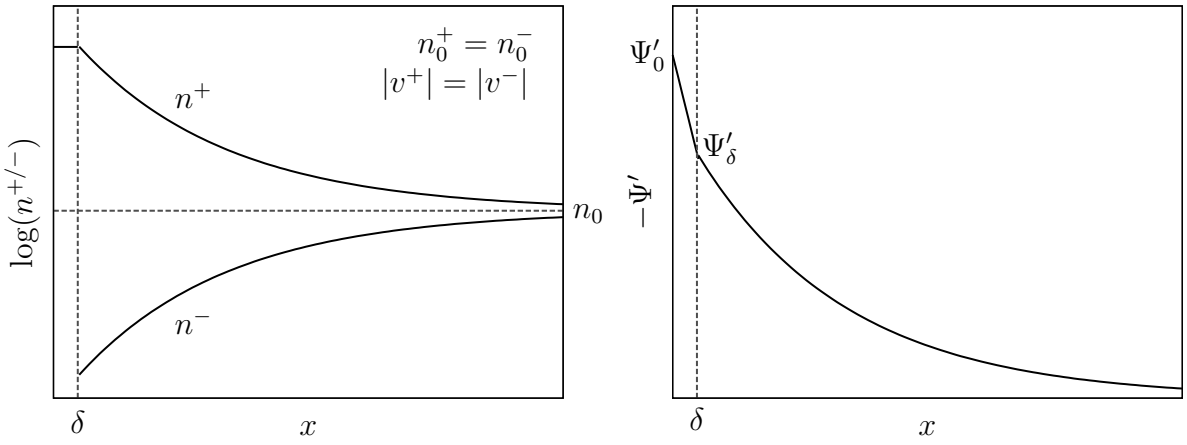

Figure 2.14: Typical distributions of cation (+) and anion (-) concentration (a) and the electric potential (b) as a function of distance to clay mineral surfaces according to Gouy-Chapman diffuse double-layer theory considering Stern-layer of thickness δ.

In addition to theoretical advancements improving the accuracy of DDL theory in estimating clay volumetric behaviour, also practical aspects of the clay mineral-water system differing from the underlying assumptions in theory have to be considered. Thereby, deviations generally refer to clay homogeneity: (i) the clay is considered to be composed of one single type of clay minerals (homomineralogic clay); (ii) the layer charge of clay mineral layers is supposed to be homogenously distributed; (iii) exchangeable cations are assumed to be of a single species (homoionic clay); (iv) clay mineral layer basal surfaces are considered to be perfectly parallel oriented; (v) basal surfaces of clay mineral layers are assumed to have an infinite dimension, i.e., clay mineral layer edges are neglected.

However, in spite of the above mentioned limitations by the use of DDL theory for estimating clay volumetric behaviour, practically, theoretical and experimental data are in quite good agreement for a wide range of surface separations relevant in the geotechnical context. Even in case of compacted clays, i.e., when deviations from perfectly parallel clay mineral surface orientation play a major role, theoretical calculations give an acceptable approximation of the actual macro-scale clay volumetric behaviour (e.g., Tripathy et al. 2004, Pusch 1982).

Diffuse double-layer theory considering polymer adsorption

From experimental studies on the electrophoretic mobility of charged particles in colloidal dispersions, it was found that due to the adsorption of non-ionic polymers on their surfaces the zeta-potential increases (e.g., Kavanagh et al. 1975). This phenomenon was theoretically discussed by Brooks (1973) and the author proposed a modified Boltzmann equation for charged surfaces having neutral adsorbed polymer layers. According to this modification, the fundamental differential equation of the diffuse double-layer (Equation 2.1) reads:

$$\frac{d^2\Psi'}{dx^2} = \left(\frac{2n_0\nu e'}{\epsilon}\right)\sinh\left(\frac{\nu e'\Psi'}{k'T} - \beta(x)\right) \tag{2.11}$$

with:

$$\beta(x) = (\phi_p(x) - \phi_{pb}) \cdot (1 - \chi_{sp} + \chi_{ip} - \chi_{si}) \tag{2.12}$$

where ϕ_p (-) is the volume fraction occupied by polymer, the subscript b refers to the bulk phase, χ (-) is the interaction parameter between two components and the subscripts s, p and i refer to the solvent, polymer and dissociated ions, respectively. Qualitatively, the influence of polymer adsorption, i.e, $\beta(x)$, increases with increasing difference in polymer volume fraction between adsorbed and bulk state as well as with increasing interaction of polymer and ions with the solvent and decreasing interaction between polymer and ions. In order to solve the nonlinear Equation 2.11 Brooks (1973) introduced a simplified form:

$$\frac{d^2\Psi'}{dx^2} = \left(\kappa e^{(-\beta(x)/2)}\right)^2 \Psi'(x) \tag{2.13}$$

With this approximation the decay of the potential with distance from the surface becomes purely exponential, which is valid for small surface potentials, i.e., $\Psi'_0 << \pm 25$ mV (van Olphen 1963).

Since one of the main challenges is the quantification of ϕ_p with distance, i.e., the geometrical arrangement of adsorbed polymers in trains loops and tails, Brooks (1973) proposed to solve Equation 2.13 by a step function with $\phi_p(x) = \phi_p$ for $0 \leq x \leq d_p$ (region 1) and

$\phi_p(x) = \phi_{pb}$ for $d_p < x$ (region 2), where d_p (m) is the thickness of the adsorbed polymer layer. Consequently, $\beta(x) = \beta$ in region 1 and $\beta(x) = 0$ in region 2. By use of the boundary conditions that for

(1) $x = 0$: $(d\Psi'/dx)_1 = -\sigma/\epsilon$ (according to Equation 2.5),

(2) $x = d_p$: $\Psi'_1 = \Psi'_2$ and $(d\Psi'/dx)_1 = (d\Psi'/dx)_2$,

(3) $x = \infty$: $\Psi'_2 = 0$ and $(d\Psi'/dx)_2 = 0$

the following expressions for the electric potential as a function of distance to a charged surface were derived (Brooks 1973):

$$\Psi'_1(x) = \left(\frac{\sigma}{\kappa_\beta \epsilon}\right)\left(\frac{\sinh\left(\kappa_\beta(d_p - x)\right) + e^{(-\beta/2)}\cosh\left(\kappa_\beta(d_p - x)\right)}{e^{(-\beta/2)}\sinh\left(\kappa_\beta d_p\right) + \cosh\left(\kappa_\beta d_p\right)}\right) \tag{2.14}$$

$$\Psi'_2(x) = \left(\frac{\sigma}{\kappa\epsilon}\right)\left(\frac{e^{(-\kappa(x-d_p))}}{e^{(-\beta/2)}\sinh\left(\kappa_\beta d_p\right) + \cosh\left(\kappa_\beta d_p\right)}\right) \tag{2.15}$$

with:

$$\kappa_\beta = \kappa e^{(-\beta/2)}$$

With respect to the proposed approach, it has to be noted that Brooks (1973) referred to colloidal dispersions composed of biological cells rather than clay minerals. Thereby, the surface charges, σ, differ significantly for both types of solids, for which reason the proposed simplified form of the differential equation for the diffuse double-layer, i.e., Equation 2.13, becomes invalid for conditions present at clay mineral surfaces (van Olphen 1963).

2.4.2 Cluster model

The Kozeny-Carman equation (Kozeny 1927, Carman 1937) is widely accepted for calculating the hydraulic permeability of soils (Mitchell & Soga 2005). By this approach, geometrical characteristics of the flow path as well as physical properties of the fluid are considered since it is based on Poiseuille's law for fluid flow through a round capillary. The

resulting equation reads as follows:

$$k_{KC} = \frac{\gamma}{\eta} \frac{1}{k_0 t^2 {S_0}^2} \frac{e^3}{1+e} \tag{2.16}$$

where k_{KC} (m/s) is the hydraulic permeability according to Kozeny-Carman approach, γ (N/m^3) and η (Ns/m^2) are the specific gravity and viscosity of the fluid, respectively, k_0 (-) and t (-) are the pore shape and tortuosity factor, respectively, S_0 (1/m) is the specific surface area of solids and e (-) is the total void ratio.

As pointed out in subsection 2.3.3, the hydraulic permeability of clays depends significantly on the clay fabric, i.e., on the type of PSD. Since bimodal PSDs, which prevail in aggregated and flocculated clay fabrics, cannot be reproduced by Kozeny-Carman equation, Olsen (1962) introduced an advanced approach valid for calculating the hydraulic permeability of clays. Thereby, additional geometrical characteristics of the clay pore system having bimodal PSDs are taken into account in order to express the deviation of effective flow rate from calculations based on Kozeny-Carman approach, which is valid for unimodal PSDs only. In the model, namely cluster model, the total void ratio is divided into two main groups of voids, i.e., the inter-cluster and intra-cluster voids, respectively, with clusters corresponding to aggregates (see Figure 2.9). It was concluded from experimental data that at high total void ratios only the inter-cluster voids change with varying total void ratio. Since fluid flow is exclusively controlled by this type of voids, the decrease in hydraulic permeability with decreasing total void ratio is more rapid than predicted by Kozeny-Carman equation. At low total void ratios intra-cluster voids start to change as well with varying total void ratio. Since fluid flow is still controlled by inter-cluster voids hydraulic permeability decreases less rapid than predicted by Kozeny-Carman equation. In order to express this behaviour theoretically, Olsen (1962) introduced the following equation:

$$\frac{k_{CM}}{k_{KC}} = N^{2/3} \frac{(1 - e_c/e_t)^3}{(1+e_c)^{4/3}} \tag{2.17}$$

where k_{CM} (m/s) is the hydraulic permeability according to cluster model, N (-) is the number of particles per cluster, e_c (-) is the intra-cluster void ratio and e_t (-) is the total void ratio.

The assumptions on the development of inter- and intra-cluster void ratios with varying total void ratio are illustrated in Figure 2.15. It is obvious that in its original form, cluster

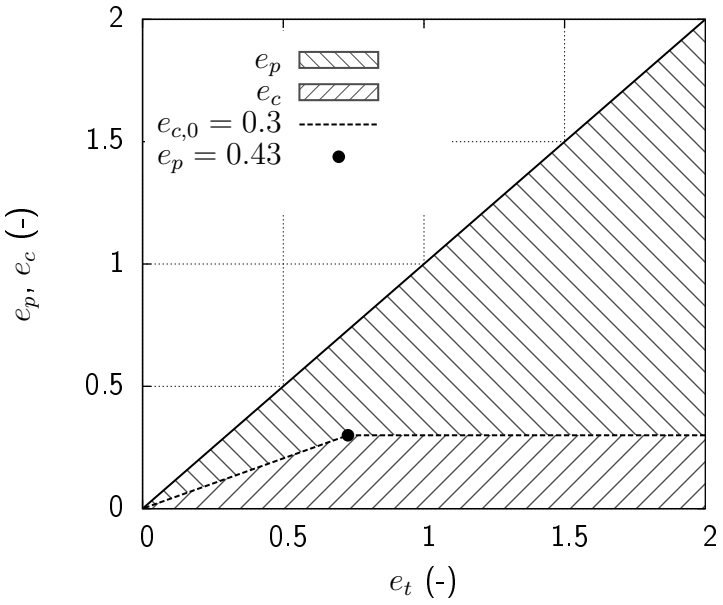

Figure 2.15: Development of inter- (e_p) and intra-cluster void ratio (e_c) with varying total void ratio (e_t) according to cluster model. Exemplary, an initial intra-cluster void ratio ($e_{c,0}$) of 0.3 is illustrated.

model implies that intra-cluster voids participate in total void ratio changes in case of inter-cluster void ratio ≤ 0.43. In this region, changes in the inter- and intra-cluster void ratios occur lineary with varying total void ratio. Advanced considerations on inter- and intra-cluster void ratio development with varying total void ratio in case of swelling clays were introduced by Achari et al. (1999) calculating the intra-cluster void ratio on the basis of DDL theory.

2.5 Clay-polymer composites for application in geotechnical and geoenvironmental engineering

2.5.1 General

It has been pointed out in section 2.3 that clay macro-scale behaviour and thus, the engineering properties, can be attributed to the micro-scale characteristics, i.e., the clay fabric, resulting from interparticle forces and external loading conditions. Since in this context,

the clay mineral surface-water interaction is of great importance, attempts have been made on the modification of the clay mineral surface-water interface, e.g., by complexation of clay minerals with organic compounds. Doing so, manipulation of the clay macro-scale properties with relevance in geotechnical and geoenvironmental engineering was enabled. For several applications the high potential of such composites has been shown with great success.

One of the most promising focus to date is on the modification of bentonite, i.e., a natural clay mixture dominated by interlayer swelling clay mineralogies, in order to stabilize its sealing capacity, e.g., in landfill lining, even when permeated with chemically aggressive electrolytes. Another promising application refers to soil conditioning in tunneling in order to modify adhesive properties of clays, i.e., to gain reduced adhesion on steel surfaces while maintaining inner strength properties. Most recently, polymer treatment as a method to reduce volume change of expansive clays has also become of growing interest.

In the following, clay-polymer composites for application in landfill technology, i.e., the hydraulic barrier performance of bentonite and bentonite-polymer composites, are focused.

2.5.2 Bentonite as hydraulic barrier material for geoenvironmental applications

Current technologies of clay based barriers in landfill lining prefer the application of geosynthetic clay liners (GCLs), which are composed of a thin layer of bentonite sandwiched between geotextiles or geomembranes. Thereby, the bentonite controls the hydraulic permeability of the system, whereas the geotextiles fulfill the constructive demands. Generally, the use of sodium bentonites, i.e., the exchangeable cations of the interlayer swelling clay minerals are dominated by sodium, is preferred since fluid flow is inhibited most effectively due to the physico-chemical clay mineral surface characteristics.

One of the most prominent problems occurring in geoenvironmental practice when using GCLs arises from cation exchange processes when the bentonite comes into contact with the leachate. Thereby, monovalent exchangeable sodium cations become preferentially replaced by di- and trivalent cations (for details see subsubsection 2.2.1.1). In consequence, clay mineral surface repulsion due to DDL overlapping decreases and surfaces tend to approach and form aggregates. By this modification of the physico-chemical clay mineral

surface characteristics, the originally dispersed clay fabric with an unimodal PSD becomes aggregated with a bimodal PSD and thus, large inter-aggregate pores promoting fluid flow (see subsection 2.3.3). It was found by several researchers that the macro-scale effect due to cation exchange processes, i.e., the increase in hydraulic permeability, can be kept to a minimum when the bentonite is prehydrated with deionized water before coming into contact with the leachate (e.g., Shackelford et al. 2000, Jo et al. 2004). Thereby, in case of previous clay fabric dispersion, i.e., in case of prehydrated bentonite, subsequent clay fabric aggregation in consequence of cation exchange is restricted rather than the cation exchange process itself. This phenomenon is illustrated in Figure 2.16.

Other factors influencing hydraulic GCL performance refer to pH and electrolyte concentration conditions of the leachates as well as to cracking mechanisms due to to desiccation of the bentonite layer (e.g., Shackelford et al. 2000, Albrecht & Benson 2001, Jo et al. 2005). Generally, special attention is turned on the long-term material behaviour since the reliability of GCL hydraulic barrier performance is of major importance in geoenvironmental practice.

2.5.3 Bentonite-polymer composites as hydraulic barrier material for geoenvironmental applications

The use of organic compounds to form complexes with clay minerals has been referred to geoenvironmental applications first by Kondo (1996) presenting a composite, which is dominantly composed of montmorillonite and highly polar propylene carbonate monomers termed 'multiswellable bentonite' (MSB). Several studies illustrated its modified swelling characteristics and hydraulic barrier performance under varying environmental conditions, i.e. ionic concentration and valence of cations in the permeant (e.g., Onikata et al. 1999, Katsumi et al. 2007). It was shown that MSB hydraulic permeability remained nearly unaffected even in case of permeation with 1.0 molar $NaCl$- and $CaCl_2$-solution as well as under long-term conditions. It is supposed that osmotic swelling in MSB appears up to higher electrolyte concentrations in the bulk fluid and thus, inhibits fluid flow under these conditions. Other approaches focus complexes composed of bentonites and anionic polymers. The resultant composites are termed 'HYPER clay' ´(Di Emidio et al. 2011) and 'bentonite-polymer nanocomposite' (BPC) (Scalia et al. 2014). Thereby, the former is composed of 2 wt% carboxymethylcellulose mixed with bentonite by *solution intercalation*, i.e., clay and

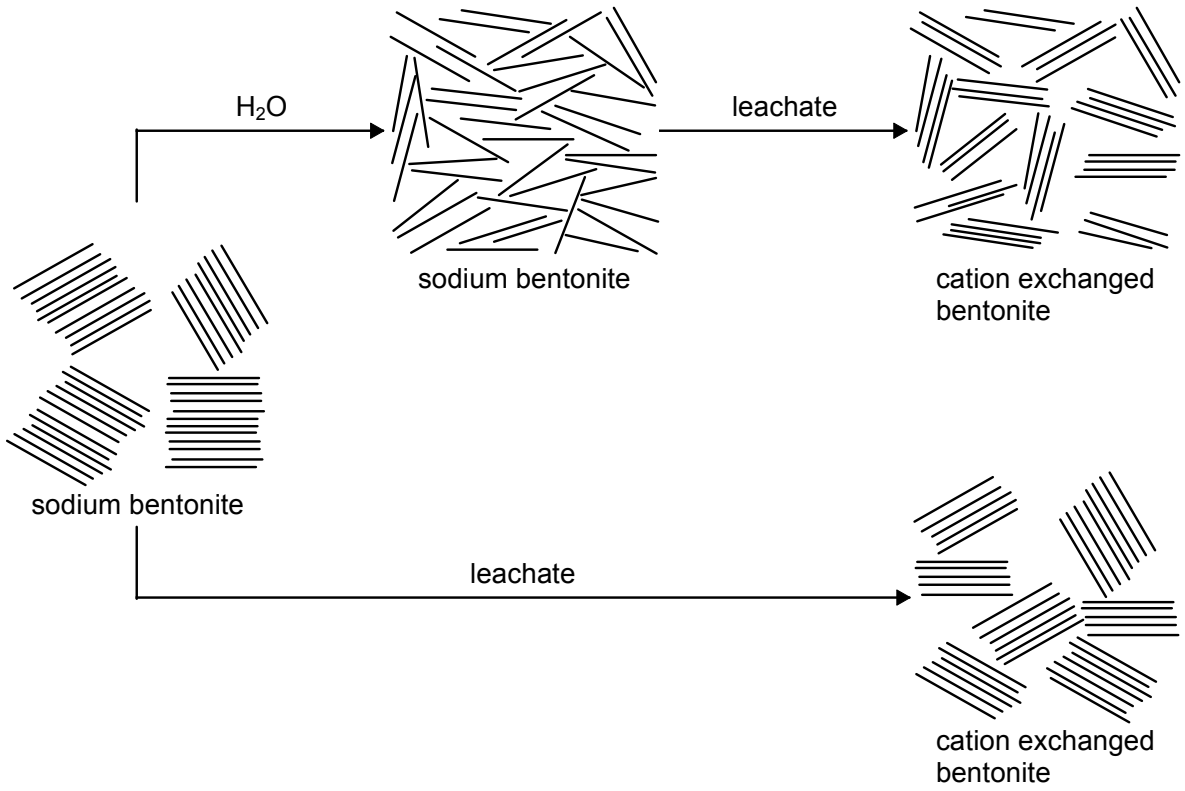

Figure 2.16: Development of bentonite fabric due to cation exchange processes with (top) and without (bottom) prehydration.

polymer are mixed in dispersion, whereas the latter is composed of 50 wt% polyacrylate mixed with the bentonite by *in situ polymerization*, i.e., clay and polymer monomers are mixed in dispersion followed by polymerization of monomers. BPC has been characterized comprehensively in the literature with respect to its hydraulic barrier performance under chemical aggressive, i.e., electrolyte concentration and pH, as well as long-term conditions, showing its excellent barrier performance (e.g., Bohnhoff & Shackelford 2014). Generally, anionic polymer addition was interpreted to inhibit fluid flow by clogging pores (Scalia et al. 2014) and altering the clay fabric due to particle bridging (Di Emidio et al. 2011). Similar interpretation is given in (Razakamanantsoa et al. 2012), where reduced hydraulic permeabilities were obtained when mixing 2 wt% of an unspecified anionic polymer with calcium activated bentonite in the dry state, i.e., by *dry powder mixing*. However, detailed investigations on the underlying mechanisms are lacking throughout the literature.

The results clearly illustrate that polymer modification of bentonites is a promising method and beneficial alternative to conventional methods on bentonite stabilization in landfill

technology, such as prehydration and activation. However, in contrast to the above materials, Ashmawy et al. (2002) illustrated the incapability as well as existing limitations, e.g., threshold electrolyte concentration or pH, of several commercially available bentonite-polymer composites. Since specific information on the materials used and mixing procedures adopted were lacking, the mechanisms and principles determining composite hydraulic performance were not interpreted.

2.6 Summary

The fundamentals of clays and clay-polymer composites relevant to this study were given. The clay mineralogical basics as well as the interaction mechanisms with water and polymers were outlined. Thereby, the importance of interlayer swelling clay mineralogies with respect to both, the adsorption of water and polymers, has been pointed out. On this basis, the micro-scale characteristics in terms of the clay and composite fabric resulting from interparticle forces and external loading conditions were discussed. Further, clay macro-scale properties in terms of the volumetric behaviour and the hydraulic permeability were summarized. Thereby, established phenomenological multiscale coupling phenomena governing clay behaviour were addressed and introduction was given to theoretical approaches on the multiscale behaviour, i.e., diffuse double-layer theory and cluster model. With respect to the former, an advanced model considering adsorbed neutral polymer layers on charged surfaces has been introduced. Thereby, its limitation in the present form with respect to clay mineral surface conditions has been pointed out. Finally, the current status of clay-polymer composites for application in geotechnical and geoenvironmental engineering was summarized. Thereby, special attention was turned on the hydraulic barrier performance of bentonite-polymer composites in landfill lining highlighting their great potential as well as the lack of knowledge on the governing mechanisms improving barrier performance.

3 Materials and methods

3.1 General

In the following chapter the research program of the study as well as the main properties of the materials used and methods adopted are introduced. Thereby, the mineralogical and soil mechanical classification of clays, the physical and chemical characteristics of polymers as well as the preparation and initial conditions of their respective composites are summarized. Further, the experimental methods for the determination of micro- and macro-scale clay-polymer composite behaviour are outlined. These include the determination of polymer adsorption characteristics by means of the adsorption isotherms as well as the determination of clay and composite fabric, plastic properties, volumetric behaviour, hydraulic permeability and water retention. In addition, the individual procedures and parameter sets used for the theoretical analysis of clay-polymer composite multiscale behaviour are summarized. Finally, the experimental procedures for investigating the hydraulic barrier performance of bentonite-polymer composites for application in geoenvironmental engineering by means of the hydraulic permeability as well as the liquid limit and swelling behaviour are outlined.

3.2 Research program

This research aims on the fundamental understanding of the mechanisms determining the hydro-mechanical behaviour of clay-polymer composites in order to illustrate their potentials and limitations with respect to the geotechnical and geoenvironmental practice and thus, enable their efficient and reliable application.

Therefore, in a first approach, i.e., the *multiscale approach*, systematic variations in the

constitutive physical and mineralogical properties combined with the experimental multi-scale analysis of composites form the basis. Additionally, by means of the experimental test results, the validity of theoretical models characterizing clay-polymer composite multiscale behaviour is examined. Thereby, one of the main objectives is to identify the governing micro- and macro-scale coupling phenomena.

In a second approach, i.e., the *application-oriented approach*, the hydraulic barrier performance of bentonite-polymer composites for application in landfill lining is explicitly addressed. Thereby, material and experimental boundary conditions cover the appropriate issues of practical demands with respect to geoenvironmental practice.

In Figure 3.1 the research program is illustrated showing the individual working steps as well as their relationships among each other. Details on the respective working steps are summarized in the following sections.

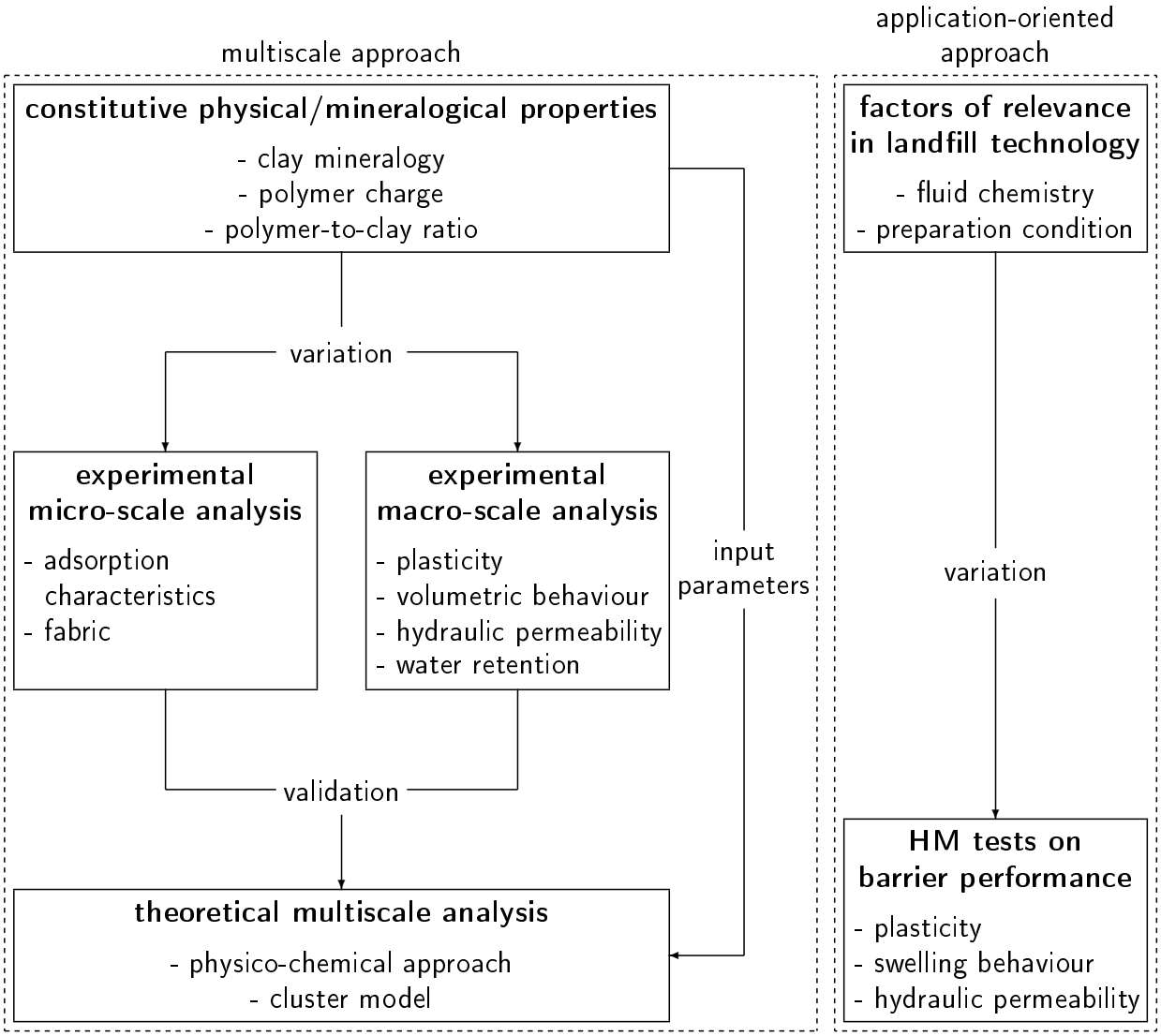

Figure 3.1: Flow chart showing the organization of the research program.

3.3 Clays, polymers and clay-polymer composites

Clays

Three different types of raw clays are used to form clay-polymer composites. From literature review it is known that clay-polymer interaction occurs most distinctive in case of interlayer swelling clay mineralogies and varies significantly with the valence of predominant exchangeable cations. Therefore, two types of montmorillonite-rich clays exhibiting predominantly mono- and divalent exchangeable cations, respectively, are selected, i.e., MX 80 and Calcigel bentonite. Additionally, a kaolinite-rich clay, i.e., Spergau kaolin, is selected having minor interaction with both, water and polymer. Their basic properties are summarized in Table 3.1. Thereby, the cation exchange capacity, CEC (meq/g), was obtained from Cu-Triethylenetetramine method according to (Meier & Kahr 1999); specific gravity, G (-), was determined by use of pycnometer method according to (ASTM D854-14 2014) with kerosene as recommended by Head (2006); liquid limit, w_l (%), and plastic limit, w_p (%), were determined according to (ASTM D4318-10e1 2010); shrinkage limit, w_s (%), was determined according to (ASTM D4943-08 2008) modified by use of fluid displacement method for volume measurement with kerosene as recommended by Péron et al. (2007). Information on the respective main mineral as well as the specific surface area (SSA), S (m^2/g), were adopted from the given references. In the following, the general terms 'Na^+-bentonite, Ca^{++}-bentonite and kaolin' are used when referring to the special types of clay used, i.e., MX 80 bentonite, Calcigel bentonite and Spergau kaolin, respectively, since by these terms the constitutive properties of clays are covered.

Polymers

The polymers used are high molar mass polyacrylamides differing in their charge characteristics, i.e., non-ionic polyacrylamide (PAA^o) in a homopolymer form as well as cationic (PAA^+) and anionic (PAA^-) polyacrylamides in a co-polymer form. Their structural formulae are illustrated in Figure 3.2 and their basic physical properties are summarized in Table 3.2. Since polyacrylamides are widely used in the research on clay mineral-polymer complex formation (e.g., Deng et al. 2006, Laird 1997, Schamp & Huylebroeck 1973, Espinasse & Siffert 1979), the novel approach on multiscale analysis can rely on previous findings in the colloid chemical context, which are beyond the scope of this study.

Clay-polymer composites

With respect to the multiscale approach, clay-polymer composites are prepared by solu-

Table 3.1: Basic properties of clays.

	MX 80 bentonite	Calcigel bentonite	Spergau kaolin
main mineral	montmorillonite*	montmorillonite*	kaolinite**
CEC (meq/g)	0.81	0.65	0.07
(Na^+,K^+,Mg^{++},Ca^{++})	(57,1,5,23)	(2,1,19,35)	(0,0,1,5)
S (m^2/g)	676***	651****	28**
G (-)	2.60	2.60	2.63
w_l (%)	588	109	51
w_p (%)	37	33	32
w_s (%)	14	13	30

*(Madsen 1998); **(Baille 2014); ***(Tripathy et al. 2013); ****(Agus 2005)

Table 3.2: Basic properties of polymers.

	PAA^+	PAA^o	PAA^-
charge	cationic	non-ionic	anionic
ionicity, I (mol-%)	40	-	40
molar mass (10^7 g/mol)	0.75	1.0	1.6

tion intercalation in order to enable distinct interaction between clay mineral surfaces and polymers. Thereby, the polymer-to-clay ratio is chosen so that the individual maximum adsorption capacity, q_{max} (mg/g), is reached. In addition, Ca^{++}-bentonite-polymer composites are also prepared with a polymer-to-clay ratio of 10% of q_{max}. In order to derive these values adsorption isotherms of each clay-polymer combination are experimentally determined in advance (see section 4.2). From literature review it is known that in addition to the individual clay and polymer characteristics, e.g., mineralogy, polymer charge, polymer chain length, the boundary conditions during solution intercalation process, e.g., temperature, pH, clay concentration, are of great importance in the adsorption process. Therefore, in the present study, the boundary conditions during adsorption tests and composite preparation are kept constant for each of the composites. Detailed information on the conditions adjusted in the present study are given in the following subsection subsection 3.4.1.

With respect to the application-oriented approach, the preparation method to form clay-polymer composites is varied since solution intercalation is a rather laborious method and thus, expensive in large-scale applications. Thus, in accordance to practical demands,

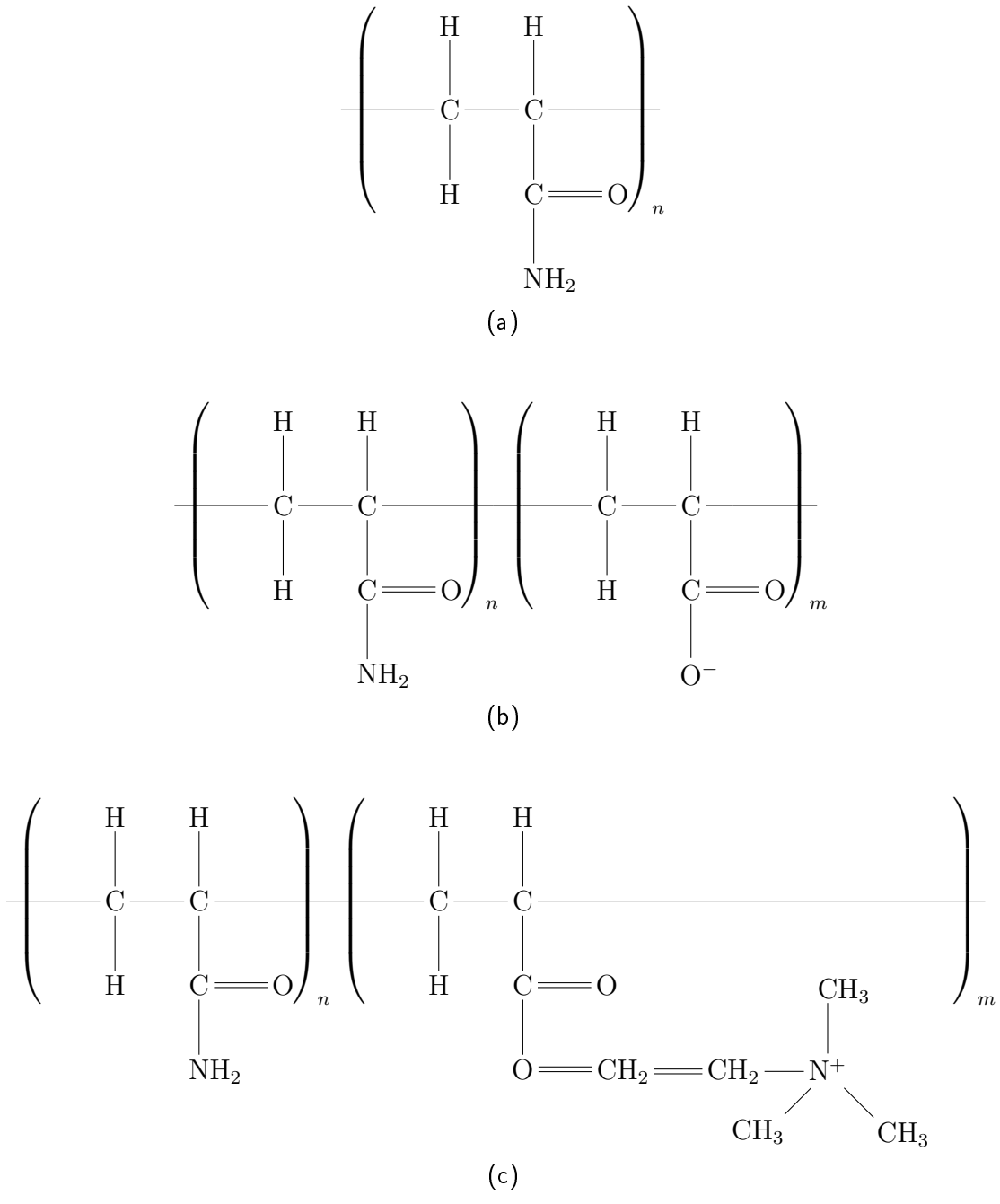

Figure 3.2: Structural formulae of polymers: non-ionic polyacrylamide (a); anionic acrylamide-acrylic acid co-polymer (b); cationic acrylamide-methylated dimethylaminoethyl acrylate co-polymer (c).

composites are additionally prepared by dry powder mixing in order to investigate the macro-scale effect of established preparation methods. The polymer-to-clay ratio is chosen to correspond to the value of 1%, which is in the same order magnitude of composites used in the literature in the geoenvironmental context (e.g., Razakamanantsoa et al. 2012, Di Emidio et al. 2011). Composites are prepared with Na^+-bentonite only since this type of clay is commonly used in GCL's, as well as with PAA^+ and PAA^- polymers, respectively.

Initial conditions of clays and clay-polymer composites

Clays and polymers are available as powders with their individual hygroscopic water contents. For adsorption tests, pre-treatment of raw materials is explained in detail in subsection 3.4.1. For fabric investigation as well as hydro-mechanical testing within the framework of the multiscale approach, pure clay and clay-polymer composites are prepared to slurry conditions, i.e., 1.1 times the individual liquid limit of clays and composites. With this initial condition, clay micro-fabric develops as a direct consequence of interaction between clay mineral-surfaces, polymers and water at approximately zero external hydraulic and mechanical loading conditions. The influence of polymer adsorption on clay mineral surfaces on the micro- and macro-scale behaviour is thus, represented most accurately. With respect to the application-oriented approach, pure Na^+-bentonite as well as Na^+-bentonite-polymer composites are compacted to proctor density of the pure bentonite, i.e., $\rho_{opt} = 1.15$ g/cm^3 with the corresponding water content, w_{opt}, of 35.4%. Compaction test results are summarized in Figure 3.3.

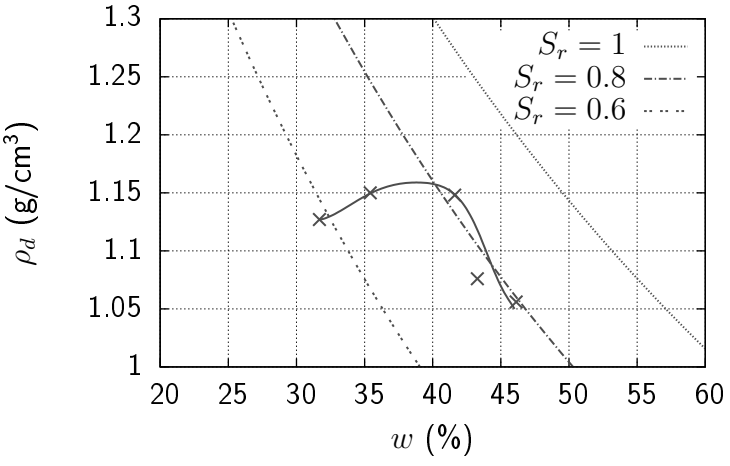

Figure 3.3: (Standard) proctor curve of Na^+-bentonite used in this study.

3.4 Experimental methods

3.4.1 Micro-scale analysis

Adsorption characteristics

The experimental procedure and boundary conditions of composite formation using solution intercalation are as follows (for schematic illustration, see Figure 3.4): Polymer adsorption is performed in a constant laboratory environment under a controlled temperature of 20°C. Clays and polymers are mixed with deionized water at pH 6.1 separately until complete dispersion (clays) and solution (polymers) is reached. Dispersions and solutions of clays and polymers are mixed together and stirred for 24 hours as the adsorption process is almost completed within this period (Greenland 1963, Schamp & Huylebroeck 1973). Clay concentrations in this step are chosen to correspond to tenfold their individual liquid limits. Polymer concentration is stepwise increased with each test in order to determine the individual relationship between adsorbed polymer mass and polymer concentration in solution at equilibrium. After adsorption, the clay-polymer dispersions are centrifuged at 4,000g for 30 min. The supernatant is analyzed for total organic carbon (TOC) to determine polymer concentration in solution after adsorption and thus, to derive the amount of polymer adsorbed on the sedimented clay. Thereby, analysis of TOC is performed by photometric measurement using standard cuvette tests. The individual relationships between TOC and PAA^{+}-, PAA^{o}- and PAA^{-}-concentration, respectively, are determined in advance and illustrated in Figure 3.5.

Fabric

Clay and composite fabrics prepared with a polymer-to-clay ratio of q_{max} are investigated using Environmental Scanning Electron Microscopy (ESEM). By use of this special mode of Scanning Electron Microscopy (SEM), the sample is placed in the pressure chamber at low vacuum conditions as against high vacuum conditions, which are adjusted in case of classical SEM in order to detect most accurate signals. As a result, ESEM enables the investigation of samples, which are equilibrated at various relative humidities of the gaseous environment and thus, having various water contents. Additionally, sample artifacts are kept to a minimum since the preparation of non-conductive materials, such as clay minerals, with a conductive coating in order to prevent charging of the sample surface isn't necessary. On the other hand, image resolution is restricted by use of this mode since numerous

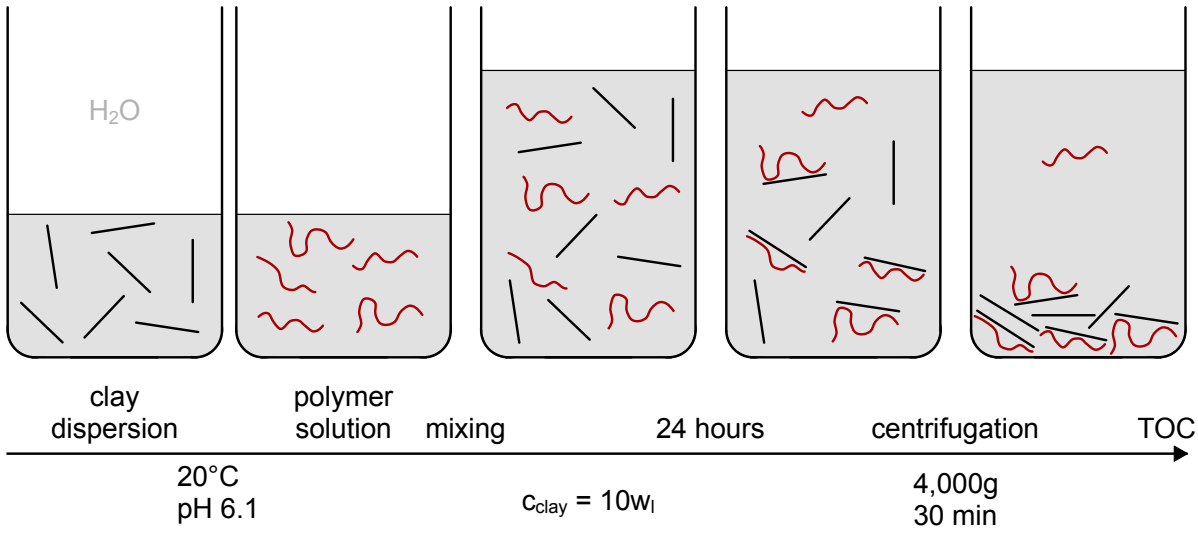

Figure 3.4: Illustration of the experimental procedure and boundary conditions for the determination of adsorption isotherms.

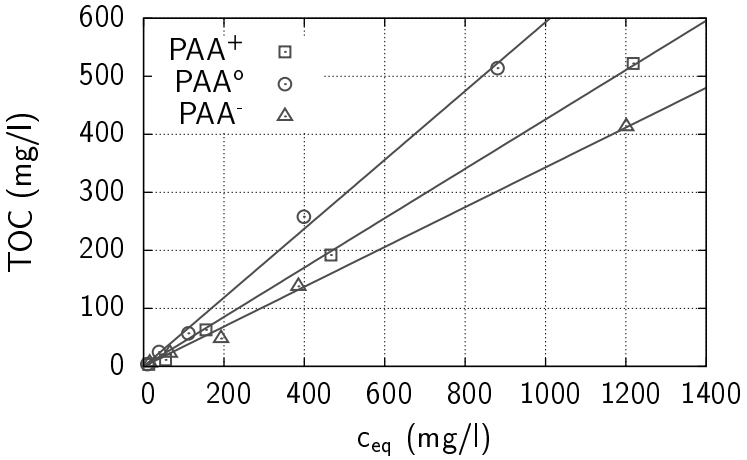

Figure 3.5: Established relations between TOC and polymer concentration for the polymers used.

collisions of electrons and water molecules in the gaseous environment occur, lowering the accuracy of detected signals.

The following conditions are chosen for sample analysis using ESEM: Clay and composite slurries are equilibrated in the pressure chamber at relative humidities of 90-95% by adjusting the temperature and chamber pressure to approximately 2°C and 6.5 mbar, respectively; the electron beam scanning the sample surface is accelerated with an electrical potential of 30 kV; the 2D surface plot of clay and composite samples is generated by detection of secondary electrons, i.e., electrons, which are bounced out from the respective position on the sample surface due to collisions with accelerated primary electrons of the electron beam.

3.4.2 Macro-scale analysis

Plasticity

Clay and composite liquid limits, w_l (%), and plastic limits, w_p (%), are determined according to (ASTM D4318-10e1 2010). For the determination of shrinkage limits, w_s (%), the procedure described in (ASTM D4943-08 2008) is modified by the use of fluid displacement method with kerosene for sample volume measurements as described in (Péron et al. 2007). For the calculation of water contents based on sample volume measurements, water densities are assumed to deviate from 1 g/cm^3 according to (Martin 1960). A summary of water densities depending on the respective mineralogy as well as clay water content as adopted in the present study are given in Table 3.3. Interim values are interpolated linearly.

Oedometer tests

Oedometer tests involve investigation of the materials in terms of their volumetric behaviour and hydraulic permeability. The prepared samples are 70 mm in diameter and 19 mm in height. Vertical loads are applied from 2 (seating load) to 800 kPa followed by unloading from 800 to 25 kPa. Compression and decompression indices, C_c (-) and C_s (-), respectively, are determined along e-$log(p')$ relationships, where e (-) is the void ratio and p' (kPa) is the applied vertical pressure. For each stress increment along the loading path, the corresponding coefficient of consolidation, c_v (m^2/s), is calculated according to Casagrande $log(t)$-method. Subsequently, the hydraulic permeability, k (m/s), is computed from the value of c_v and the coefficient of volume compressibility, m_v (m^2/kN).

Table 3.3: Water densities, ρ_w (g/cm^3), of pore water in clays according to Martin (1960).

w (%)	montmorillonite	kaolinite
0.4		1.68
0.8		1.12
0.9		1.03
6.5		0.99
11.6	1.41	
16.6	1.37	
28.4	1.32	
46.0	1.16	
244.0	1.02	
301.0	1.02	

Water retention tests

Clays and clay-polymer composites are investigated in terms of their water retention behaviour under unconfined conditions (i) along the first drying curve, i.e., from zero to 350 MPa suction and (ii) along the subsequent (scanning) wetting curve, i.e., from 350 to 0.1 MPa suction. Application of suction to the samples is achieved using osmotic method (OM) (drying) as well as axis translation technique (ATT) (wetting) in the low suction range, i.e., from 0.1 to 10 MPa, and vapour equilibrium technique (VET) in the high suction range, i.e., from 2.5 to 350 MPa. The summary of suction steps applied to the samples is given in Table 3.4. Thereby, each suction step is performed as single step suction application test.

Application of the various techniques is chosen for practical reasons, although it is known, that the osmotic component of total suction in the pore water is assumed to remain unaffected in the OM and ATT, whereas it is affected in the VET. However, in (Tripathy et al. 2014) it is shown that differences in the results of sample water contents by use of the three techniques are negligible in account of this fact.

In the following, only the individual boundary conditions adopted in the present study by use of the three methods are explained since details of the techniques can be found elsewhere, (e.g., Delage et al. 1998, Fredlund & Rahardjo 1993). In Figure 3.6 a schematic illustration of soil sample conditions during suction application is given.

OM is performed using polyethylene glycol (PEG)-water mixtures of 20,000 g/mol molec-

Table 3.4: Summary of suction steps of single step suction application tests for determination of water retention.

material	inital suction	applied suction (MPa)			
	(MPa)	OM	VET		ATT
Na^+-bentonite-(composites)	0	0.1			
	0	0.4			
	0	1.0			
	0	4.0			
	0	10.0			
	0		21	KCl	
	0		37	NaCl	
	0		83	$Mg(NO_3)_2$	
	0		154	$MgCl_2$	
	0		354	NaOH	
	354		83	$Mg(NO_3)_2$	
	354		21	KCl	
	354		3	K_2SO_4	
	354				0.1
Ca^{++}-bentonite-(composites)	0	0.1			
	0	0.4			
	0	1.0			
	0	4.0			
	0	10.0			
	0		21	KCl	
	0		37	NaCl	
	0		83	$Mg(NO_3)_2$	
	0		154	$MgCl_2$	
	0		286	LiCl	
	0		354	NaOH	
	354		83	$Mg(NO_3)_2$	
	354		21	KCl	
	354		3	K_2SO_4	
	354				0.1
kaolin-(composites)	0	0.1			
	0	0.4			
	0	1.0			
	0		3	K_2SO_4	
	0		9	KNO_3	
	0		21	KCl	
	0		83	$Mg(NO_3)_2$	
	0		286	LiCl	
	262		37	NaCl	
	262		9	KNO_3	
	262		3	K_2SO_4	
	262				1.0
	262				0.1

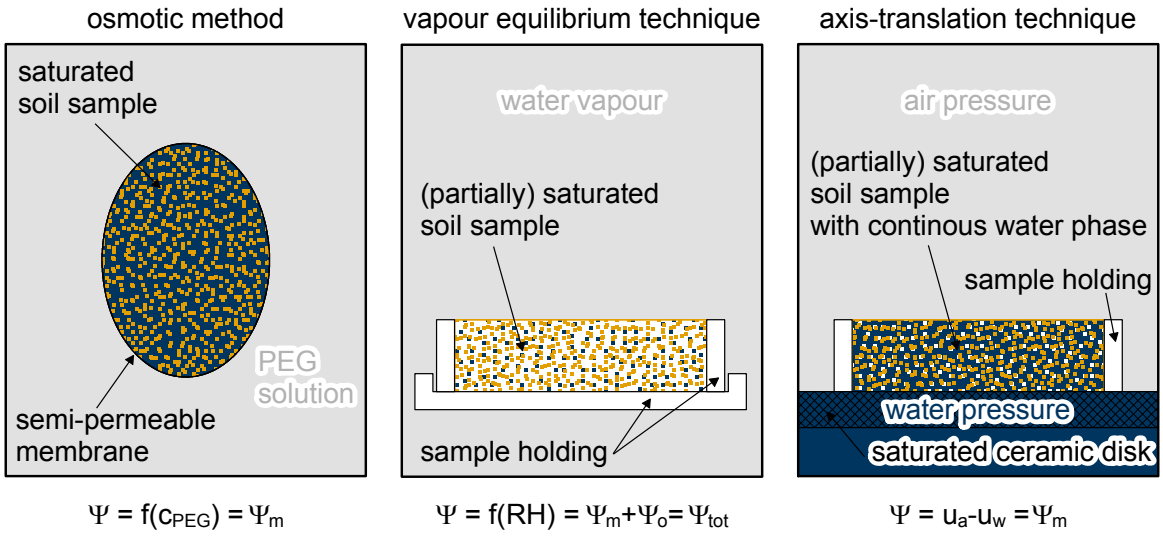

Figure 3.6: Illustration of clay and composite boundary conditions for the determination of water retention using osmotic method, vapour equilibrium technique and axis translation technique.

ular weight of PEG. Suctions applied to the samples, which depend on the respective PEG concentration, are calculated according to the relationship established by Tripathy et al. (2013) for this type of polymer:

$$\Psi_m = -3.9139c_{PEG}^3 + 14.692c_{PEG}^2 - 1.1336c_{PEG} \tag{3.1}$$

where Ψ_m (MPa) is the matric suction applied and c_{PEG} (g/g) is the related PEG concentration. Sample conditions as applied in this study are constrained to the saturated state, i.e., no air is allowed to enter the system.

In the high-suction range, VET is adopted using saturated salt solutions. Relative humidities and temperatures of the ambient air of the samples placed in desiccators are controlled and converted to their respective suction values by the adoption of Kelvin's law:

$$\Psi_{tot} = \frac{RT}{Mg} \ln(RH) \tag{3.2}$$

where Ψ_{tot} (MPa) is the total suction; R (J mol/K) is the ideal gas constant; T (K) is the absolute temperature; M (g/mol) is the molar mass of water; g (m/s^2) is the gravity acceleration and RH (-) is the relative humidity, i.e., the ratio of partial and saturated

water vapour pressure.

For the low suction range in the wetting process of samples, ATT is adopted using pressure plate apparatuses equipped with ceramic disks of various air entry values. Therefore, samples are placed on prewetted filter papers in order to enable continuity of the water phase between pore water and the water saturated ceramic disk artificially. The matric suction applied to the samples using this technique is calculated as the difference between the pore air and pore water pressure, u_a and u_w, respectively:

$$\Psi_m = u_a - u_w \tag{3.3}$$

After equilibration of the samples, the water contents and, in case of VET and ATT, the volumes of the samples are determined. Thereby, volume measurement is conducted by fluid displacement using kerosene following the method described in (Péron et al. 2007). For the OM, the volumes of samples are calculated based on fully saturated conditions.

For the representation of clay and composite soil-water characteristic curve (SWCC), the degree of saturation, S_r (-), is plotted over the respective value of soil suction, Ψ (MPa), for each suction step of the first drying curve. By means of the experimental data, fitting curves are generated following the relationship given by Fredlund & Xing (1994) since it was found to give the best fit among the most popular equations proposed in literature (Leong & Rahardjo 1997):

$$S_r = C(\Psi)\frac{1}{\left\{\ln\left[e + \left(\frac{\Psi}{a}\right)^n\right]\right\}^m} \tag{3.4}$$

where $C(\Psi)$ (-) is a correction function assumed to be unity (Leong & Rahardjo 1997) and n, m and a are fitting parameters. In order to calculate S_r for each suction step, water densities depending on the respective mineralogy as well as the water content established in (Martin 1960) are adopted (Table 3.3).

3.4.3 Hydro-mechanical tests on bentonite-polymer composite hydraulic barrier performance

In order to evaluate clay and composite barrier performances with respect to practical demands, various material characteristics are determined. (i) the liquid limit and the swelling

behaviour as well as (ii) the hydraulic permeability. With respect to the latter, the hydraulic barrier performance is directly addressed, whereas by the determination of the former characteristics it is indirectly addressed since they are correlated to the hydraulic permeability in case of clays (Mitchell & Soga 2005) and thus, indicators of material hydraulic barrier performance. In practice, the index properties are of great importance since their experimental determination is much less laborious and time consuming as compared to hydraulic permeability tests. Thereby, the swelling behaviour is generally determined by means of the swell index according to (ASTM D5890-11 2011).

The liquid limits of Na^+-bentonite-polymer composites are determined according to (ASTM D4318-10e1 2010). Swelling behaviour as well as hydraulic permeability of clay and composites are determined successively by use of the same sample. Therefore, samples of 20 mm height and 50 mm diameter are prepared and saturated with deionized and deaired water under isochoric conditions. Therefore, a burette is connected to the bottom of the sample and saturation is permitted under atmospheric pressure conditions. The development of the axial swelling pressure, p_s (kPa), is measured during the saturation process by a load cell and water uptake is recorded by means of the burette scaling. After equilibration, samples are permeated with deionized and deaired water by using a volume and pressure control device (VPC) connected to the bottom of the sample. Thereby, the pressure is increased successively to 36, 100, 200 and finally 500 kPa while the pressure at the sample top equals atmospheric conditions. Thus, a maximum hydraulic gradient of 2,500 is adjusted. During permeation, the sample inflow and outflow are monitored by the VPC as well as by means of the burette scaling, which is placed at the sample top. For each pressure step, hydraulic permeability is determined for constant pressure conditions according to the following equation:

$$k = \frac{Q\Delta l}{A\Delta h} \tag{3.5}$$

where k (m/s) is the hydraulic permeability, Q (m^3/s) is the flow rate permeating the sample, A (m^2) is the cross-sectional area of the sample permeated by the fluid, Δh (m) is the difference between inflow and outflow pressure heads and Δl (m) is the length of the sample permeated by the fluid. After equilibration at 500 kPa, i.e., the inflow equals the outflow and the hydraulic permeability remains constant, the permeation fluid is replaced by a deaired 0.5 molar $CaCl_2$ solution in order to initiate cation exchange process of exchangeable sodium cations. Using the salt solution, sample permeation is continued until the pore volume is replaced completely.

It has to be noted, that according to ASTM D5084-03 (2003) a maximum hydraulic gradient of 30 is recommended in order prevent sample consolidation during testing. However, by Rad et al. (1994) it was shown that in case of GCL conditions, i.e., sample thicknesses of about 20 mm, hydraulic gradients up to 2,800 do not essentially affect hydraulic permabilities. Thus, in order to reduce testing duration a hydraulic gradient of 2,500 is adjusted in the present study. In Figure 3.7 a schematic illustration of the experimental setup used for the determination of swelling pressure and hydraulic permeability of Na^{+}-bentonite as well as its respective composites is given. Details on the equipment used, i.e., the isochoric cell as well as the VPC device, can be found in (Khan 2012).

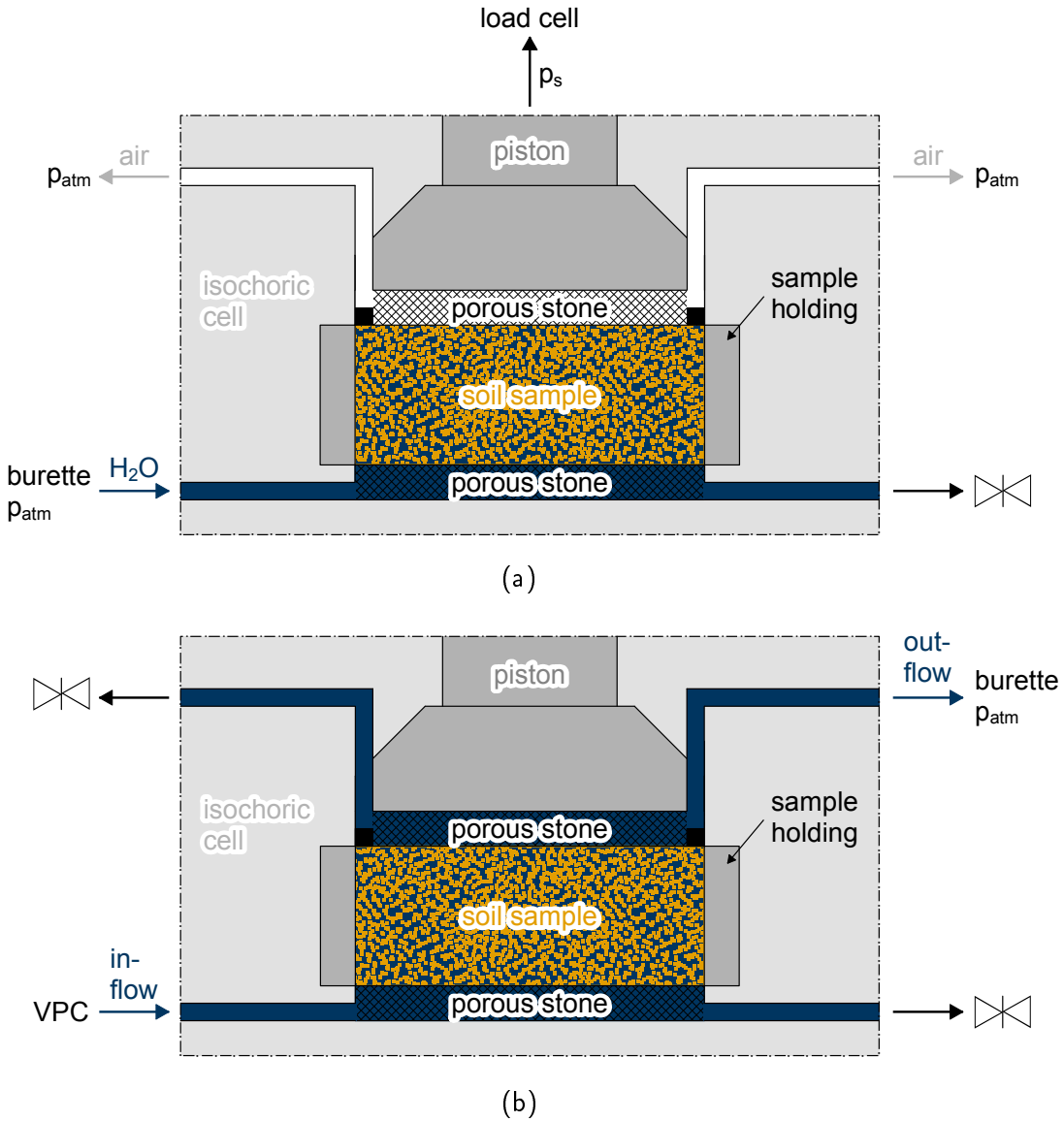

Figure 3.7: Illustration of the experimental setup used for the determination of swelling pressure (a) and hydraulic permeability (b) of Na^+-bentonite as well as its respective composites.

3.5 Theoretical methods

3.5.1 Physico-chemical approach

The volumetric behaviour of pure bentonites and bentonite-PAA°-composites, determined experimentally by oedometer compression tests on their respective slurries, are theoretically analysed by use of (modified) DDL theory. Therefore, the fundamental Poisson-Boltzman equation of the DDL (Equation 2.1) as well as its modified form considering non-ionic polymer adsorption on charged surfaces (Equation 2.11) are used. As pointed out in subsection 2.4.1, the solution obtained by Brooks (1973) is valid for small surface potentials only, i.e., $\Psi'_0 << \pm 25$ mV (van Olphen 1963), since it is based on a simplified form of the original nonlinear equation. However, in case of interlayer swelling clay mineralogies, clay mineral surface potentials amount around -275 mV, for which reason the existing solution is invalid for clay mineral surface conditions. This is illustrated in Figure 3.8, where the effect of non-ionic polymer adsorption on the electric potential in the near-field of charged surfaces is illustrated for varying values of β and d_p. It is obvious that the calculated values of $\Psi'(x)$ become enormous and definitely unrealistic, when applying the proposed equations to clay conditions (Figure 3.8b), whereas the approximation is valid in case of small surface potentials (Figure 3.8a). Therefore, in the present study, new equations are introduced obtained by semi-analytical solution of the original nonlinear Equation 2.11 in order to account for the influence of adsorbed non-ionic polymers on clay mineral surfaces on DDL formation characteristics. The novel approach is introduced in subsection 6.2.1:

3.5.2 Cluster model

Analysis of pure clay as well as composite hydraulic permeability as a function of total void ratio is performed on the basis of cluster model (see subsection 2.4.2). The following conditions are considered for theoretical calculation by use of Equation 2.17 and Equation 2.16:

In case of water being the pore fluid at 20°C, γ and η amount 9810 N/m^3 and 0.001005 Ns/m^2, respectively. k_0 and t amount 2.5 and $\sqrt{2}$, respectively, which is valid for uniform pore size distributions and thus, for Kozeny-Carman approach (Mitchell & Soga 2005). According to the underlying assumptions in cluster model, e_c, i.e., the intra-cluster void ratio, begins

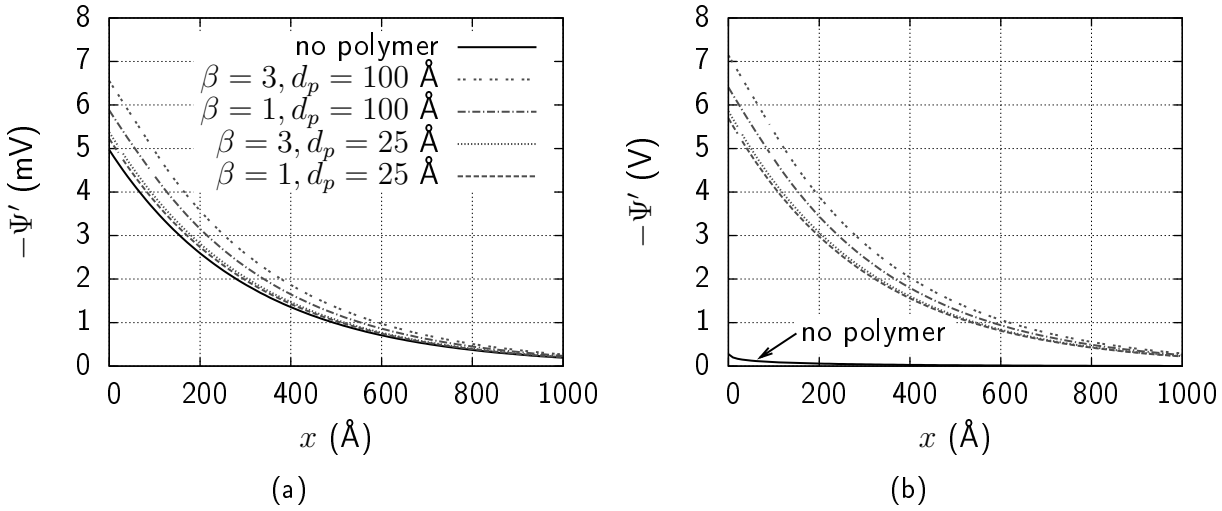

Figure 3.8: Electric potential versus distance to charged surface plots following Equation 2.4 (no polymer) and Equation 2.14 & 2.15 (with polymer) with $n_0 = 10^{-4}$ mol/l, $\nu = 1$, $\epsilon = 7.1 \cdot 10^{-10}$ C^2/Jm, T = 298 K: Small surface potential of Ψ'_0 = -5 mV (a); clay mineral surface conditions of Ψ'_0 = -275 mV (b).

to participate in compression process when the inter-cluster void ratio, e_p, falls below the value of 0.43. Thus, for $e_p \geq 0.43$, e_c equals $e_{c,0}$, whereas e_p decreases by the same value as the total void ratio, e_t, decreases. In case of $e_p < 0.43$, both void ratios, e_c and e_p, decrease linearly with decreasing e_t (see Figure 2.15). Therefore,

$$\begin{aligned} e_c &= e_{c,0} \\ e_p &= e_t - e_c \qquad\qquad \text{for} \quad e_p \geq 0.43 \end{aligned} \tag{3.6}$$

and

$$\begin{aligned} e_c &= \frac{e_{c,0}}{(0.43 + e_{c,0}) \cdot e_t} \\ e_p &= e_t - e_c \qquad\qquad \text{for} \quad e_p < 0.43 \end{aligned} \tag{3.7}$$

Finally, the unknown values of the initial intra-cluster void ratio, $e_{c,0}$, as well as the number of particles per cluster, N, are derived by fitting the cluster model approach, i.e., Equation 2.17, with the respective experimental data of oedometer time-compression test results. Thereby, it is assumed that the initial fabric of clay and composite slurries is

formed at zero external loading conditions, i.e.,

$$e_{c,0} \leq \ e_{t,0} - 0.43 \tag{3.8}$$

3.6 Summary

The fundamentals on the study's approach, the materials used as well as the experimental and theoretical methods adopted were summarized. In the beginning, the organization of the research program was defined. Thereby, the multiscale approach focusing on the systematic multiscale experimental and theoretical investigation of clay-polymer composites as well as the application-oriented approach focusing on the identification of the governing mechanisms determining the hydraulic barrier performance of polymer enhanced bentonite barriers were distinguished.

With respect to the multiscale approach, variations of the constitutive properties in terms of the clay mineralogy, the polymer charge as well as the polymer-to-clay ratio were defined. Further, the experimental methods of micro-scale analysis in terms of the adsorption characteristics by means of the adsorption isotherms as well as the fabric were introduced. Similarly, the experimental methods of macro-scale analysis in terms of the plastic properties, the volumetric behaviour, the hydraulic permeability as well as the water retention were given. With respect to the theoretical multiscale analysis, i.e., (modified) DDL theory and cluster model, the individual procedures, parameter sets and boundary conditions were summarized. These involve the development of new equations on the basis of modified DDL theory by solving the original non-linear differential equation introduced in chapter 2 within the framework of the thesis.

With respect to the application-oriented approach, variations of the constitutive properties in terms of the polymer charge and composite preparation method were defined. Further, the testing boundary conditions, especially concerning the determination of swelling pressure and subsequently the hydraulic permeability were outlined.

4 Experimental results of micro-scale analysis

4.1 General

In the following chapter, the results of clay and composite experimental micro-scale analysis are presented and discussed. Firstly, consideration is given to the adsorption characteristics of each clay-polymer combination. Thereby, the results obtained are discussed in terms of polymer adsorption spots on clay mineral surfaces as well as its shape in the adsorbed state based on the state-of-the-art knowledge summarized in subsection 2.2.3. In the second part of this chapter, experimental results of microscopic clay and composite investigations are presented and discussed in terms of their fabrics based on the definitions given in subsubsection 2.2.1.3 and subsection 2.2.4. Thereby, interpretation of clay and composite fabrics aims on the identification of physico-chemical as well as steric mechanisms caused by the presence of adsorbed polymer on clay mineral surfaces. Parts of the results presented in the following have been published in (Haase & Schanz 2015, Haase & Schanz 2016).

4.2 Adsorption characteristics

Test results on the adsorption characteristics of PAA^{+}, PAA^{o} and PAA^{-} on Na^{+}- and Ca^{++}-bentonite as well as kaolin are given in Figure 4.1 showing the respective adsorption isotherm, i.e., the mass of adsorbed polymer per gram clay, q (mg/g), over the concentration of polymer in solution, c_{eq} (mg/l), each for the state of equilibrium. In accordance to previous findings on the adsorption characteristics of polyacrylamide polymers on clay mineral surfaces, e.g., by Schamp & Huylebroeck (1973), adsorption isotherms can be

characterized most suitable by the Langmuir-type, following the equation:

$$q = \frac{K q_{max} c_{eq}}{1 + K c_{eq}} \tag{4.1}$$

Where, K (-) is the Langmuir adsorption coefficient and q_{max} (mg/g) is the maximum adsorption capacity. The parameters K and q_{max} describing the individual shape of the adsorption isotherm are summarized in Table 4.1 for each clay-polymer combination. It is obvious that both, the clay mineralogy as well as the polymer charge have significant influence on the maximum adsorption capacity.

With respect to the polymer charge, the highest amount of polymer adsorption was found to occur in case of PAA^{o}, followed by PAA^{+}. This behaviour is in accordance to similar findings, e.g., by Denoyel et al. (1990), on the influence of polymer cationicity on adsorption characteristics, and can be explained by the geometrical shape of polymers in the adsorbed state. Randomly coiled PAA^{o} chains adsorb with large loops and tails, whereas stretched geometries of PAA^{+} result in a large portion of train segments. The adsorbed volume and thus, mass, is therefore reduced in case of PAA^{+}, even if the coverage of clay mineral surfaces is equal. In case of PAA^{-}, the maximum adsorption capacity is in a quite lower order of magnitude as observed for PAA^{o} and PAA^{+}. This indicates that the governing mechanisms of anionic polymer adsorption, i.e., anion exchange on clay mineral edges and cation bridging on multivalent exchangeable cations, are significantly less in quantity as compared to cation exchange, which is the governing mechanism in cationic polymer adsorption. Additionally, ion-dipole and dipole-dipole bonding to polar parts of the polymer chain, as observed e.g., by Deng et al. (2006) for all three types of polymers, are of minor significance in case of the anionic polymer.

With respect to the clay mineralogy, polymer adsorption occurs most distinctive in case of

Table 4.1: Adsorption parameters according to Langmuir-type adsorption isotherms.

	PAA^{+}			PAA^{o}		PAA^{-}	
	K (-)	q_{max} (mg/g)	q_{max}* (meq/g)	K (-)	q_{max} (mg/g)	K (-)	q_{max} (mg/g)
Na^{+}-bentonite	0.017	185.18	0.70	0.033	201.60	-	-
Ca^{++}-bentonite	0.011	32.63	0.12	0.009	67.88	0.026	2.01
kaolin	0.009	9.26	0.04	0.014	16.11	0.033	0.53

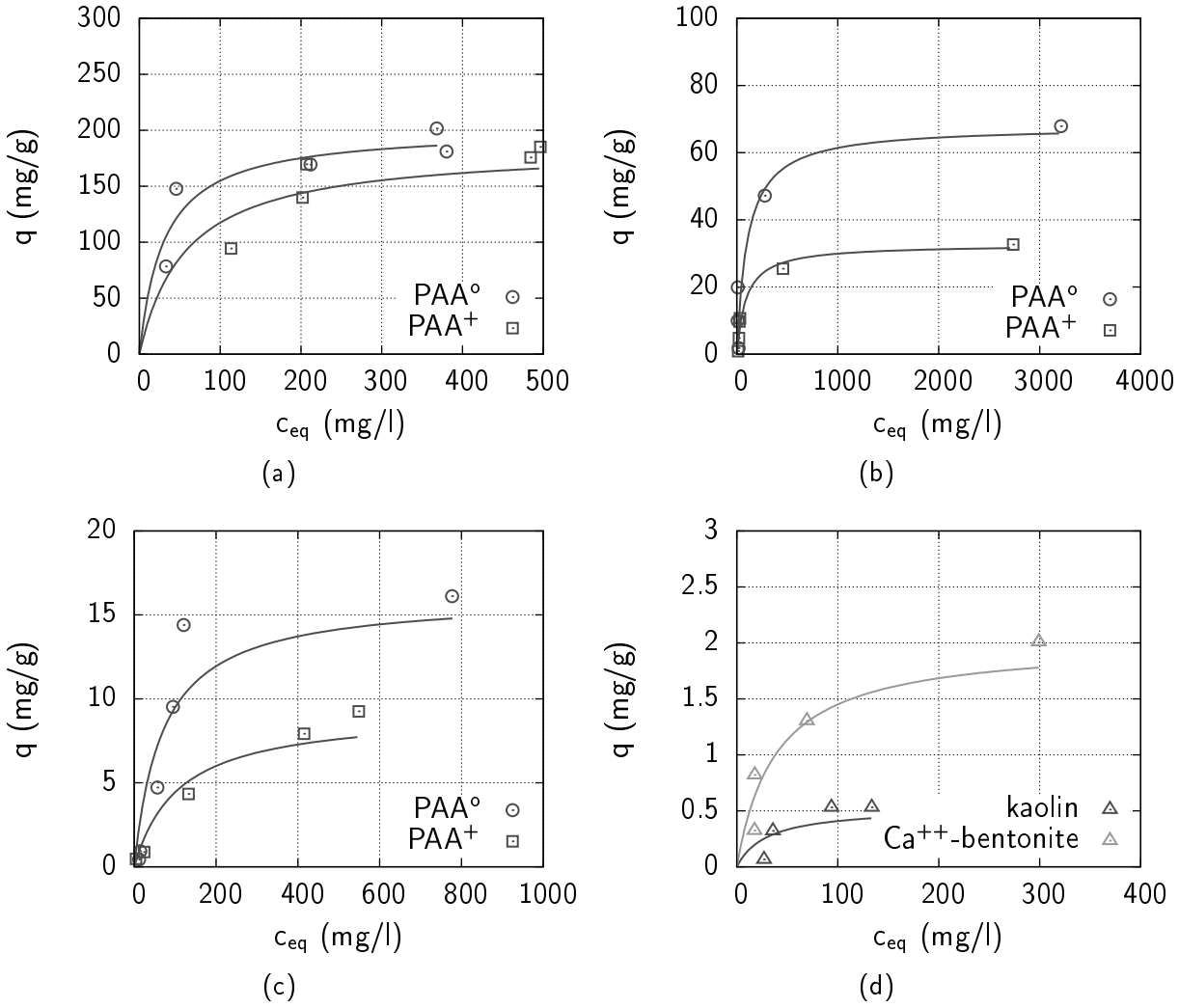

Figure 4.1: Adsorption isotherms of polyacrylamide polymers on clays: PAA^+ and PAA° on Na^+-bentonite (a), Ca^{++}-bentonite (b) and kaolin (c); PAA^- on Ca^{++}-bentonite and kaolin (d).

Na^+-bentonite, followed by Ca^{++}-bentonite and kaolin. These results are in good agreement with the respective surface accessibilities for polymer adsorption on clay mineral surfaces since inner surface adsorption is possible in the presence of interlayer swelling clay minerals only, i.e., in case of bentonites. Additionally, for the Ca^{++}-bentonite, restrictive access to the inner surfaces of interlayer swelling clay minerals can be expected since DDL repulsion of clay mineral surfaces is decreased in the presence of multivalent exchangeable cations, which accounts for its lower maximum adsorption capacity as compared to Na^+-bentonite. Quantitative information on the individual surface accessibilities of the bentonites studied can be obtained when incorporating PAA^+ ionicity, I^+ (mol-%), as well as the respective molar masses, M (g/mol), of acrylamide and methylated dimethylaminoethylacrylate monomers into the corresponding results on maximum adsorption capacity of PAA^+. By use of the following equation,

$$q_{max}* = \left(M^o \cdot \frac{(1 - I^+/100)}{I^+/100} + M^+ \right)^{-1} \cdot q_{max} \tag{4.2}$$

q_{max} (mg/g) can be rewritten as $q_{max}*$ (meq/g), where M^o (g/mol) is the molar mass of acrylamide, i.e., 71.08 g/mol, and M^+ (g/mol) is the molar mass of methylated dimethylaminoethylacrylate, i.e., 158.21 g/mol. Finally, by the ratio $q_{max}*/CEC$, an indication of clay mineral surface occupancy can be given leading to the conclusion that polymer chains do not intercalate completely into montmorillonite layers. Thereby, calculations assume that by each cationic monomer adsorbed an exchangeable cation is replaced. In case of Ca^{++}-bentonite, an average amount of 5 stacked montmorillonite layers with the inner surfaces remaining inaccessible for polymer adsorption can be concluded since only 19% of the exchangeable cations were replaced by the adsorption of PAA^+. In case of Na^+-bentonite, on the other hand, an average amount of 1.2 montmorillonite layers per stack was calculated and thus, almost complete polymer intercalation. Since kaolinite minerals are characterized by a very low layer charge the above assumptions, i.e., by each cationic monomer adsorbed an exchangeable cation is replaced, do not apply for the kaolin clay and thus, the corresponding calculations will not be considered.

It has to be noted, that in case of Na^+-bentonite, actually no adsorption of PAA^- was detected leading to the conclusion that multivalent cation bridging, which are present in considerable amount only in case of Ca^{++}-bentonite and kaolin, is the dominant mechanism in PAA^- adsorption rather than anion exchange. This conclusion is in agreement with the fact, that under the present pH conditions, i.e., pH 6.1, clay mineral edges are approxi-

mately neutral or rather slightly negatively charged and thus, do not have an appreciable amount of exchangeable anions.

4.3 Fabric

Results of microscopic investigation using ESEM are illustrated in Figure 4.2a - Figure 4.4d. With respect to the pure clay fabrics, it is obvious that bentonites are characterized by a homogeneous smooth surface of the clay (Figure 4.2a & 4.3a) without visible pore systems on the particular scale. However, individual units, i.e., (stacked) layers, can be identified rudimentary smearing into each other rather than having finite dimensions. Thus, preferential clay mineral layer/stack orientations in terms of well-defined F-F, E-F and E-E orientations, respectively, cannot be identified. Generally, the diffuse effect of layer/stack smearing is more pronounced in case of the Na^{+}-bentonite indicating that clay mineral layers are more dispersed as compared to the Ca^{++}-bentonite, which is in accordance to the findings on polymer adsorption characteristics, i.e., 1.2 versus 5 layers per stack (see section 4.2). The fabric of pure kaolin, on the other hand, is dominated by the existence of individual finite units, i.e., particles and aggregates, with the latter having well-defined F-F particle orientations. In consequence, large inter-aggregate pores can be identified between F-F aggregates and assemblages of dispersed and deflocculated particles indicating the existence of a bimodal PSD. These observations are in accordance to the physico-chemical surface characteristics of the particular clay minerals. In case of montmorillonite, clay mineral basal surface repulsion due to DDL overlapping dominates, whereas in case of kaolinite, basal surface attraction due to London-van der Waals forces is dominant. In consequence, the existing units in bentonites are single montmorillonite layers as well as stacks of few layers in a dispersed and deflocculated state appearing as a 'clay mass' on the particular scale. Kaolinite layers on the other hand, form large units, i.e., several thousands of stacked layers, which can be identified distinctly as particles on the particular scale.

It is obvious that due to composite formation with PAA^{+}, bentonite fabrics rearrange from the initial smooth surface and form large units, i.e., aggregates, each consisting of an assemblage of numerous clay mineral layers and stacks with inter-aggregate pores between them (Figure 4.2b & 4.3b). Thereby, the diffuse effect of (stacked) layers as observed in pure bentonites, persists within aggregates, for which reason a dominant intra-aggregate orientation of clay mineral layers and stacks is still not obvious. Since PAA^{+} polymers

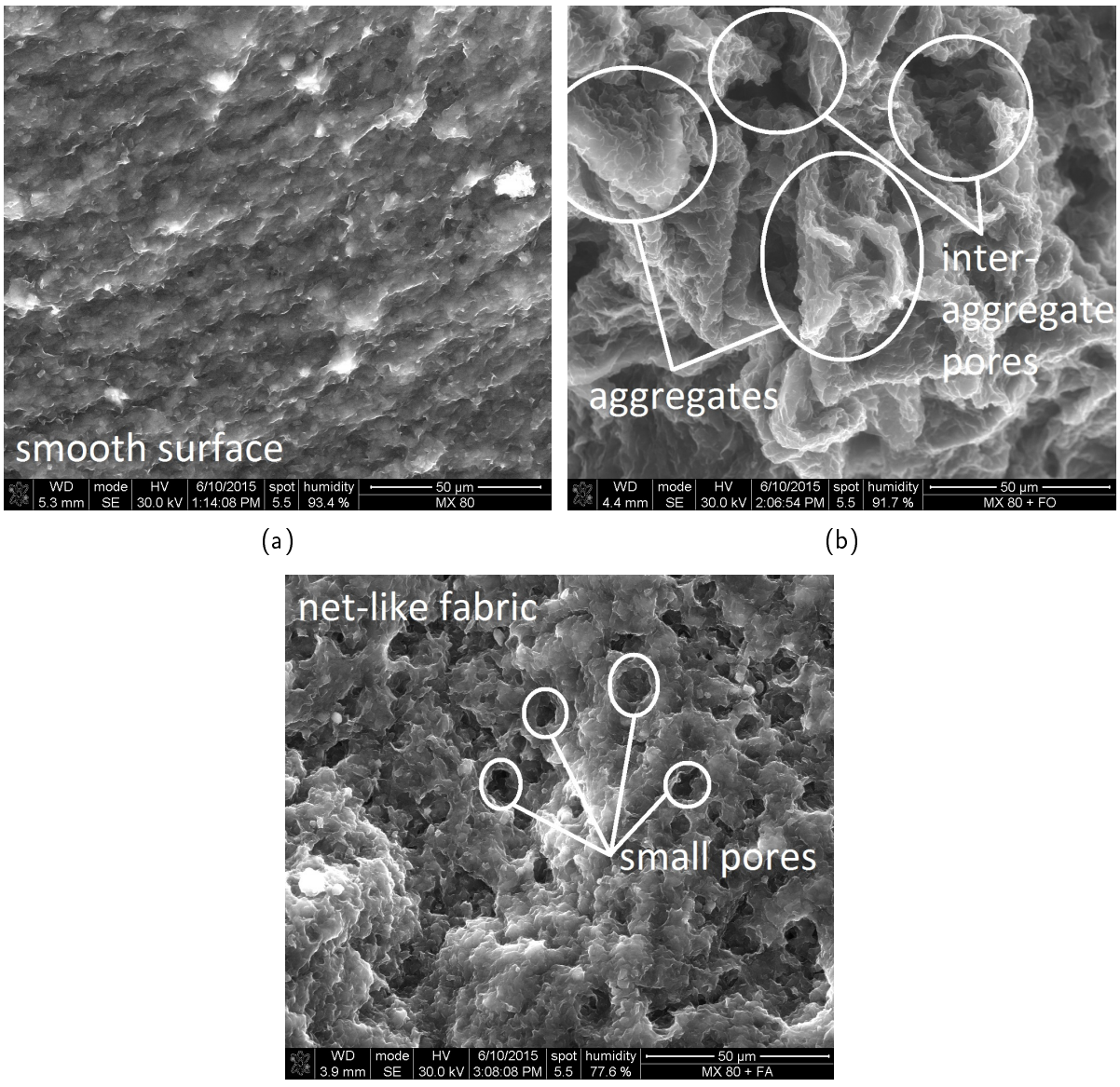

Figure 4.2: ESEM images of Na^+-bentonite (a), PAA^+ (b) and PAA^o (c) composites.

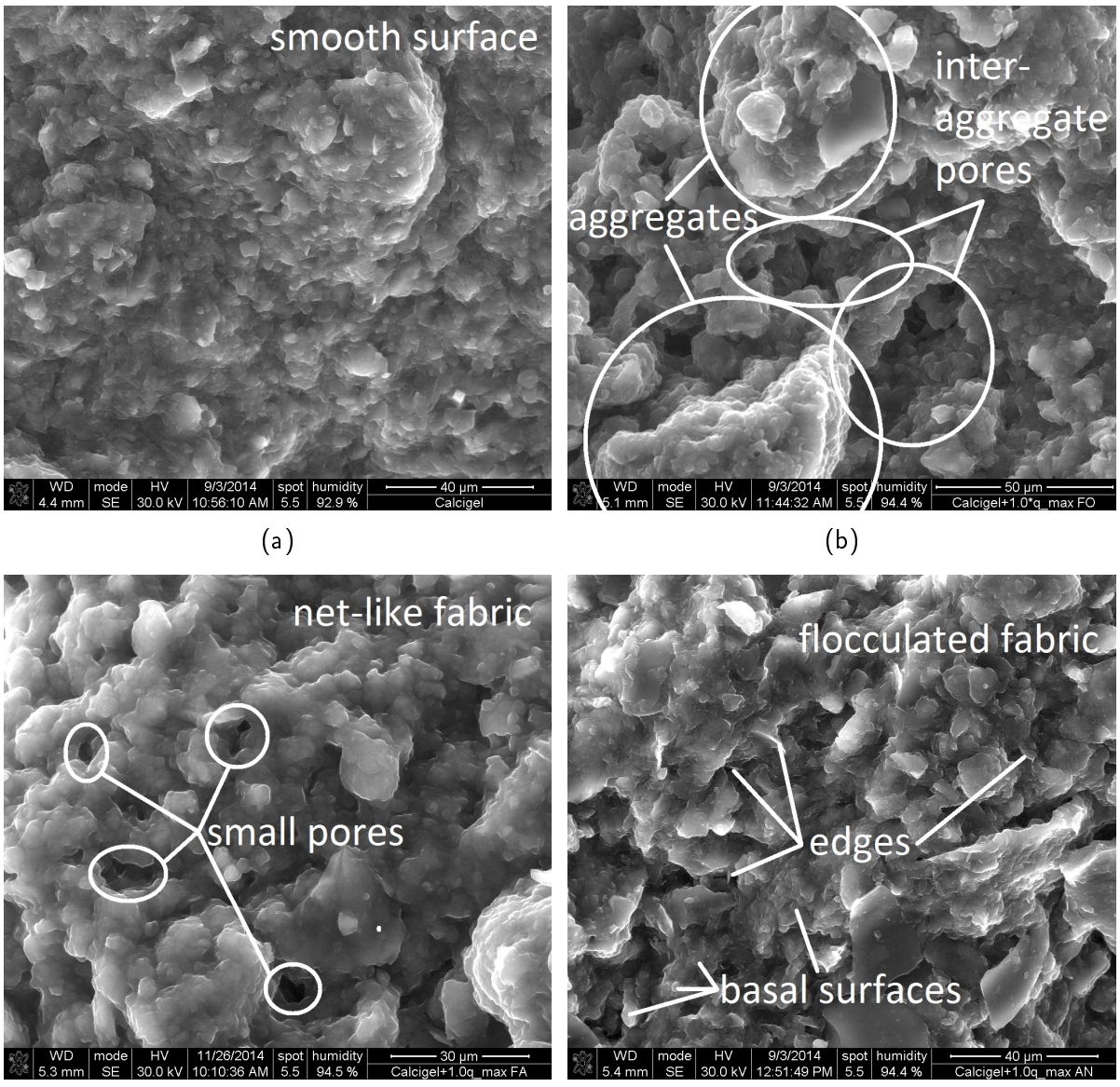

Figure 4.3: ESEM images of Ca^{++}-bentonite (a), PAA^{+} (b), PAA^{o} (c) and PAA^{-} (d) composites.

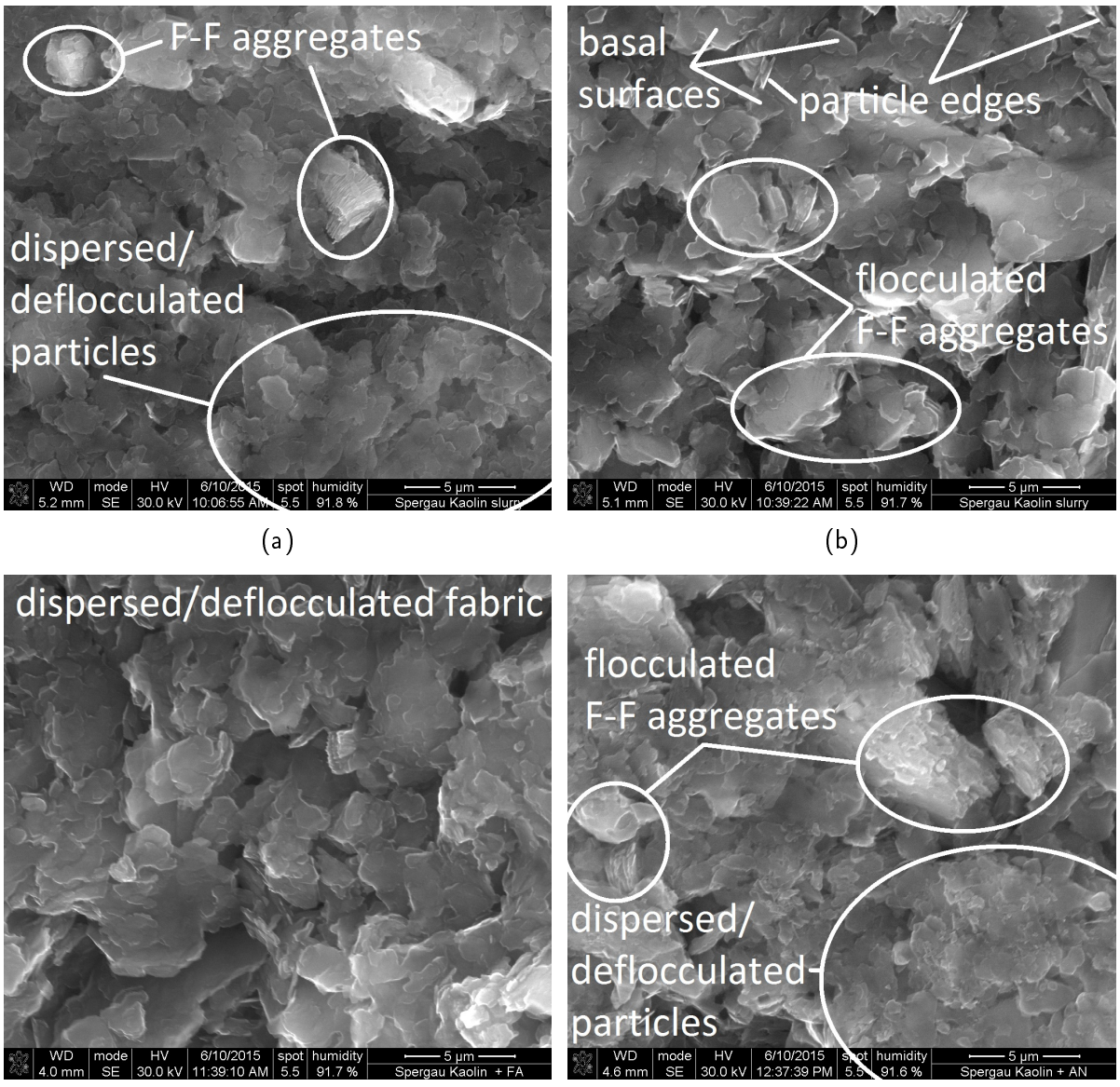

Figure 4.4: ESEM images of kaolin (a), PAA^{+} (b), PAA^{o} (c) and PAA^{-} (d) composites.

adsorb by cation exchange as the governing mechanism, the surface charge of clay mineral layers becomes significantly lowered and eliminated, respectively. Thus, DDL repulsion decreases and clay mineral layers approach forming larger units, i.e., aggregates. Thereby, as it is obvious from microscopic investigation, layers and stacks approach irregularly in dependence on their initial orientation rather than forming well-defined particles, which accounts for the persisting diffuse effect within aggregates. The kaolin-PAA^+ composite fabric (Figure 4.4b), on the other hand, differs from its pure clay counterpart by having smaller F-F associated clay particle aggregates, i.e., aggregates are composed of a less amount of particles. However, the smaller aggregates are additionally associated with each other by E-F and E-E flocculation forming further units. Additionally, individual particles tend to flocculate, which is obvious from the alternating particle orientation within particle assemblages. Thus, intra-aggregate fabrics differ from pure kaolin, whereas the inter-aggregate pore-system remains nearly unaffected. As a result of these differing fabrics, an additional pore size fraction can be identified in case of the kaolin-PAA^+ composite, i.e., intra-aggregate pores between small aggregates. Since DDL repulsion and thus, the reduction of surface charges due to cation exchange by PAA^+ adsorption is insignificant in case of kaolinite, the mechanisms determining composite fabric differ from the governing effects in the bentonites. As it has been pointed out in subsubsection 2.2.3.2, cationic polymer shape in the adsorbed state tends to form large loop and tail segments, if the clay mineral surface can be electrostatically equilibrated by the remaining train segments only. This is particularly significant in case of kaolinite having a very low layer charge and thus, extensive loop and tail segments of the adsorbed polymer. Under these conditions, cationic polymers promote interparticle bridging since they act as long-distance connectors. Obviously, this effect occurs between individual particles as well as F-F associated aggregates resulting in their respective flocculation.

The micro-fabric observed in case of bentonite-PAA^o composites is characterized by a net-like surface of the clay (Figure 4.2c & 4.3c), i.e., the smooth surface, which is similar to that of pure bentonite, is interrupted by a large number of small pores with the clay still forming a continuous mass rather than individual units, i.e., aggregates. However, the diffuse effect of (stacked) layers persists within the clay, for which reason preferential layer and stack orientations are still not obvious. From colloid chemical point of view, non-ionic polymer adsorption is assumed to promote dispersion and deflocculation by an increase in DDL repulsion as well as steric stabilization between clay mineral surfaces (see subsection 2.2.4), which accounts for the observation of a continuous clay mass similar to

that of pure bentonite. However, the formation of small pores may be attributed to local variations in the physico-chemical surface characteristics of clay mineral layers originated from, e.g., non-uniform polymer adsorption, i.e., surfaces having adsorbed layers and surfaces without adsorbed layers co-exist, as well as variations in the specific polymer shape, i.e., the individual extent of loops and tails. Since the net-like fabric is very similar to the 'honeycomb-fabric' as observed in some silts, its metastable nature, i.e., collapse under the action of applied stresses, can be assumed accordingly (see Mitchell & Soga (2005)). In case of the kaolin-PAA^{o} composite, it is obvious that its fabric is characterized by a single particle association without having aggregated or flocculated units (Figure 4.4c), i.e., the fabric is dispersed and deflocculated. In consequence, only interparticle pores, i.e., an unimodal PSD, can be observed. This effect of non-ionic polymer adsorption on kaolin fabric is therefore in accordance to the concept of steric stabilization between clay mineral surfaces since F-F aggregation of particles is suppressed by preventing particle approaching into each others attraction sphere.

PAA^{-} composites of Ca^{++}-bentonite as well as kaolin were found to deviate from pure clay fabrics by the formation of preferred E-F flocculation. This is most obvious in case of the Ca^{++}-bentonite composite with the ESEM image clearly illustrating alternating orientation of stacks (Figure 4.3d). Thereby, the formation of large units having flocculated intra-aggregate fabrics cannot be identified and thus, the PSD remains unimodal. With respect to the kaolin composite, E-F flocculation occurs between F-F associated aggregates, whereby assemblages of single particles remain dominantly dispersed and deflocculated since distinct alternation in particle orientation is lacking. Thereby, F-F aggregates are composed of a similar amount of particles as observed in pure kaolin and thus, intra-aggregate pores between them are in the same order of magnitude as inter-aggregate pores between assemblages of flocculated aggregates and assemblages of single particles. From adsorption results (section 4.2), it was concluded that PAA^{-} interacts via divalent cation bridging with the clay mineral surface. In doing so, long-distance bridging between clay mineral surfaces is enabled since adsorption spots, i.e., the local excess of positive surface charges, are rarely as compared to the polymer anionicity. Consequently, flocculation between the existing units, i.e., layers/stacks and aggregates, respectively, occurs. However, in case of kaolin, assemblages of single particles remain unaffected by the flocculating effect of PAA^{-} indicating that the existence of adsorption spots on the kaolinite surface, i.e., the local excess of positive surface charges originated by the presence of divalent exchangeable cations, correlates with the tendency of particle F-F aggregation.

4.4 Summary

Micro-scale analysis of clays and clay-polymer composites has been performed including the experimental determination of adsorption isotherms as well as the microscopic investigation of clay and composite fabrics prepared with a polymer-to-clay ratio of q_{max}. The concluding findings are as follows:

Adsorption isotherms of each clay-polymer combination were found to follow the Langmuir-type adsorption. Their individual maximum adsorption capacities were found to be in the following orders of magnitude: $PAA^o > PAA^+ >> PAA^-$ as well as Na^+-bentonite > Ca^{++}-bentonite > kaolin, which is in agreement with the respective constitutive characteristics dominating the interaction between clay mineral surfaces and polymers, i.e., polymer shape in the adsorbed state, the amount of adsorption spots on clay mineral surfaces as well as clay mineral surface accessibility. With respect to the latter, adsorption results were confirmed by microscopic investigation indicating distinctive layer dispersion in the Na^+-bentonite, layer stacking in the Ca^{++}-bentonite as well as the existence of particles and F-F aggregates in the kaolin. Thereby, calculations of PAA^+ maximum adsorption capacity let to the conclusion of an average amount of 5 layers per stack in case of Ca^{++}-bentonite.

PAA^+ adsorption was found to promote aggregated clay fabrics in case of bentonites due to the reduction in DDL repulsion, whereas in case of kaolin, flocculation was promoted due to long-distance interparticle and inter-aggregate bridging. PAA^o adsorption, on the other hand, was found to cause dispersed clay fabrics due to an increase in DDL repulsion as well as steric stabilization between clay mineral surfaces. However, in the slurry condition, bentonite composites tend to develop a net-like fabric similar to the well-known honeycomb-fabric, which is assumed to be sensitive to the stress level. PAA^- adsorption was found to promote flocculated clay fabrics due to long-distance interparticle bridging. Thereby, multivalent cation bridging was concluded to be the governing mechanism in adsorption process rather than anion exchange since in case of Na^+-bentonite having a very little amount of multivalent exchangeable cations no adsorption of PAA^- has been detected. In Figure 4.5 & 4.6 the results are summarized schematically.

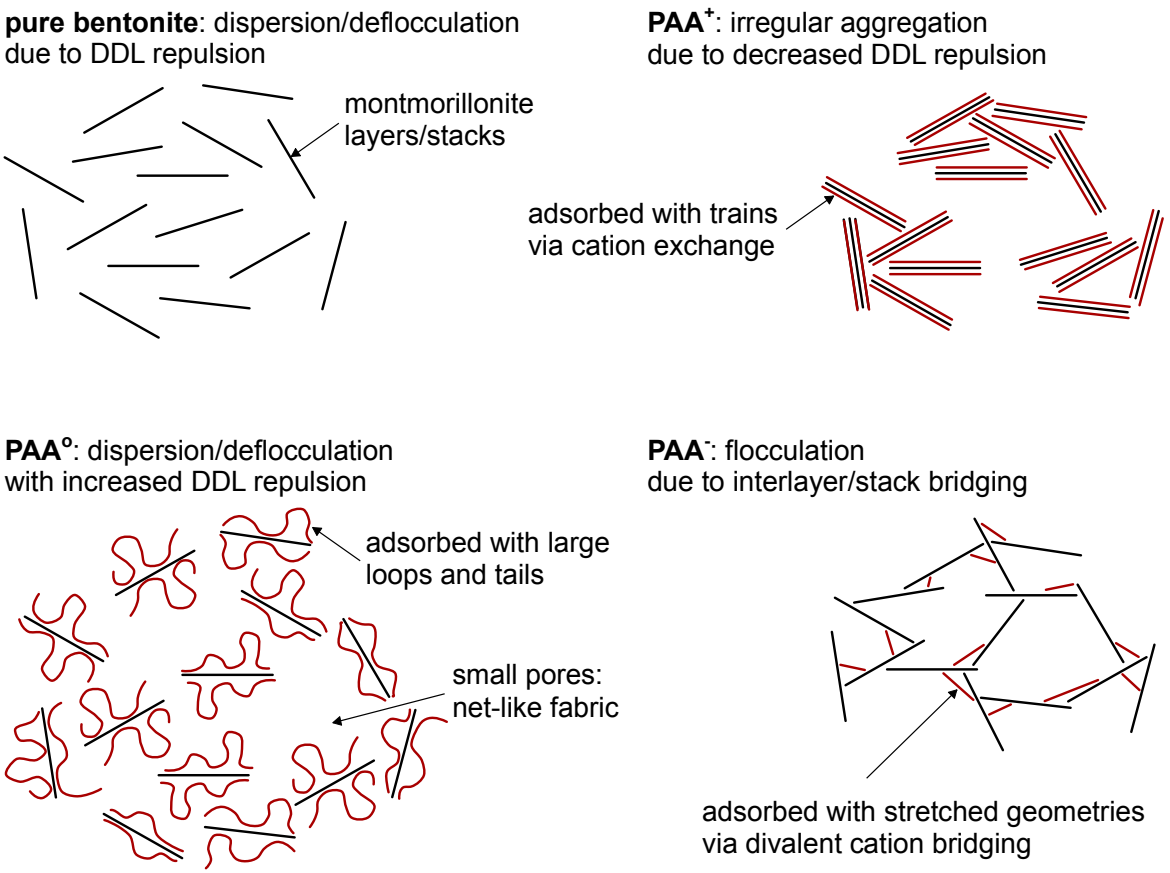

Figure 4.5: Summary of clay and composite micro-scale analysis - bentonite fabric.

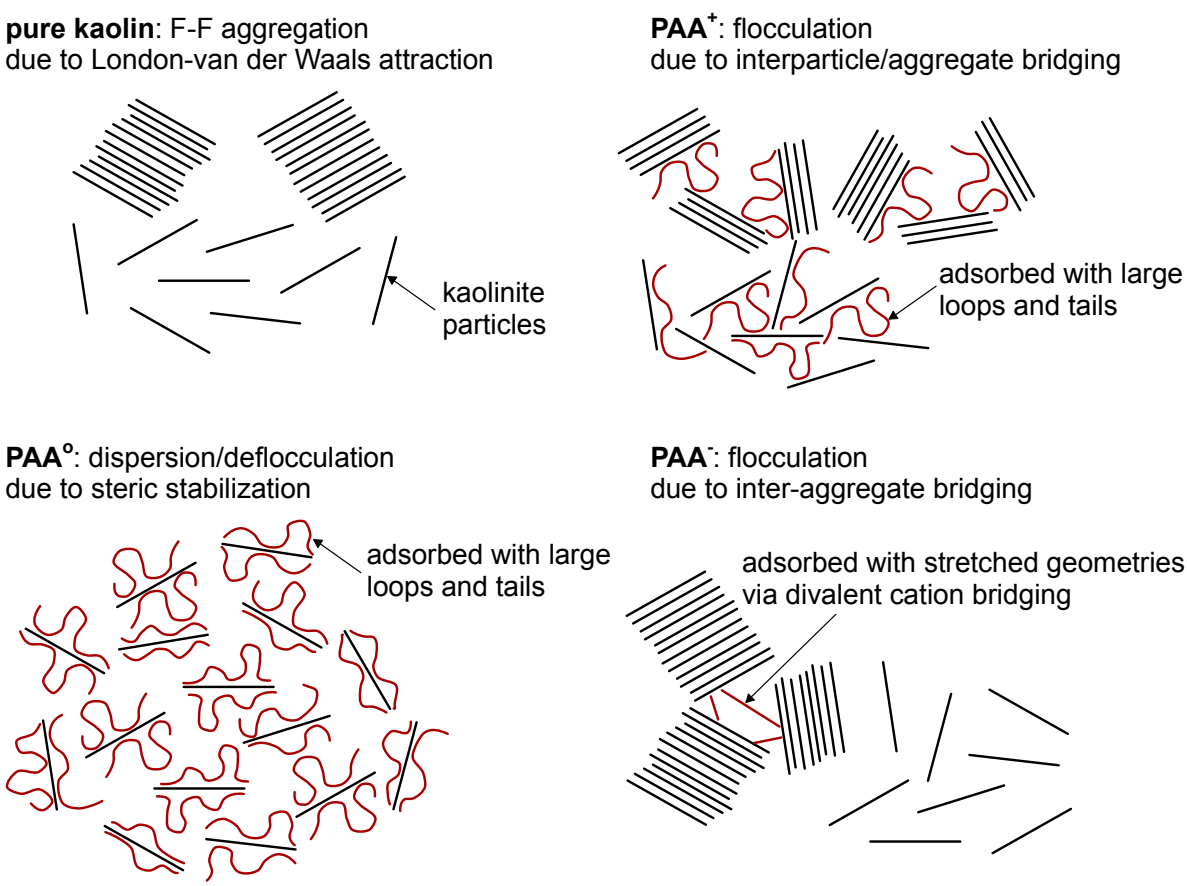

Figure 4.6: Summary of clay and composite micro-scale analysis - kaolin fabric.

5 Experimental results of macro-scale analysis

5.1 General

In the following chapter, the results of clay and composite experimental macro-scale analysis are presented and discussed. Thereby, consideration is given to the plastic properties as well as oedometer and unconfined water retention test results performed on clay and composite slurries. In order to enable comparison of composite macro-scale properties to their respective pure clay counterparts, modified definitions in terms of the water content as well as the void ratio are introduced:

$$w^* = \frac{m_w}{m_c} \cdot 100 \tag{5.1}$$

$$e_{clay} = \frac{V_v + V_p}{V_c} \tag{5.2}$$

where w^* (%) is the modified water content indicating the influence of polymer adsorption on the physico-chemical properties of clay mineral surfaces; m_w (g) is the mass of water; m_c (g) is the mass of clay; e_{clay} (-) is the modified void ratio indicating the influence of polymer adsorption on clay fabric, i.e., clay mineral solid separation and orientation; V_v (cm^3) is the volume of voids; V_p (cm^3) is the volume of polymer and V_c (cm^3) is the volume of clay mineral solids.

Interpretation of clay and composite macro-scale behaviour is based on fundamental multiscale relationships established for clays (see section 2.3) taking into account the results of micro-scale analysis. Parts of the results presented in the following have been published in (Haase & Schanz 2016, Haase & Schanz 2015).

5.2 Plasticity

It is established in literature that in case of montmorillonite being the predominant clay mineral the extent of DDLs controls the order of liquid limits, whereas in case of kaolinite being th predominant clay mineral the fabric is the governing factor (Sridharan et al. 1986, Sridharan et al. 1988). Thereby, with increasing degree of DDL extent and flocculation, respectively, w_l-values are increased. Nonetheless, both mechanisms exist simultaneously in montmorillonitic as well as kaolinitic clays with different degree of intensity and may act opposed to each other (Sridharan 2002). In addition, both mechanisms directly influence shrinkage limits, i.e., with increasing extent of DDLs in case of montmorillonite w_s-values decrease as well as with increasing degree of flocculation in case of kaolinite w_s-values increase. With respect to the former relationship, the accompanying effect of fabric dispersion in consequence of extensive DDL formation is reflected (for details see subsection 2.3.2). The results on composite plastic behaviour, i.e., the liquid, plastic and shrinkage limits, summarized in Table 5.1 largely reflect these relationships when taking into account their respective micro-scale characteristics:

In case of kaolin clay, w_l^*- as well as w_s^*-values of PAA^+ and PAA^- composites are increased, which is in accordance to the flocculating effect of polymer adsorption identified in section 4.3. In addition, the particular degree of flocculation, as illustrated in Figure 4.6, correlates to the absolute values of w_l^* and w_s^*. With respect to the kaolin-PAA^o composite, fabric dispersion and deflocculation has been identified (see section 4.3), in which consequence a decrease in liquid and shrinkage limits is expected based on the established relationships on micro- and macro-scale coupling. However, since an increase in w_l^*- and w_s^*-values can be identified, the effect of polymer adsorption in terms of steric stabilization, as illustrated in Figure 4.6, is assumed to dominate the effect of dispersion and deflocculation, i.e., the interparticle pore-space is increased rather than decreased, which is macroscopically similar to the effect of flocculation.

In case of bentonite composites, aggregated and flocculated fabrics have been identified to exist in PAA^+ and PAA^- composites. In consequence, both types of composites have significantly increased w_l^*-values. Thereby, it has to be noted that the effect of PAA^+-adsorption in terms of fabric aggregation dominates the effect of clay mineral surface charge equalization and thus, reduction in DDL extent, by which the reverse effect on the value of liquid limit is promoted. In case of Ca^{++}-bentonite-PAA^o composites prepared

Table 5.1: Modified consistency limits of clay-polymer composites.

	pure	PAA^+	PAA^o	PAA^-
Na^+-bentonite prepared with q_{max}				
w_l^* (%)	588	654	-[1]	-[2]
w_p^* (%)	37	-[1]	-[1]	-[2]
w_s^* (%)	14	7	10	-[2]
Ca^{++}-bentonite prepared with q_{max}				
w_l^* (%)	109	153	173	171
w_p^* (%)	33	-[1]	-[1]	38
w_s^* (%)	13	17	12	12
Ca^{++}-bentonite prepared with 10% of q_{max}				
w_l^* (%)	109	139	163	138
w_p^* (%)	33	34	53	30
w_s^* (%)	13	14	12	12
kaolin prepared with q_{max}				
w_l^* (%)	51	113	96	57
w_p^* (%)	32	75	49	37
w_s^* (%)	30	42	40	39

[1]determination failed, standard test method unsuitable; [2]composites were not considered (see section 4.2)

with a polymer-to-clay ratio of q_{max} and 10% of q_{max}, respectively, the increase in DDL extent due to polymer adsorption is reflected by their liquid limits, i.e., w_l^*-values are significantly increased. However, in case of the Na^+-bentonite-PAA^o composite standard test methods for the determination of liquid limit were found to be not applicable, for which reason no w_l^*-value was obtained. With respect to the shrinkage limits of bentonite-PAA composites, it is obvious that significant deviations from pure bentonite values occur in case of Na^+-bentonite-PAA composites only, i.e., the shrinkage limits are decreased. This behaviour is not consistent with established w_l^*-w_s^*-relationships, on which basis the increased w_l^*-value due to aggregation in case of the Na^+-bentonite-PAA^+ composite is expected to be accompanied by an increase in w_s^*. Since the polymer-to-clay ratio is very high for both Na^+-bentonite-PAA composites, it is concluded that polymer specific characteristics, such as the flexibility of polymer chains as against the rigidity of clay mineral layers, dominate the formation of residual composite fabrics during shrinking. In

contrast, in case of Ca^{++}-bentonite-PAA composites, consistent w_s^*-values can be observed for the PAA^+ and PAA^o composites, i.e., slightly increased and decreased values due to fabric aggregation and DDL increase, respectively, whereas in case of PAA^- composites, w_s^*-values are inconsistent with the corresponding w_l^*-values, i.e., they are slightly decreased in spite of fabric flocculation and thus, increased w_l^*-values. With respect to the effect of polymer-to-clay ratio, Ca^{++}-bentonite-PAA composites prepared with q_{max} and 10% of q_{max}, respectively, show similar tendencies in w_l^*- and w_s^*-values with the more pronounced effect in case of composites prepared with q_{max}. w_l^*-w_s^* relationships of clays and composites are illustrated in Figure 5.1.

Since the determination of plastic limits failed for many of the composites, interpretation of the values in terms of general relationships cannot be given.

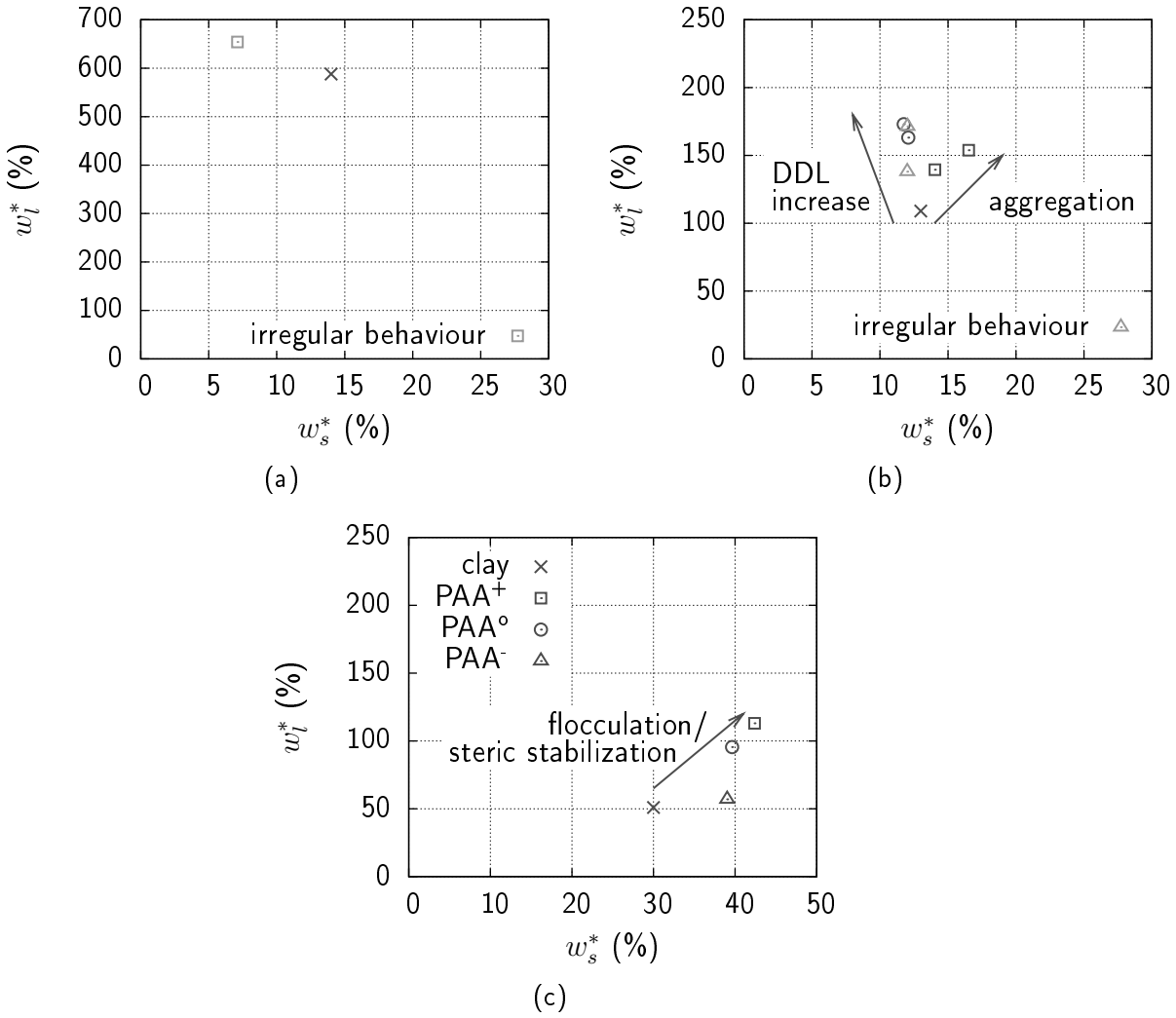

Figure 5.1: w_l^*-w_s^*-relationships of clays and composites: Na^+-bentonite (a); Ca^{++}-bentonite (b); kaolin (c).

5.3 Volumetric behaviour

The results obtained experimentally by oedometer compression and rebound tests on the volumetric behaviour of pure clays and clay-polymer composites prepared with a polymer-to-clay ratio of q_{max} are shown in Figure 5.2. They indicate that the changes in volumetric behaviour due to composite formation have similar tendencies independently on the dominant clay mineralogy, even though e-log(p') relationships have different orders of magnitude for kaolinite- and montmorillonite-rich clays dominated by mono- and divalent exchangeable cations, respectively. It is obvious that composites have generally higher void ratios at the same applied pressure as compared to their pure clay counterparts. Since the void ratio expressed in terms of e_{clay} implicates that the volume of polymer adsorbed on clay mineral surfaces is treated as voids the contribution of polymer volumes to the calculated void volumes is indicated by dashed lines for high polymer-to-clay ratios (Figure 5.2). Thereby, polymer volumes are neglected completely for the calculation of void ratios. Doing so, it is obvious that the higher void ratios in case of composites cannot be attributed to polymer volumes only and additional factors dominate composite volumetric behaviour. The general tendency of increased void ratios at the same applied pressure in case of composites can be further differentiated by polymer charge as follows:

In case of PAA^+ composites, the abovementioned behaviour can be observed most significantly for all the three clays as well as along the whole pressure range tested. This behaviour is in accordance to the micro-scale findings on clay fabric, i.e., aggregated and flocculated fabrics in case of bentonites and kaolin, respectively. Thereby, it was found that the bentonite-PAA^+ composite fabrics differ from the pure bentonite fabrics by having large inter-aggregate pores and thus, a bimodal PSD as against the unimodal PSD in pure bentonites. The kaolin-PAA^+ composite, on the other hand, differs from the pure clay fabric by having increased intra-aggregate pores between flocculated small aggregates, whereas inter-aggregate pores, that can also be found in the pure kaolin fabric, remain unchanged. However, for both types of predominant clay mineralogies a bimodal PSD exists in the PAA^+ composite fabrics, whereas the pore size fraction accounting for distinctly increased void ratios is different for montmorillonite and kaolinite dominated clays.

With respect to PAA^o composites, it can be observed that in case of bentonites, composite e-log(p') relationships tend to approach to the respective relationship of pure clays with increasing pressure. At 800 kPa their corresponding dashed line approximately equals the

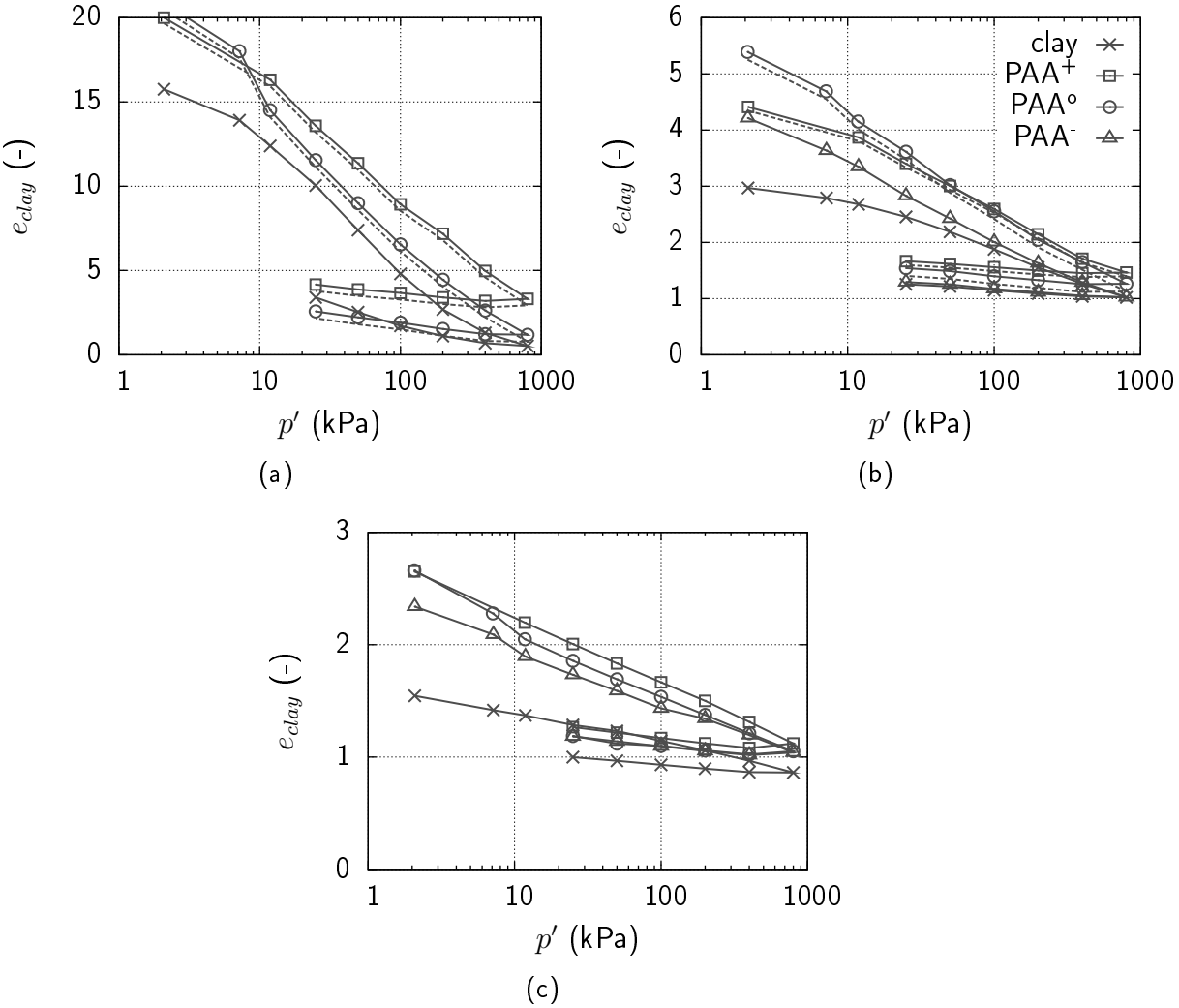

Figure 5.2: (De)compression curves of clays and composites prepared with a polymer-to-clay ratio of q_{max}: Na^{+}-bentonite (a); Ca^{++}-bentonite (b); kaolin (c).

value e_{clay} of pure clays. However, the kaolin-PAA^{o} composite has no tendency to approach to the e-log(p') relationship of pure clay. This differing behaviour can be attributed to the fact that the mechanisms of non-ionic polymer adsorption on clay fabric formation are different and depend on the predominant mineralogy, although the qualitative effect on clay fabric, i.e., dispersed and deflocculated fabrics, is equal. In case of montmorillonite, polymer adsorption causes an increase in DDL repulsion of clay mineral surfaces, whereas in case of kaolinite, the mechanism of 'steric stabilization' governs kaolinite surface separation. Since the latter mechanism dominates for physical reason independently on the stress level differences in e_{clay} exist for each applied pressure. However, due to decreased differences with increasing stress level, it can be assumed that polymer shape rearranges, i.e., loop and tail sizes become reduced and train parts are increased with increasing pressure applied. In case of increased DDL repulsion due to PAA^{o}-adsorption, on the other hand, the effect has less dominance with increasing clay mineral surface approaching and thus, stress level. This can be attributed to additional attractive forces acting between adsorbed polymer parts and the opposing clay mineral surface, i.e., dipole-dipole and ion-dipole attraction, causing 'forced polymer bridging' between clay mineral surfaes. Additionally, the influence of attractive London-van der Waals forces has to be considered since due to the adsorbed polymer chains separation of solids is distinctly smaller than separation of clay mineral surfaces as referred to by e_{clay}. Thus, clay mineral surface separations, at which attractive forces become relevant can be assumed to differ from the findings in literature on pure clay mineral surfaces (see subsection 2.4.1). Further, since in the high pressure range differences in e_{clay} can be attributed to the polymer volume between montmorillonite solids only, the initial polymer shape in terms of large loops and tails becomes rearranged with increasing pressure, i.e., train segments are increased. Taking additionally into account the results of micro-scale investigations, i.e., the presence of a net-like fabric, which is morphologically similar to the honeycomb fabric, the assumption of its metastable nature is confirmed by oedometer compression test results.

In case of PAA^{-} composites, increased e-log(p') relationships have least extent in comparison to the PAA^{+} and PAA^{o} composites. Further, for the Ca^{++}-bentonite composite it can be observed that its e-log(p') relationship approaches to that of pure clay at an applied vertical pressure of about 100 kPa. However, the kaolin composite has no tendency to approach to its corresponding pure clay e-log(p') relationship. In both cases, E-F flocculation was found to dominate the clay fabric, which accounts for the general increase. In addition, when taking into account the respective differences in clay fabrics, i.e., E-F flocculation

between stacks (Ca^{++}-bentonite) and aggregates (kaolin), the latter fabric can be expected to have higher resistance against loading induced particle rearrangement, which is caused by an increase in shearing resistance between flocculated units due to an increase in the shearing area. Thus, E-F flocculation of the Ca^{++}-bentonite-PAA^{-} composite is highly sensitive to the stress level, which obviously applies for anisotropic as well as isotropic loading conditions, i.e., the sensitivity is indicated by oedometer compression test results as well as the w_s^*-value, which is inconsistent to the corresponding w_l-value (see section 5.2).

With respect to the influence of polymer-to-clay ratio, oedometer (de)compression curves of Ca^{++}-bentonite-PAA composites prepared with q_{max} and 10% of q_{max} are similar in a qualitative manner (see Figure 5.3). Thereby, the effect of polymer adsorption as discussed in the previous paragraphs is more pronounced for the higher polymer-to-clay ratio. Thus, differences in composite fabric as proposed in literature in terms of flocculation by interparticle bridging in case of moderate amounts of adsorbed polymer and steric stabilization in case of high amounts of adsorbed polymer cannot be confirmed by the results obtained.

The compression and decompression indices, C_c (-) and C_s (-), obtained by linearization of e-$\log(p')$ relationships between 25 and 800 kPa vertical stress are listed in Table 5.2. The pure clay values of both parameters follow the order Na^{+}-bentonite >> Ca^{++}-bentonite > kaolin. With respect to the composites, slightly increased values of C_c can be identified. Since the compression index was proposed by Sridharan (2002) to be correlated to w_s-values in dependence on the predominant clay mineralogy the individual C_c-w_s^* relationships are illustrated in Figure 5.4. Thereby, inconsistencies with established relationships on micro- and macro-scale coupling, which have been identified in section 5.2 on the basis of w_l^*-w_s^* relationships as well as the results of fabric investigation, are confirmed, i.e., decreased w_s^*-values of Na^{+}-bentonite-PAA composites due to polymer chain flexibility as well as decreased w_s^*-values of Ca^{++}-bentonite-PAA^{-} composites due to fabric sensitivity to the stress level. Kaolin-PAA composites as well as Ca^{++}-bentonite-PAA^{+} and -PAA^{o} composites, on the other hand, show very good agreement between macro-scale C_c-w_s^* relationships and their respective micro-scale characteristics. The individual mechanisms are indicated in Figure 5.4. The C_s-values amount 10 - 35% of the corresponding C_c-values, which is in accordance to ratios given by Mitchell & Soga (2005). Generally, the influence of polymer adsorption is most obvious in case of Na^{+}-bentonite-PAA composites, i.e., C_s-values are signifiantly decreased, which additionally emphasizes the relevance of attractive forces at small clay mineral surface separations due to adsorbed polymer layers.

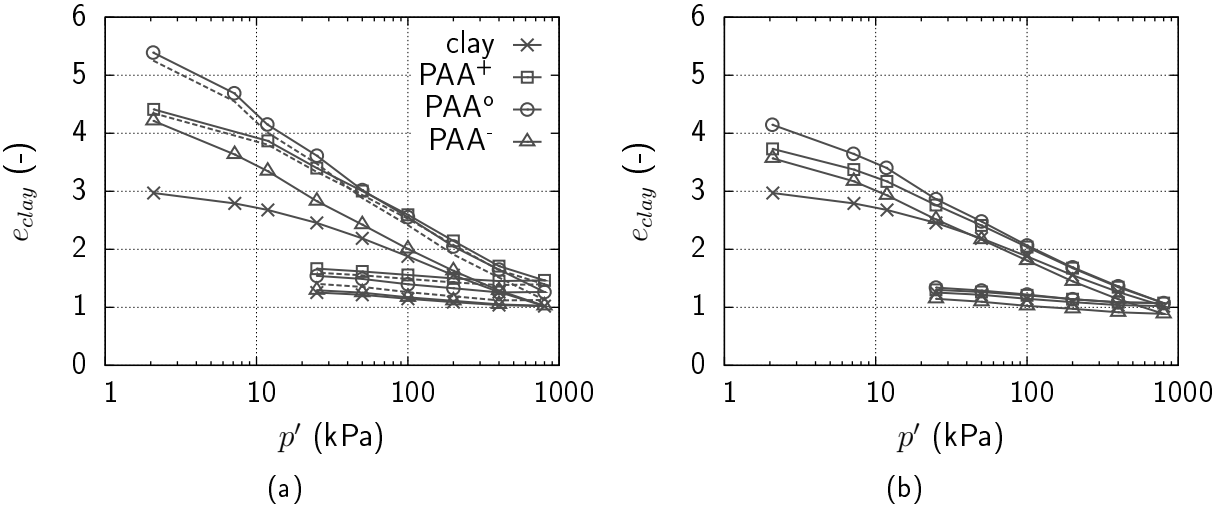

Figure 5.3: (De)compression curves of Ca^{++}-bentonite and its composites prepared with a polymer-to-clay ratio of q_{max} (a) and 10% of q_{max} (b).

Table 5.2: (De)compression indices of clays and composites.

	pure	PAA^{+}	PAA^{o}	PAA^{-}
Na^{+}-bentonite prepared with q_{max}				
C_c (-)	6.46	6.85	6.93	-[1]
C_s (-)	1.95	0.62	0.98	-[1]
Ca^{++}-bentonite prepared with q_{max}				
C_c (-)	0.97	1.33	1.22	1.55
C_s (-)	0.17	0.15	0.21	0.19
Ca^{++}-bentonite prepared with 10% of q_{max}				
C_c (-)	0.97	1.14	1.10	1.20
C_s (-)	0.17	0.16	0.19	0.18
kaolin prepared with q_{max}				
C_c (-)	0.28	0.58	0.53	0.45
C_s (-)	0.10	0.11	0.10	0.11

[1]composites were not considered (see section 4.2);

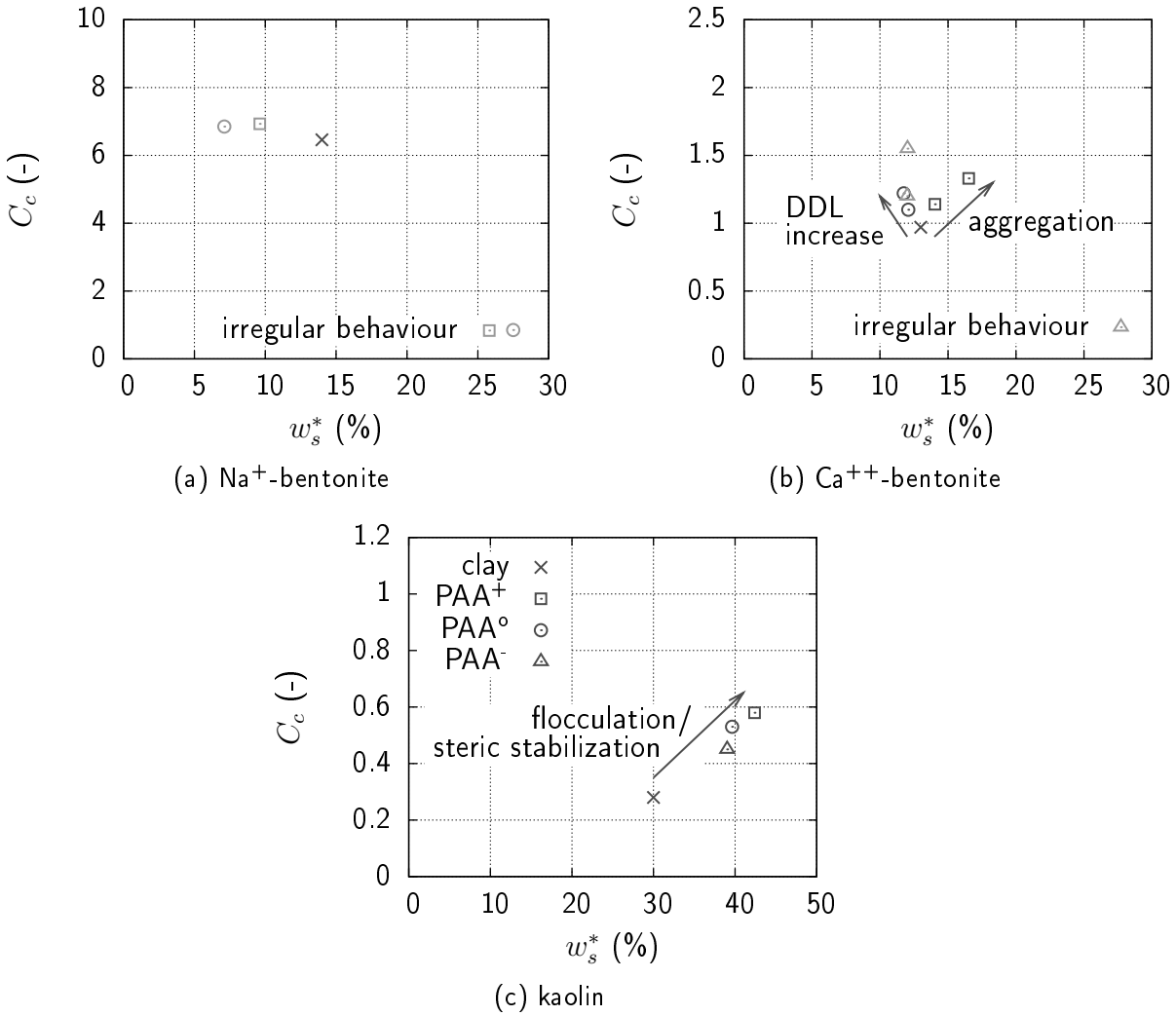

(a) Na^+-bentonite

(b) Ca^{++}-bentonite

(c) kaolin

Figure 5.4: C_c-w_s^*-relationships of clays and composites: Na^+-bentonite (a); Ca^{++}-bentonite (b); kaolin (c).

5.4 Hydraulic permeability

Hydraulic permeabilities of pure clays and clay-polymer composites obtained by the analysis of time-compression curves for each stress increment along the loading path of oedometer compression tests are illustrated in Figure 5.5 & 5.6 as a function of total void ratio e_{clay}. For each type of clay as well as their respective composites, hydraulic permeability decreases exponentially with decreasing void ratio. Additionally, as expected, pure clay values of k follow the order Na^{++}-bentonite < Ca^{++}-bentonite << kaolin, which can be attributed to the respective clay fabrics and thus, fluid flow paths, in consequence of physico-chemical clay mineral surface characteristics. With respect to clay-polymer composites prepared with a polymer-to-clay ratio of q_{max}, it is obvious that hydraulic permeabilities differ from their pure clay counterparts by different tendencies depending on polymer charge as follows:

In case of PAA^+ composites, a general increase in hydraulic permeability can be observed. For bentonites, this increase amounts about 0.5 - 1 order of magnitude along the whole void ratio range tested. It has to be noted that time-compression curves of the Na^+-bentonite-PAA^+ composite were found to have established distributions in the high pressure range only. k-values were therefore obtained for 200, 400 and 800 kPa vertical loading instead of each stress increment. In contrast to the bentonite-PAA^+ behaviour, kaolin-PAA^+ composite does not differ significantly from its pure clay counterpart in terms of the hydraulic permeability. The differences are in accordance to the findings of microscopic investigation summarized in section 4.3. Thus, increased k-values of bentonite-PAA^+ composites are caused by the formation of aggregated clay fabrics including bimodal PSDs exhibiting preferential fluid flow paths. The kaolin-PAA^+ composite, on the other hand, was found to be altered with respect to the intra-aggregate pores, whereas the inter-aggregate pores remained unchanged. Since the fluid flow is controlled by the latter, macro-scale behaviour in terms of the hydraulic permeability remains unchanged as well.

In case of PAA^o composites, the tendency is vice versa, i.e., hydraulic permeabilities are decreased. This behaviour is most evident for the kaolin-PAA^o composite with reductions by about 2 orders of magnitude. This is in accordance to the micro-scale characteristics of pure kaolin and kaolin-PAA^o composite since PSDs were identified as bimodal and unimodal, respectively. Thus, a decrease in maximum pore radii in case of the kaolin-PAA^o composite causes decreased hydraulic permeabilities. However, PAA^o composites of bentonites have reduced hydraulic permeabilities in case of Na^+-bentonite only, whereas in

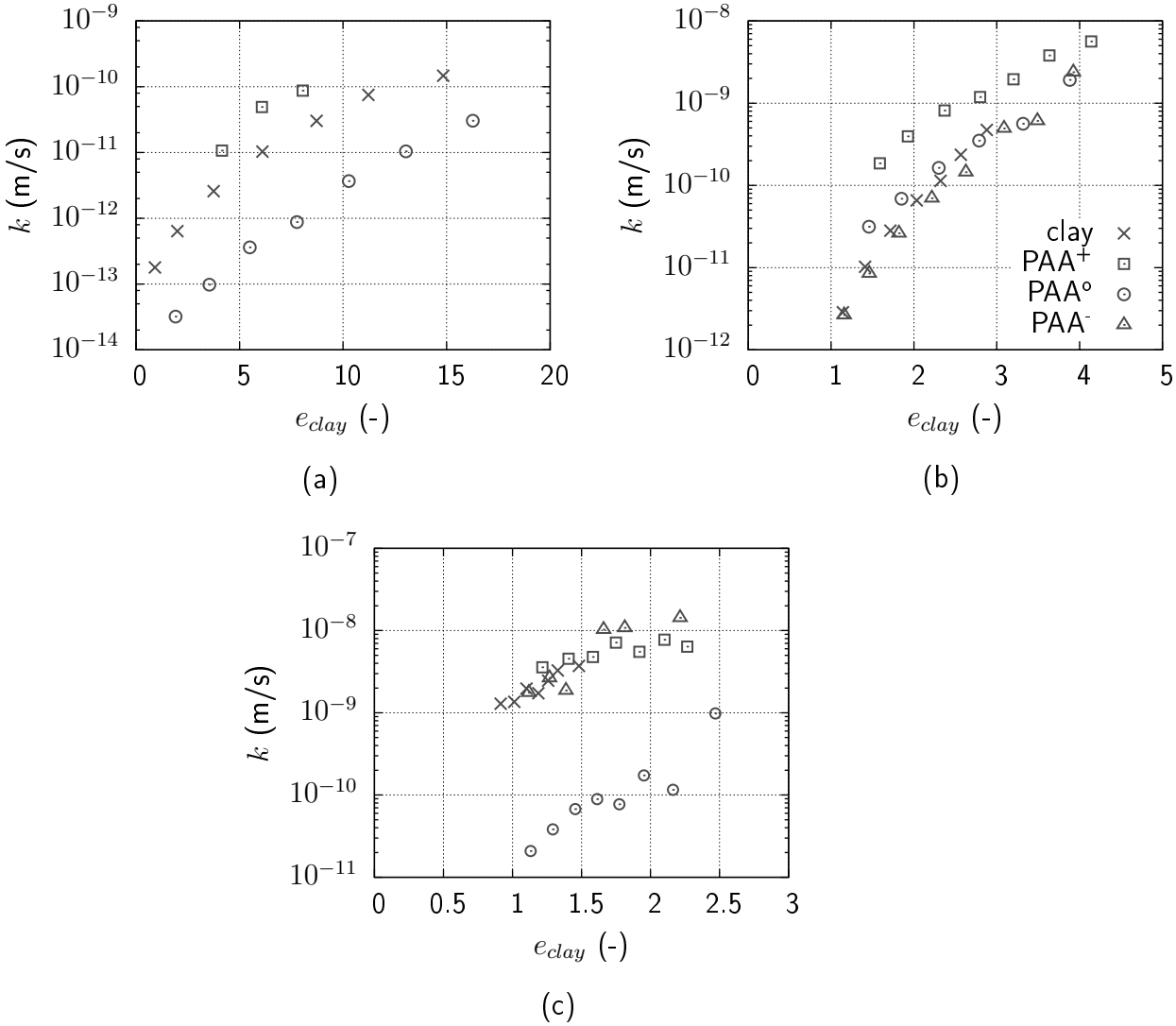

Figure 5.5: Hydraulic permeability versus void ratio plots of clays and composites prepared with a polymer-to-clay ratio of q_{max}: Na^{+}-bentonite (a); Ca^{++}-bentonite (b); kaolin (c).

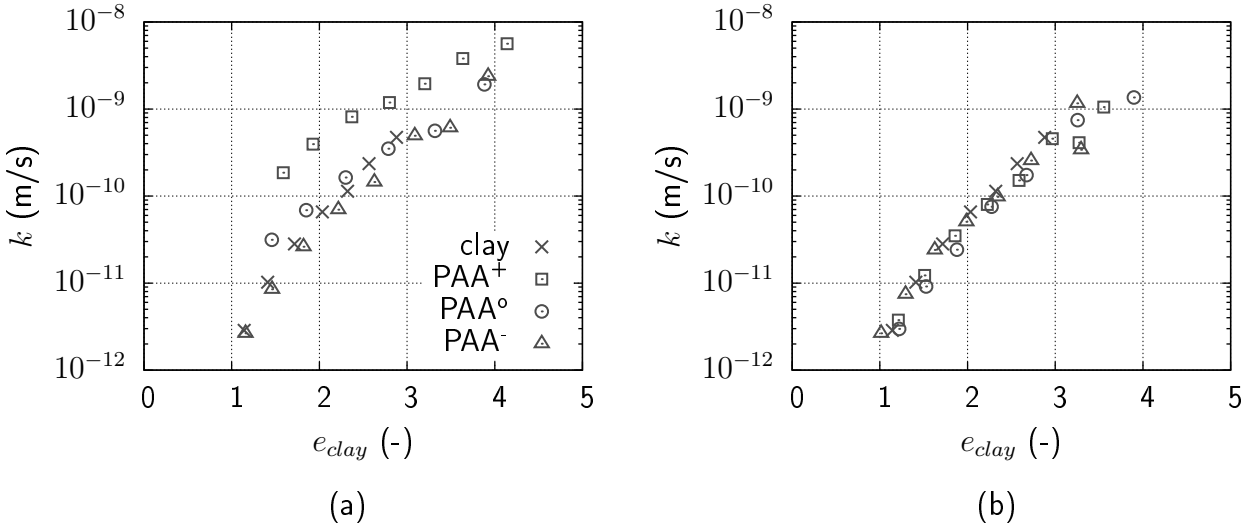

Figure 5.6: Hydraulic permeability versus void ratio plots of Ca^{++}-bentonite and its composites prepared with a polymer-to-clay ratio of q_{max} (a) and 10% of q_{max} (b).

case of Ca^{++}-bentonite, composite hydraulic permeabilities do not differ from pure bentonite values. Since pure bentonite as well as composite fabrics were found to be dispersed and deflocculated for both types of predominant exchangeable cations, an additional factor controlling fluid flow in case of monovalent exchangeable cations has to be considered, e.g., the influence of DDL formation on clay mineral surfaces on water viscosity, which has also been discussed by Olsen (1962). Thus, PAA^{o}-adsorption causing an increase in DDL extent, impacts composite macro-scale behaviour in terms of the hydraulic permeability in case of distinct DDL formation, i.e., monovalent exchangeable cations, whereas its impact is negligible in case of slight DDL formation, i.e., divalent exchangeable cations.

The effect of PAA^{-} composite formation on hydraulic permeability is of no significance, which is independent of the dominant clay mineralogy. This behaviour can be attributed to the fact, that in spite of the micro-scale alterations of the clay fabric in terms of E-F flocculation, the PSD remains unchanged, i.e., unimodal in case of Ca^{++}-bentonite and bimodal in case of kaolin. The respective units in both types of clays, i.e., stacks, particles and aggregates, persist regardless of their orientations. Thus, fluid flow paths are determined by the same type of pores in case of pure clays as well as clay-PAA^{-} composites, for which reason k as a function of the total void ratio remains unchanged.

With respect to the effect of polymer-to-clay ratio, the macro-scale hydraulic permeabilities of Ca^{++}-bentonite-PAA composites prepared with 10% of q_{max} equal the pure clay

values (Figure 5.6). Thus, in spite of slightly altered clay fabrics, which are indicated by composites volumetric behaviour (see section 5.3), fluid flow paths in dependence of global void ratio are widely unchanged.

5.5 Water retention

The results of unconfined water retention tests of clays and composites prepared with q_{max} are illustrated in Figure 5.7 - Figure 5.10. Thereby, S_r, w^* and e_{clay} versus suction plots are illustrated. With respect to material SWCCs, i.e., the fitting curves of S_r-Ψ relationships of the first drying curves generated according to the equation proposed by Fredlund & Xing (1994), the corresponding air entry values, Ψ_{AEV} (MPa), are listed in Table 5.3. The results can be summarized as follows:

Based on their respective SWCCs, the drying behaviour of pure clays in terms of their air entry values follows the order Na^+-bentonite > Ca^{++}-bentonite >> kaolin, which is in accordance to their respective plastic properties, i.e., the more plastic the clay, the greater the air entry value (Fredlund & Xing 1994), as well as to results obtained on similar materials in literature (e.g., Tripathy et al. 2014). Further, composite formation results in a decrease of Ψ_{AEV} in case of Na^+-bentonite, whereas it results in an increase of Ψ_{AEV} in case of Ca^{++}-bentonite and kaolin clay. Since the degree of saturation depends on the amount of water adsorbed as well as the void space in between solids related to the equilibrium state of the respective value of suction, the physico-chemical clay mineral surface characteristics as well as the clay fabric govern the desaturation behaviour. For this reason, the corresponding values of w^* and e_{clay} indicating the physico-chemical (polymer layered) clay mineral surface characteristics and the clay fabric, respectively, have to be taken into account in order to interpret the above findings on composite desaturation behaviour. In the low suction range of the first drying curve, composites have generally increased values of w^* and e_{clay}, while maintaining the saturated state. This is in accordance to the results on composites liquid limits and can be attributed to the same governing mechanisms, i.e., increased DDL repulsion as well as fabric flocculation, aggregation and steric stabilization, respectively, providing an increased pore space to be filled with water (for details see section 5.2). With increasing suction, composite w^*- and e_{clay}-values approach to their pure clay counterparts, whereas differing characteristics can be observed with varying clay mineralogy and polymer charge as follows:

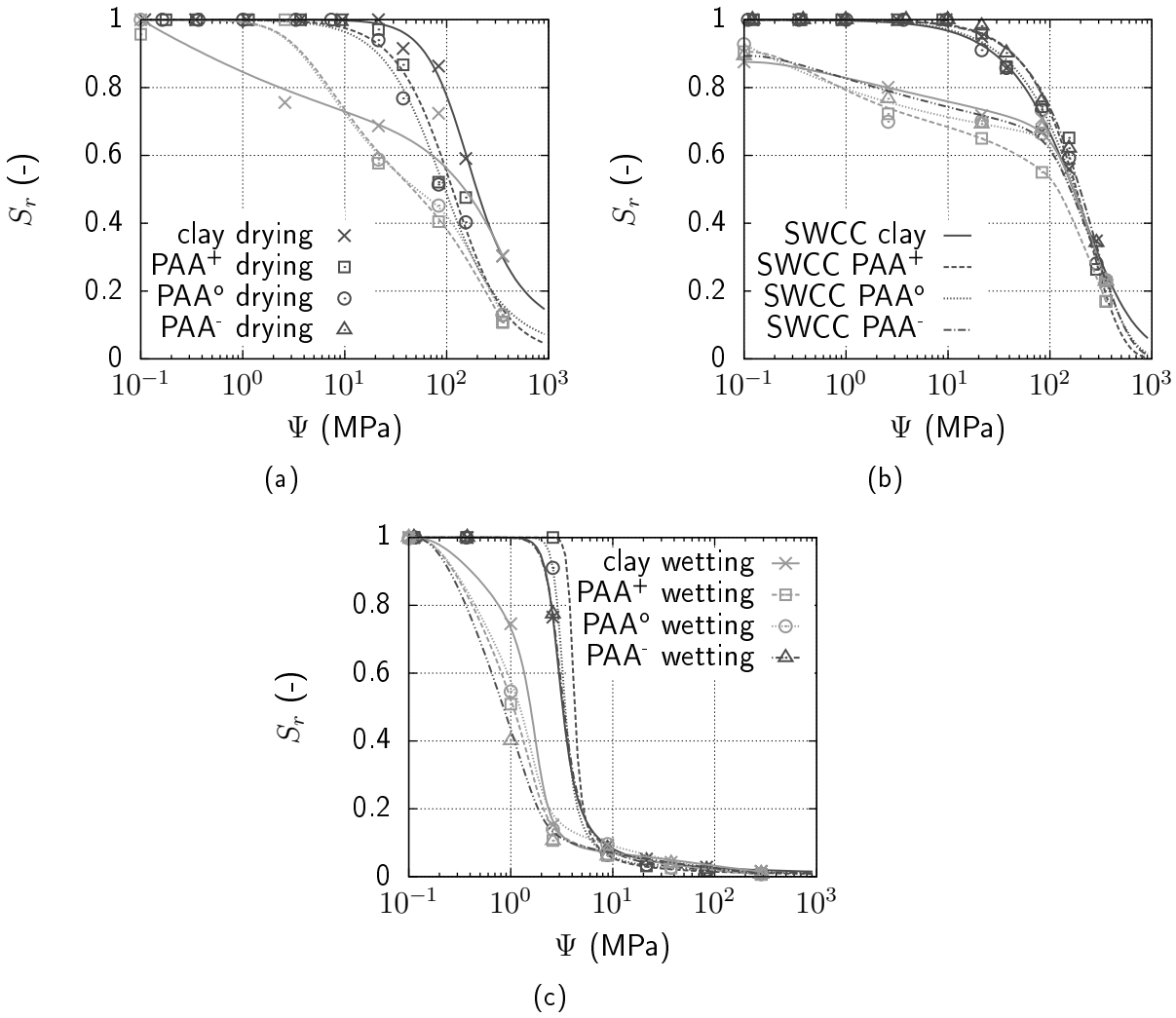

Figure 5.7: Degree of saturation versus suction plots of clays and composites prepared with a polymer-to-clay ratio of q_{max}: Na^{+}-bentonite (a); Ca^{++}-bentonite (b); kaolin (c).

Table 5.3: Air entry values of clays and composites.

	pure	PAA^+	PAA°	PAA^-
Na^+-bentonite prepared with q_{max}				
Ψ_{AEV} (MPa)	60	30	20	
Ca^{++}-bentonite prepared with q_{max}				
Ψ_{AEV} (MPa)	35	60	35	50
Ca^{++}-bentonite prepared with 10% of q_{max}				
Ψ_{AEV} (MPa)	35	35	35	45
kaolin prepared with q_{max}				
Ψ_{AEV} (MPa)	2.1	2.9	2.3	2.1

In case of bentonite-PAA^+ composites, drying curves of w^* cross their respective pure clay counterparts and have thus, decreased values of w^* in the high suction range (Figure 5.8a & 5.9a). Thereby, the corresponding suction at intersection is close to the individual air entry value of the respective composite. Values of e_{clay}, on the other hand, remain permanently increased in comparison to their pure clay counterparts (Figure 5.8b & 5.9b). Thereby, differences in e_{clay} correspond approximately to the volume occupied by the polymer in between clay mineral solids, i.e., ≈ 0.1 and ≈ 0.4 in case of Ca^{++}- and Na^+-bentonite, respectively. This finding indicates that fabric changes in terms of aggregation including the formation of bimodal PSDs, which have been observed microscopically and confirmed by macro-scale oedometer test results, do not persist in the high suction range > 20 MPa. This kind of fabric rearrangement can be attributed to the flexible characteristic of polymer chains, which has also been concluded from a significantly decreased shrinkage limit in case of the Na^+-bentonite-PAA^+ composite having a very high polymer-to-clay ratio and thus, a significant ratio of flexible solids. Further, since the shrinkage limit in case of the Ca^{++}-bentonite-PAA^+ composite having a moderate polymer-to-clay ratio was found to be increased due to the persisting dominance of fabric aggregation, the rearrangement of clay fabric is concluded to additionally depend on the drying rate, i.e., it is partly suppressed in case of rapid drying (shrinkage limit testing conditions), whereas it is permitted in case of moderate drying rates (water retention testing conditions). In summary, bentonite-PAA^+ composites are characterized by decreased values of w^* in the high suction range indicating significantly altered physico-chemical characteristics of the (polymer layered)

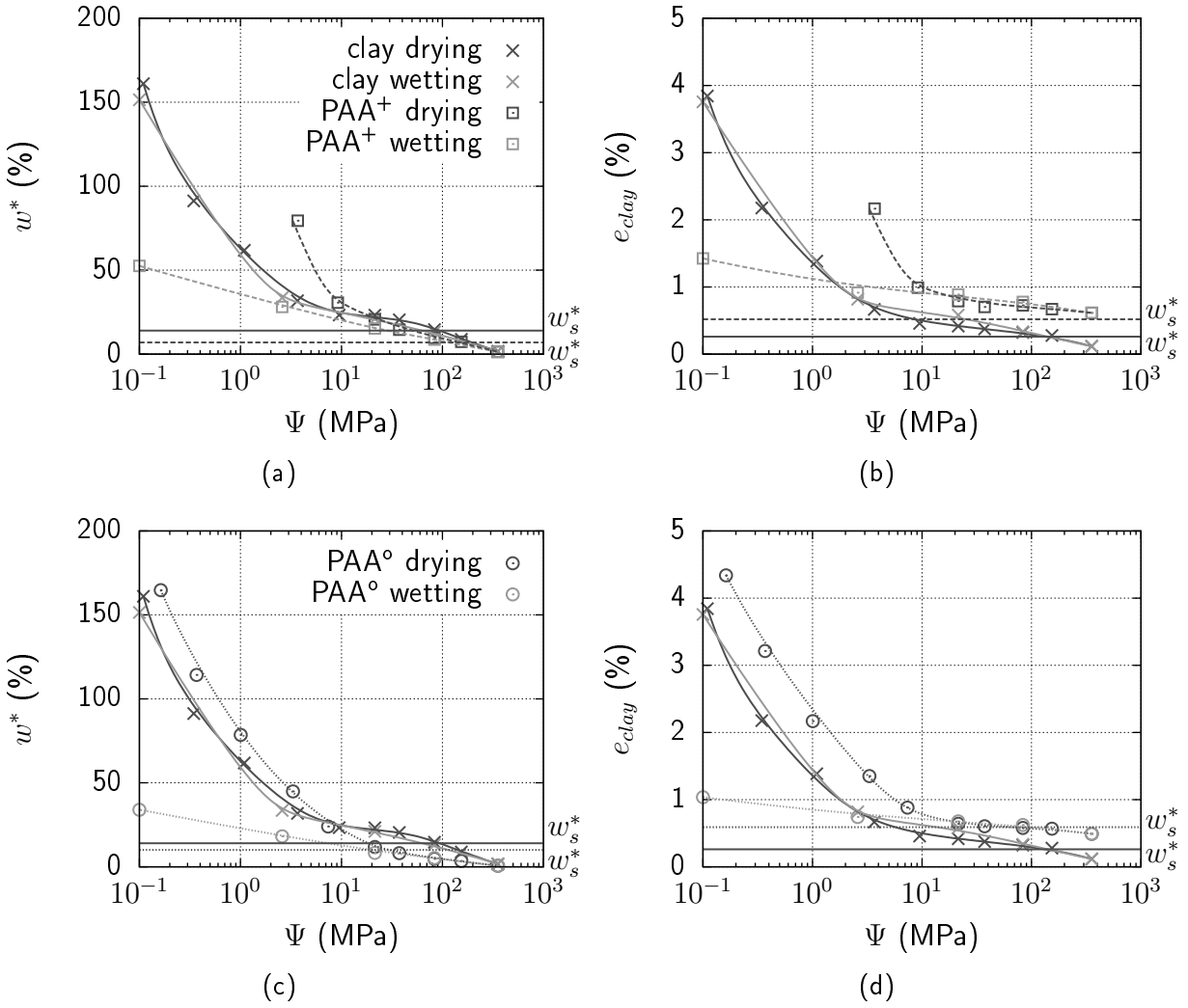

Figure 5.8: Water content and void ratio versus suction plots of Na^+-bentonite and its composites prepared with a polymer-to-clay ratio of q_{max}: PAA^+ (a) & (b); PAA° (c) & (d).

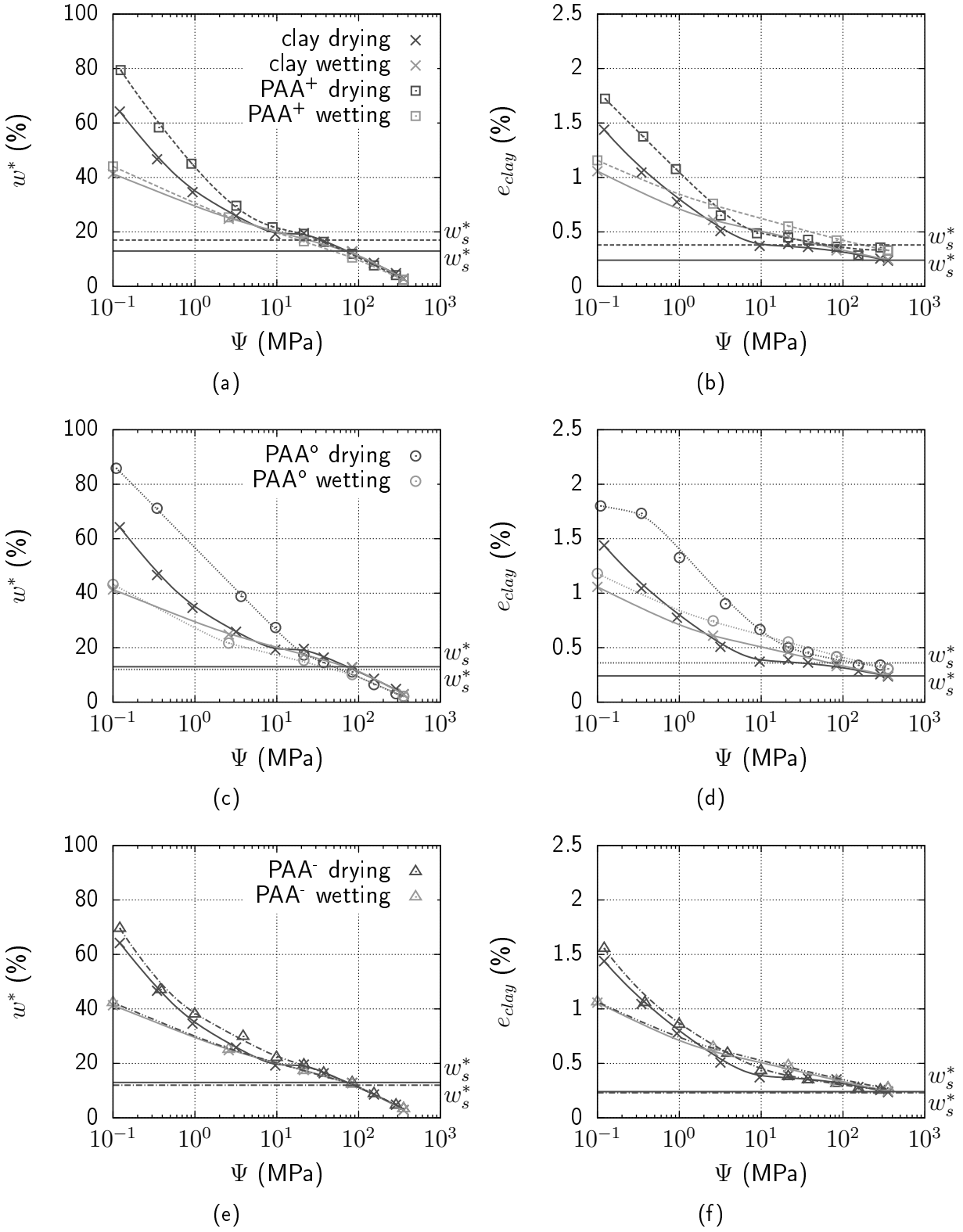

Figure 5.9: Water content and void ratio versus suction plots of Ca^{++}-bentonite and its composites prepared with a polymer-to-clay ratio of q_{max}: PAA^{+} (a) & (b); PAA° (c) & (d); PAA^{-} (e) & (f).

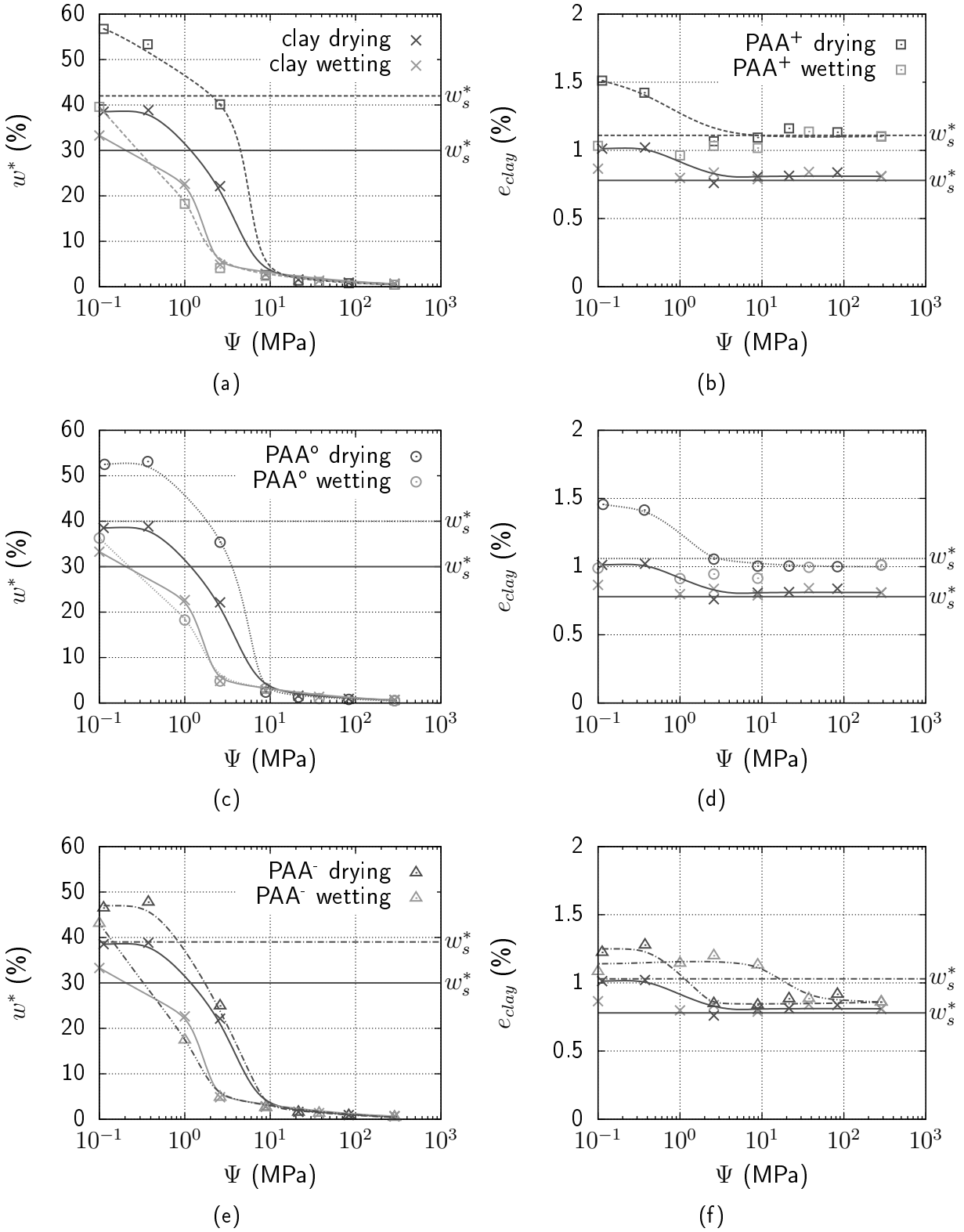

Figure 5.10: Water content and void ratio versus suction plots of kaolin and its composites prepared with a polymer-to-clay ratio of q_{max}: PAA$^+$ (a) & (b); PAA$^\circ$ (c) & (d); PAA$^-$ (e) & (f).

clay mineral surface in terms of its hydration. In addition, an approximate agreement of e_{clay}-values can be observed in the high suction range when taking into account the polymer volume between clay mineral solids. In consequence, Na^{+}-bentonite-PAA^{+} composite's air entry value is decreased since the amount of adsorbed water is decreased in the relevant suction range while the void volume between composite solids is equal to its pure clay counterpart. Ca^{++}-bentonite-PAA^{+} composite's air entry value, on the other hand, is increased, which can be attributed to the dominance of clay fabric rearrangement due to polymer chain flexibility in the relevant suction range of air entry. In case of the kaolin-PAA^{+} composite, differences in w^* in the high suction range are marginal, whereas e_{clay}-values of composites remain distinctly increased in comparison to the pure kaolin clay values (Figure 5.10a & 5.10b). Thus, polymer induced fabric rearrangement is of less significance in case of kaolinite dominated clays, which can be attributed to the distinctly lower amount of adsorbed polymer and thus, flexible solids. However, in the relevant suction range of air entry, i.e., in the medium suction range, an increase in composite w^* dominates the effect of an increase in e_{clay} resulting in an increase of Ψ_{AEV}. Thereby, based on micro-scale findings on the kaolin-PAA^{+} composite fabric, especially in terms of polymer shape in the adsorbed state (see Figure 4.6), the increase in w^* in the medium suction range can be attributed to the distinct interaction between non-adsorbed parts of the cationic polymer chain (trains and loops bridging aggregates) and water rather than an alteration of physico-chemical clay mineral surface characteristics since adsorption spots on kaolinite surfaces and thus, polymer layered surfaces are rarely.

In case of bentonite-PAA^{o} composites w^*- and e_{clay}-Ψ relationships of the first drying curves are very similar to the behaviour identified for bentonite-PAA^{+} composites, i.e., w^* drying curves of composites cross their respective pure bentonite counterparts and have thus, decreased values of w^* in the high suction range, whereas e_{clay}-values remain increased by approximately the volume of polymer between clay mineral solids (Figure 5.8c - 5.8d & Figure 5.9c - 5.9d). From the latter behaviour it can be concluded that polymer shape in the adsorbed state rearranges from its initial state, which is characterized by large loops and tails (see section 4.2), and reduces loop and tail sizes while increasing train parts with increasing suction. This is in accordance to the results of oedometer compression tests at maximum vertical loading. However, the deviations from pure bentonite behaviour in terms of w^* are more pronounced in case of PAA^{o} composites, whereas deviations in terms of e_{clay} are approximately equal since the volume of adsorbed non-ionic and cationic polymer, respectively, is in the same order of magnitude. The former finding can be attributed

to the differences in physico-chemical characteristics of the polymer layered clay mineral surface, i.e., clay mineral surface and exchangeable cation hydration is reduced in case of adsorbed PAA^{o} as compared to adsorbed PAA^{+}. This is caused by the fact that non-ionic polymer chains exclusively replace hydration water molecules, whereas cationic polymer chains additionally provide charge carriers, i.e., cationic monomers, which become hydrated with water molecules. Thus, the decrease in adsorbed water due to water molecule replacement by non-ionic monomers of the polymer chain is partially balanced in case of PAA^{+} by the hydration of cationic monomers of the polymer chain. Further, this difference in surface hydration accounts for the finding that $\Psi_{AEV}(PAA^{+}) > \Psi_{AEV}(PAA^{o})$ since the fabrics have become approximately equal in the relevant suction range of air entry. Similar to composite behaviour of bentonites, the kaolin-PAA^{o} composite is characterized by the same features as observed for the kaolin-PAA^{+} composite in terms of its w^{*}- and e_{clay}-Ψ relationships of the first drying curve (Figure 5.10c & 5.10d). However, in the relevant suction range of air entry, differences between PAA^{o} and PAA^{+} composites primarily exist in terms of w^{*}, whereas the respective e_{clay}-values are approximately equal, i.e., the water content of the PAA^{+} composite exceeds the water content of the PAA^{o} composite accounting for the finding that $\Psi_{AEV}(PAA^{+}) > \Psi_{AEV}(PAA^{o})$. This behaviour is in accordance to the differing interaction characteristics of non-adsorbed parts of the polymer chain with water, i.e., interaction in terms of DDL formation and hydration on polymer chain surfaces is increased in case of PAA^{+} as compared to PAA^{o}.

With respect to composites prepared with PAA^{-}, significant differences in terms of increased values of w^{*} and e_{clay} can be observed in case of kaolin composites in the low suction range < 1 MPa only (Figure 5.9e - 5.9f & Figure 5.10e - 5.10f). This is in accordance to the results of oedometer compression tests indicating that PAA^{-} composite micro-scale properties in terms of E-F flocculation are highly sensitive to the stress level. Further, the higher resistance of E-F flocculated F-F aggregates in case of kaolin as compared to E-F flocculated stacks in case of Ca^{++}-bentonite is confirmed by the results of water retention tests. However, slightly increased values persist along the whole suction range, indicating that (i) fabric rearrangement from the E-F flocculated state occurs imperfectly under isotropic stress conditions, which is indicated by e_{clay}, and (ii) interaction of non-adsorbed parts of PAA^{-} chains and water is significant, which is indicated by w^{*}. In consequence, composite SWCCs result in an increased value of Ψ_{AEV} in case of Ca^{++}-bentonite indicating that polymer chain-water interaction governs the macro-scale behaviour, whereas a nearly unchanged air entry value can be observed in case of kaolin, which can be attributed to

the very low amount of adsorbed polymer and thus, polymer chain-water interaction.

With respect to clay and composite (scanning) wetting curves, the effect of hysteresis in terms of decreased values of S_r, w^* and e_{clay}, respectively, as compared to the first drying curves can be observed independently on clay mineralogy and polymer charge. In spite of this behaviour, the fully saturated state is reached at the minimum applied suction of 0.1 MPa in case of Na^+-bentonite as well as kaolin clay, whereas in case of Ca^{++}-bentonite pure clay and composite S_r-values remain permanently below the value of 1.0 (Figure 5.7). Thus, a general irreversibility of the fully saturated state due to air entrapment and cracks as proposed e.g., by Fleureau et al. (2001) cannot be confirmed from the results obtained. However, when taking into account the corresponding w^*- and e_{clay}-Ψ relationships the following characteristics of pure clay and composite wetting behaviour can be observed:

Pure Na^+-bentonite wetting curves are characterized by the complete reversibility of w^* and e_{clay} drying curves, which is in accordance to the dominance of DDL repulsion in volume change behaviour (Bolt 1956). Thereby, it has to be noted that in case of oedometer compression and rebound tests, the e-$\log(p')$ relationship during compression was found to be irreversibly, which has been attributed to attractive forces dominating at small clay mineral surface separations and thus, preventing interlayer expansion during unloading. Since under anisotropic loading conditions clay mineral layer base surface orientations are assumed to be parallel attractive London-van der Waals forces are of great importance in case of oedometer tests. In case of isotropic loading, on the other hand, base surface orientations are randomly accounting for the insignificance of attractive forces in case of unconfined water retention tests and thus, complete reversibility during drying and wetting cycles. However, Na^+-bentonite composites differ significantly from pure bentonite behaviour, i.e., w^*- and e_{clay}-values of the wetting curves remain distinctly below the corresponding values of the drying curves (Figure 5.8). A similar behaviour has been observed during oedometer testing with distinctly decreased C_s-values in case of Na^+-bentonite composites. This behaviour has been mainly attributed to an increase in attractive (polymer layered) surface forces between parts of the adsorbed polymer chain and the opposing clay mineral surface. This mechanism of 'forced polymer bridging' is therefore of great importance with respect to both, isotropic and anisotropic (un)loading conditions. Obviously, in consequence of this mechanism, the fully saturated state is reached at a higher value of applied suction during the wetting process.

In case of Ca^{++}-bentonite as well as its composites w^*- and e_{clay}-Ψ relationships of the

wetting curves differ insignificantly from each other (Figure 5.9). Thus, polymer bridging at small surface separations as concluded from Na^+-bentonite composite wetting curves cannot be observed, which is in accordance to the results of oedometer rebound tests, i.e., nearly unchanged C_s-values. However, PAA^+ and PAA^o composites are characterized by slightly increased values of w^* and e_{clay} as compared to the pure Ca^{++}-bentonite behaviour indicating that the respective initial composite fabrics become partially reconstituted, whereas this tendency cannot be observed for the PAA^- composite, i.e., E-F flocculation is rearranged irreversibly during the drying process.

In case of kaolin composites, on the other hand, the effect of fabric reconstitution is most obvious for the PAA^- composite, whereas e_{clay}-values of kaolin-PAA^+ and -PAA^o composites remain approximately constant during wetting (Figure 5.10). However, since even in the high suction range of the drying process PAA^+ and PAA^o composite e_{clay}-values remain distinctly increased as compared to the pure kaolin clay values, it can be assumed that the initial fabrics (partially) persist during the complete process of drying and wetting accounting for the insignificance of fabric reconstitution during wetting. In consequence of initial fabric reconstitution and persistence, respectively, composite S_r-Ψ relationships during wetting are characterized by continously decrased values of S_r as compared to their respective pure clay counterpart. However, finally the fully saturated state is reached at the minimum applied suction of 0.1 MPa.

With respect to the effect of polymer-to-clay ratio, the macro-scale behaviour in terms of S_r-Ψ relationships of the first drying curve as well as the subsequent (scanning) wetting curve of Ca^{++}-bentonite-PAA composites prepared with 10% of q_{max} equals the pure clay behaviour (Figure 5.11). Thereby, w^*- and e_{clay}-Ψ relationships are characterized by slightly increased values in case of PAA^+ and PAA^o composites in the low suction range only (Figure 5.12). Thus, the alteration of physico-chemical (polymer layered) clay mineral surface properties as concluded from bentonite-PAA^+ and -PAA^o composites prepared with q_{max} is insignificant in case of the reduced polymer-to-clay ratio. Further, the influence of non-adsorbed parts of PAA^- chains in terms of their interaction with water is negligible.

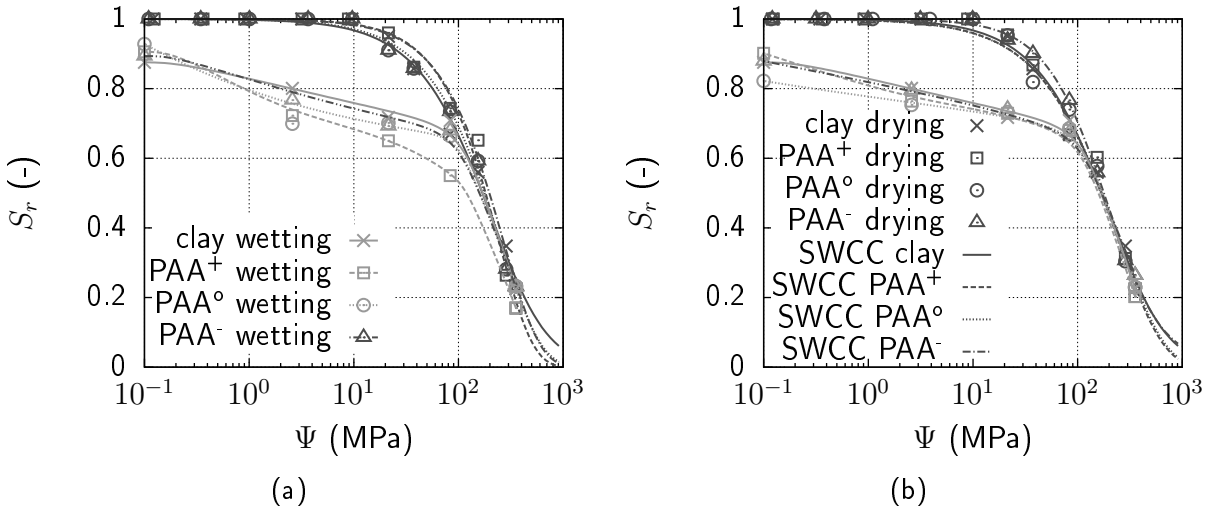

Figure 5.11: Degree of saturation versus suction plots of Ca^{++}-bentonite and its composites prepared with a polymer-to-clay ratio of q_{max} (a) and 10% of q_{max} (b).

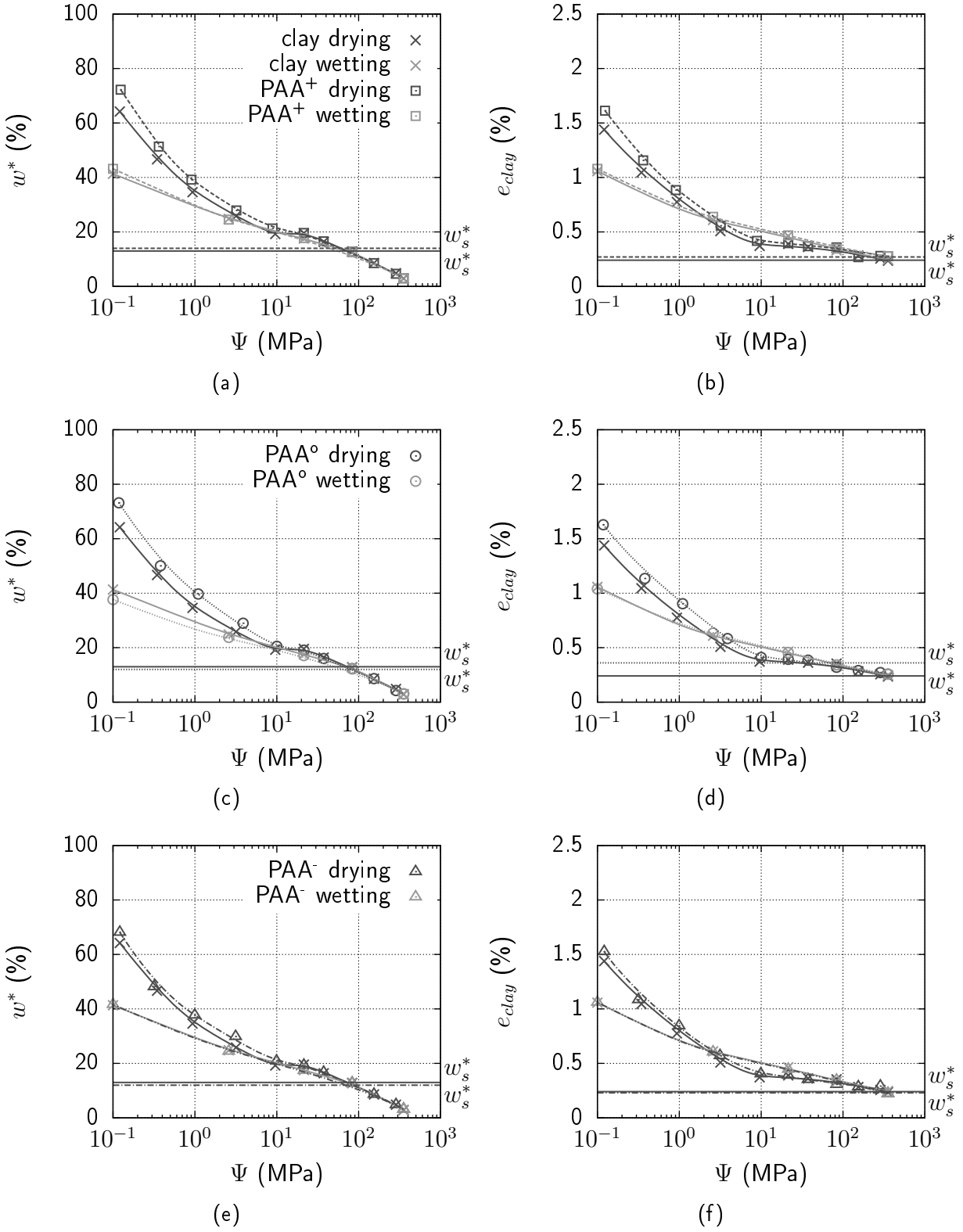

Figure 5.12: Water content and void ratio versus suction plots of Ca^{++}-bentonite and its composites prepared with a polymer-to-clay ratio of 10% of q_{max}: PAA^{+} (a) & (b); PAA° (c) & (d); PAA^{-} (e) & (f).

5.6 Summary

Macro-scale analysis of clays and clay-polymer composites has been performed including the experimental determination of materials' plastic properties, the volumetric behaviour and saturated hydraulic permeability by oedometer compression and rebound tests as well as the water retention by unconfined drying and wetting tests. The results can be summarized as follows:

In general, considerable agreement with the micro-scale findings has been found when taking into account established relations on micro- and macro-scale coupling. Thus, aggregated fabrics in case of PAA^+ adsorption on montmorillonite surfaces result in an increase of the liquid and shrinkage limits as well as the compressibility and hydraulic permeability. Flocculated fabrics as promoted by PAA^+ adsorption on kaolinite surfaces as well as PAA^- adsorption, on the other hand, have no influence on material hydraulic permeability since the development of preferential fluid flow paths is lacking, whereas the liquid and shrinkage limits as well as the compressibility are increased. Further, the micro-scale effect of non-ionic polymer adsorption, i.e., fabric dispersion and deflocculation due to increased DDL repulsion and steric stabilization, respectively, causes an increase in liquid limit and compressibility as well as a decrease in hydraulic permeability by reducing the maximum pore radii of the governing fluid flow paths. In addition, shrinkage limits are decreased in case of DDL repulsion being the governing effect of PAA^o adsorption (bentonite) and increased in case of steric stabilization being the governing effect of PAA^o adsorption (kaolin). With respect to composite water retention behaviour similar mechanisms can be observed, e.g., increased water contents and void ratios in the low suction range < 1 MPa due to fabric aggregation, flocculation, steric stabilization as well as increased DDL repulsion. In addition, with increasing suction, especially in the partially saturated state, additional mechanisms have been observed, i.e., a decrease in (polymer layered) clay mineral surface hydration due to water molecule replacement by adsorbed PAA^+ and PAA^o chains in case of montmorillonite surfaces as well as increased water adsorption due to distinct interaction of non-adsorbed parts of polymer chains and water, which is relevant in case of PAA^- adsorption as well as PAA^+ and PAA^o adsorption on kaolinite surfaces. Finally, due to the versatile effects participating in the water retention behaviour, composite SWCCs have various tendencies, i.e., the resulting air entry values are increased in case of Na^+-bentonite, whereas they are decreased in case of Ca^{++}-bentonite and kaolin.

However, in addition to the findings showing good agreement between micro- and macro-scale composite properties some unique features related to the presence of adsorbed polymer chains have been identified:

- In case of high polymer-to-clay ratios (Na^{+}-bentonite) the flexibility of polymer chains may cause complete clay fabric rearrangement with increasing loading to the point of minimum void space between clay mineral layer and polymer chain solids. In addition, during subsequent unloading the mechanism of 'forced polymer bridging' between clay mineral surfaces is obvious, which is manifested in distinctly decreased values of C_s as well as distinct hysteresis in case of water retention wetting curves.

- Even with very low polymer-to-clay ratios in case of PAA^{-} composites, flocculated clay fabrics are highly sensitive to the stress level. Thereby, E-F flocculation of stacks (Ca^{++}-bentonite) becomes destroyed at vertical loadings of about 100 kPa, whereas E-F flocculation of aggregates (kaolin) persists up to isotropic suction loadings of about 10 MPa.

- The redistribution of non-ionic polymer shape in the adsorbed state with increasing loading, i.e., loop and tail sizes become reduced, whereas train segments are increased, is obvious from composite volumetric behaviour under anisotropic oedometer testing conditions as well as isotropic unconfined water retention testing conditions.

6 Theoretical analysis

6.1 General

In the following chapter, the hydro-mechanical behaviour of clays and composites is analyzed theoretically by use of classical approaches on micro- and macro-scale coupling in clays, i.e., DDL theory and cluster model. With respect to the former approach, the volumetric behaviour of bentonites as well as bentonite-PAA^{o} composites is calculated theoretically and compared to the experimental results of oedometer compression tests performed on clay and composite slurries. Therefore, based on a modified form of the fundamental differential equation of the diffuse double-layer proposed by Brooks (1973) new equations for calculating the electric potential as a function of distance to clay mineral surfaces having adsorbed layers of non-ionic polymers are presented by solving the nonlinear differential equation. With respect to cluster model approach, the hydraulic permeability of pure clays as well as clay-PAA^{o} and -PAA^{+} composites obtained by oedometer time-compression test results are recalculated by theory. Thereby, special focus is set on the resulting values of fitting parameters characterizing clay and composite fabric in order to compare the theoretical results with micro-scale characteristics of clay and composite fabrics summarized in Figure 4.5 and Figure 4.6. Parts of the results presented in the following have been published in (Haase & Schanz 2015, Haase & Schanz 2016).

6.2 Physico-chemical approach

6.2.1 Theoretical solution for the determination of bentonite-non-ionic polymer composite volumetric behaviour

The following solutions are based on the modified form of the fundamental nonlinear differential equation of the diffuse double-layer at charged surfaces proposed by Brooks (1973) taking into account adsorbed layers of non-ionic polymers, i.e., Equation 2.11. Thereby, in accordance to the author's suggestion, $\beta(x)$ is simplified by a step function. Thus, by use of the substitutions introduced in Equation 2.2, the fundamental differential equations in region 1 ($\beta(x) = \beta$) and region 2 ($\beta(x) = 0$) read:

$$\left(\frac{d^2y}{d\xi^2}\right)_1 = \sinh(y - \beta) \qquad 0 \leq \xi \leq \xi_{d_p} \tag{6.1}$$

$$\left(\frac{d^2y}{d\xi^2}\right)_2 = \sinh(y) \qquad \xi_{d_p} < \xi \tag{6.2}$$

By use of the boundary conditions that for

(1) $\xi = \infty$: $y_1 = y_2 = 0$, $(dy/d\xi)_1 = (dy/d\xi)_2 = 0$ and $\beta = 0$

the following semi-analytical solutions for the potential functions $y_{1,2}$ can be found:

$$y_1 = \beta + 2\ln\left[\coth\left(\frac{1}{2}(\xi - C_1)\right)\right] \tag{6.3}$$

$$y_2 = 2\ln\left[\coth\left(\frac{1}{2}(\xi - C_2)\right)\right] \tag{6.4}$$

where the integration constants C_1 and C_2 can be derived by the boundary conditions that for

(2) $\xi = \xi_{d_p}$: $y_1 = y_2$ and

(3) $(\sigma\nu e)/(\epsilon\kappa kT) = (dy/d\xi)_{1,\xi=\xi_{dp}} - (dy/d\xi)_{1,\xi=0} - (dy/d\xi)_{2,\xi=\xi_{dp}}$:

$$C_2 = \ln\left(\frac{\coth\left(\frac{1}{2}\left(\xi_{dp} - C_1\right)\right)\sqrt{e^{\beta}} - 1}{\coth\left(\frac{1}{2}\left(\xi_{dp} - C_1\right)\right)\sqrt{e^{\beta}} + 1}\right) + \xi_{dp} \tag{6.5}$$

$$\begin{aligned}\left(\frac{\sigma\nu e}{2kT\kappa\epsilon}\right) = &-\sinh\left(\ln\left[\coth\left(\frac{\xi_{dp} - C_1}{2}\right)\right]\right) \\ &+\sinh\left(\ln\left[\coth\left(-\frac{C_1}{2}\right)\right]\right) \\ &+\sinh\left(\ln\left[\coth\left(\frac{\xi_{dp} - C_2}{2}\right)\right]\right)\end{aligned} \tag{6.6}$$

By this approach, the electric potential as a function of distance to the clay mineral surface refers to single DDLs. However, in the context referred to in the present study, the condition of interacting DDLs is of specific significance. Therefore, Equation 2.9 is used to correlate $\Psi'_{x=d}$, i.e., the electric potential calculated for a single DDL at distance d to the charged surface, to its corresponding value of Ψ'_d, i.e., the electric potential at the midplane calculated for interacting DDLs of charged surfaces separated by distance $2d$. Similarly, for calculating the midplane potential between pure clay mineral surfaces without having layers of adsorbed polymers, the approach of calculating $\Psi'_{x=d}$ for single DDLs (Equation 2.4) and subsequently converting it to its corresponding value of Ψ'_d (Equation 2.9) is used. The suitability of this method is illustrated in Figure 6.1 showing good agreement between the empirical relationship proposed by Bharat et al. (2013), i.e., $\Psi'_d = f(\Psi'_{x=d})$, and the results obtained based on numerical calculations of interacting DDLs as proposed by Tripathy et al. (2004) for typical clay-water conditions. On the other hand, by summation of the potentials of two single DDLs at the midplane as proposed by van Olphen (1963) for weak interaction, i.e., $\Psi'_d = 2\Psi'_{x=d}$, the results deviate significantly from the exact solution in case of surface separations < 800 Å (Figure 6.1). Finally, $2d$-$\log(p)$ relationships are obtained by use of Equation 2.10, i.e., by relating the midplane potential, Ψ'_d, to its corresponding repulsive pressure, p. The procedure for calculating $2d$-$\log(p)$ relationships of bentonites and bentonite-PAA^{o} composites is summarized in Figure 6.2.

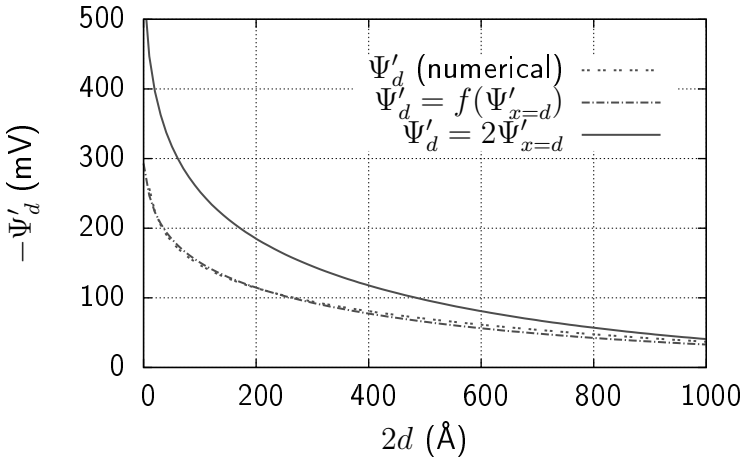

Figure 6.1: Electric potential at the midplane versus surface separation plots following (i) Equation 2.4, where $\Psi'_d = 2\Psi'_{x=d}$, (ii) Equation 2.6, where $\sigma = const.$ and (iii) Equation 2.4, where $\Psi'_d = f(\Psi'_{x=d})$ (Equation 2.8) with n_0 = 10^{-4} mol/l, ν = 1, ϵ = 7.1·10^{-10} C^2/Jm, T = 298 K and σ = -0.125 C/m^2.

6.2.2 Determination of bentonite-PAA^o composite volumetric behaviour

In order to determine bentonite-PAA^o composite volumetric behaviour theoretically by use of the equations proposed in the previous subsection, special attention is turned on the two unknown parameters of the clay-polymer-water system, i.e., the thickness of the adsorbed non-ionic polymer layer, d_p, as well as the polymer-electrolyte interaction parameter, β. In Figure 6.3 the influence of both parameters is illustrated for typical conditions of the clay-polymer-water system. Obviously, with increasing values of both, d_p and β, the electric potential at the midplane of two opposing polymer layered clay mineral surfaces separated by a certain distance, $2d$, and thus, the repulsive pressure is increased. Thereby, d_p is increased with increasing loop and tail size of the adsorbed polymer chain, whereas β is increased with increasing density of the adsorbed polymer layer (ϕ_p) as well as with increasing interaction of polymer and ions with water (χ_{sp}, χ_{si}) and decreasing interaction between ions and polymer (χ_{ip}). It is noteworthy that the latter components governing the value of β, i.e., the interaction parameters, χ, are constant for a given clay-polymer-water system. The former component governing the value of β, ϕ_p, as well as the value of d_p, on the other hand, may vary with varying polymer layered clay mineral surface separation, especially in case of extensive loop and tail sizes in the initial state. Theoretically, these

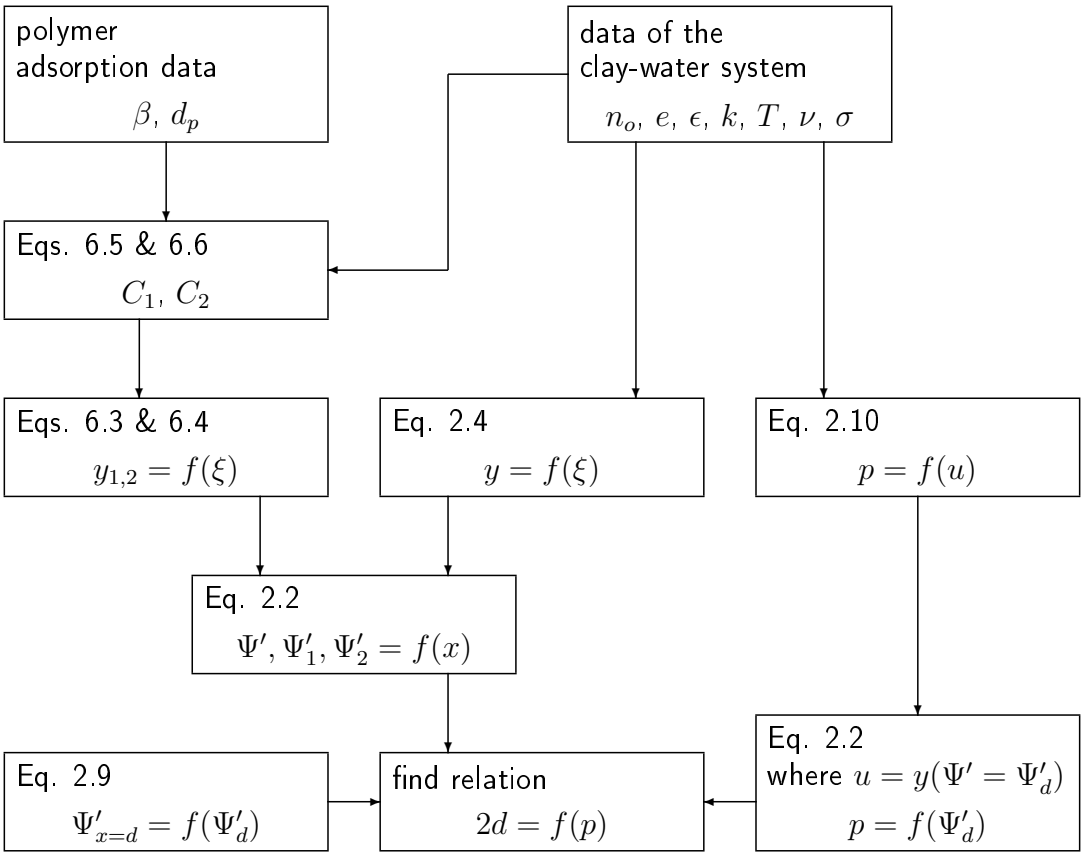

Figure 6.2: Flow chart showing the determination of $2d$-log(p) relationships of bentonites (having non-ionic polymer layered clay mineral surfaces) by use of (modified) DDL theory.

variations occur since the persistence of, e.g., $d_{p,0} = 100$ Å is unlikely in case of $2d < 200$ Å due to polymer overlapping and becomes sterically impossible in case of $2d < 100$ Å. Practically, these variations have been concluded from the experimental results on macro-scale composite behaviour (see chapter 5). Thereby, in consequence of a decrease in d_p, ϕ_p and thus, β increases.

In Figure 6.4 the experimental results of bentonite and bentonite-PAA^o composite volumetric behaviour obtained by oedometer compression tests are illustrated and compared to the theoretical $2d$-log (p) relationships obtained by use of the (modified) approach based on DDL theory according to the procedure given in Figure 6.2. Thereby, calculation of

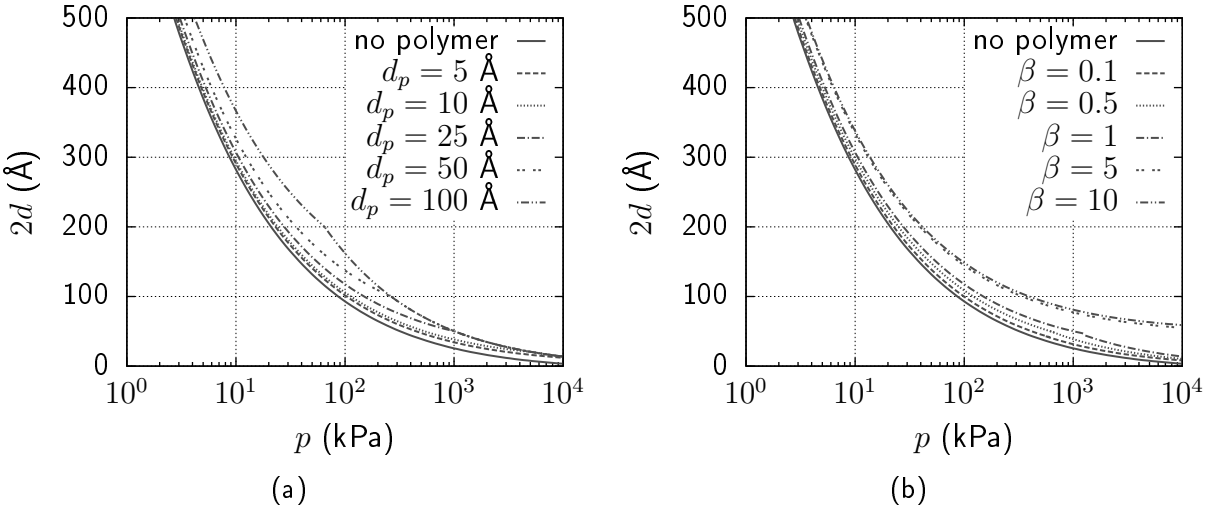

Figure 6.3: Surface separation versus repulsive pressure plots of bentonites (having non-ionic polymer layered clay mineral surfaces) following the procedure given in Figure 6.2 with n_0 = 10^{-4} mol/l, $\nu = 1$, ϵ = 7.1·10^{-10} C^2/Jm, T = 298 K and σ = -0.125 C/m^2: Influence of d_p with $\beta = 1$ (a); Influence of β with $d_p = 25$ Å (b).

$2d$-values follows the approximation given by Bolt (1956) for saturated clays:

$$e_{clay} = G\rho_w 10^6 Sd \tag{6.7}$$

For pure bentonites, it is obvious that by theoretical analysis, surface separation is overestimated as compared to the experimental results. This is in accordance to previous observations, e.g., by Schanz et al. (2013) and Tripathy et al. (2013), for the pressure range tested in this study. In case of Ca^{++}-bentonite, the discrepancies between theoretical and experimental results, especially in the low pressure range up to 400 kPa, are more significant in comparison to the Na^{+}-bentonite. For montmorillonites having predominantly divalent exchangeable cations, these great discrepancies have already been observed, e.g., by Blackmore & Warkentin (1960) and Schanz & Tripathy (2009). In the former study, it was suggested that due to divalent exchangeable cations and thus, increased attractive forces between cations and negatively charged clay mineral surfaces, stacks of montmorillonite layers are present with DDLs only acting at their outer surfaces. The conventional approach, on the other hand, suggests complete layer separation with DDLs also acting at the inner surfaces. From PAA^{+} adsorption test results, stacks with an average amount of 5 montmorillonite layers were concluded to exist in Ca^{++}-bentonite. On this basis, the experimental $2d$-log (p) relationship is recalculated by fixing 4/5 of the layer distances to

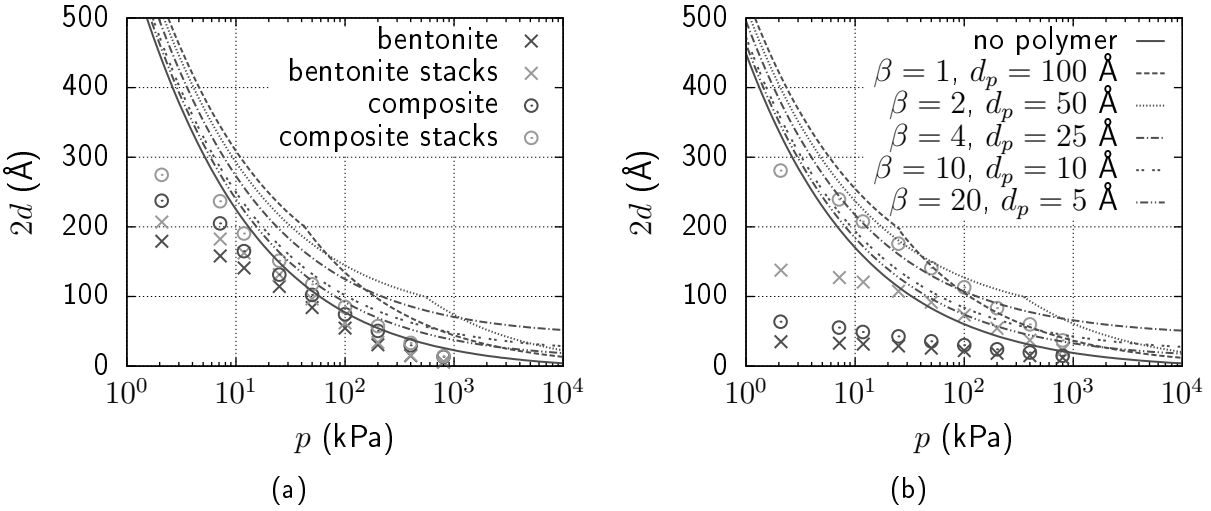

Figure 6.4: Surface separation versus repulsive pressure plots of bentonites and bentonite-PAA° composites prepared with a polymer-to-clay ratio of q_{max} based on (i) experimental oedoemter compression test results with $p = p'$ and (ii) theoretical analysis following the procedure given in Figure 6.2: Na^+-bentonite (a); Ca^{++}-bentonite (b).

$2d = 9.4$ Å (Mitchell & Soga 2005), i.e., the maximum layer separation when exchangeable cations are hydrated, and calculating layer separations between stacks. The results are also shown in Figure 6.4 indicating that overestimated layer separations as obtained by DDL theory can be explained by this approach, i.e., agreement between theoretical and experimental results increases significantly. Similarly, in case of Na^+-bentonite, which has few divalent exchangeable cations as well, an average amount of 1.2 montmorillonite layers per stack was calculated based on PAA^+ polymer adsorption and the respective corrections to the experimental results are plotted in Figure 6.4. Generally, the prediction of bentonite volumetric behaviour by use of DDL theory is limited, even though a good approximation can be given for the stress range investigated in this study. Thereby, the limitations can be attributed to the assumptions of DDL theory, rather than additional acting forces, which have been found to be insignificant for the layer separations studied (for details see subsection 2.4.1), i.e., discrepancies between theory and experiments in the low pressure range < 25 kPa can be mainly attributed to existing deviations from perfectly parallel clay mineral surface orientations. However, in the medium pressure range (25 - 400 kPa), good agreement between experimental and theoretical $2d$-$\log(p)$ relationships can be observed for both types of bentonites.

Taking into account the limitations of DDL theory in reproducing bentonite volumetric

behaviour accurately, especially in the low pressure range < 25 kPa, the modified approach proposed in the present study for the calculation of bentonite-PAA^o composite volumetric behaviour gives a good approximation to the experimental results (Figure 6.4). Thereby, the aforementioned behaviour of polymer shape in the adsorbed state during compression is confirmed by theory, i.e., d_p has to be considered as a function of interlayer distance rather than a constant since experimentally, composite $2d$-values tend to approach to their respective pure bentonite counterpart with increasing pressure, which is vice versa by theoretical treatment assuming constant values of d_p and β. Thus, d_p decreases with decreasing $2d$ and adsorbed polymer shapes tend to reduce loop and tail extensions while increasing train segments with decreasing surface separation. In consequence, the value of β increases by the same factor as d_p decreases since in the special case treated in the present study it can be assumed that $\phi_{pb} = 0$. On this basis, bentonite-PAA^o composite volumetric behaviour can be reproduced by modified DDL theory according to the following procedure:

1. From experimental results in the high pressure range, i.e., at very small surface separations with sterically restricted polymer layer extension, d_p is estimated in its residual state ($d_{p,res} \approx 5$ Å).

2. The corresponding value of β is derived by fitting so that the experimental behaviour of composites is matched within the limitations of classical DDL theory ($\beta_{res} \approx 20$).

3. Various states of the polymer layered clay mineral surface during compression in terms of $d_{p,i}$ and β_i are calculated, where $\beta_i = d_{p,res}/d_{p,i} \cdot \beta_{res}$.

The resulting $2d$-log (p) relationships for various states of the polymer layered clay mineral surface are illustrated in Figure 6.4. Obviously, composite volumetric behaviour as found from experiments can be reproduced quite accurately by modified DDL theory in the medium pressure range (25 - 400 kPa) with β varying between 1 and 20 and d_p varying between 100 and 5 Å.

6.3 Cluster model

Figure 6.5 - 6.7 summarize the results on reproducing clay and composite hydraulic permeability as a function of total void ratio theoretically by use of (i) Kozeny-Carman approach

as well as (ii) cluster model approach. Since the experimental results obtained in case of Na^+-bentonite cannot be reproduced accurately detailed analysis and discussion is limited to Ca^{++}-bentonite and kaolin as well as their respective composites. It is supposed that due to the great influence of physico-chemical forces acting at montmorillonite surfaces having predominantly exchangeable Na^+ cations, additional factors, such as the decreased viscosity of water in the near-field of clay mineral surfaces, have to be taken into account in order to express hydraulic permeability by theoretical relations. Similar conclusions were drawn from the macro-scale finding of reduced hydraulic permeabilities due to PAA^o adsorption in case of Na^+-bentonites only (see section 5.4). In case of Ca^{++}-bentonite and kaolin, on the other hand, the experimental results can be reproduced quite accurately by cluster model theory, whereas by use of the Kozeny-Carman approach great discrepancies between experiments and theory can be identified.

With respect to the cluster model approach, the influence of the unknown parameters N. i.e., the number of particles per cluster, and $e_{c.initial}$, i.e., the initial intra-cluster void ratio, is illustrated taking into account the individual clay mineralogical conditions. Finally, the resulting $\log(k)$-e_{clay} relationships based on parameter fitting according to the boundary conditions given in subsection 3.5.2 are shown graphically and the corresponding fitting parameters are summarized in Table 6.1. It is obvious that the conclusions derived qualitatively by phenomenological analysis of clay and composite hydro-mechanical behaviour as well as their micro-scale characteristics agree with the quantitative results obtained. For both clays, the increase in cluster particle number due to PAA^+ adsorption, i.e., from 60 to 400 (Ca^{++}-bentonite) and from 80 to 1200 (kaolin), is significant. In addition, the kaolin-PAA^o composite has a distinctly reduced value of N, i.e., 1.5, whereas it remains

Table 6.1: Cluster model fitting parameters of Ca^{++}-bentonite and kaolin as well as their respective PAA^+ and PAA^o composites.

	pure	PAA^+	PAA^o
Ca^{++}-bentonite prepared with q_{max}			
N (-)	60	400	60
$e_{c,0}$ (-)	0.9	0.8	0.8
kaolin prepared with q_{max}			
N (-)	80	1200	1.5
$e_{c,0}$ (-)	1.1	2.1	1.7

constant in case of Ca^{++}-bentonite. It has to be noted that the values of N refer to mineral layers in case of bentonite, whereas they refer to particles in case of kaolin. This is caused by the differences in clay mineral surface accessibility of the predominant clay minerals kaolinite and montmorillonite, respectively, during SSA measurements since this parameter is incorporated in the calculations. The results on N values reveal that the formation of aggregated fabrics is the main reason for increased hydraulic permeabilities due to PAA^{+} adsorption in case of Ca^{++}-bentonite. Further, in case of kaolin, PAA^{o} adsorption causes an increase in clay particle dispersion accounting for significantly decreased hydraulic permeabilities. These findings completely agree to the micro-scale observations on clay and composite fabrics, summarized in Figure 4.5 & Figure 4.6. Similarly, the information obtained on $e_{c,0}$ confirms the experimental findings on micro- and macro-scale. The kaolin-PAA^{+} composite fabric derived by microscopic investigation was found to be characterized by E-F and E-E flocculated small F-F associated aggregates. As a result, the intra-aggregate pores were concluded to be altered due to the formation of an additional pore size fraction, i.e., intra-aggregate pores between small aggregates, whereas the inter-aggregate pore-system controlling fluid flow remains nearly unaffected. This interpretation is confirmed by the increase in initial intra-cluster void ratio, $e_{c,0}$, i.e., from 1.1 to 2.1 due to PAA^{+} composite formation with kaolin. The kaolin-PAA^{o} composite, on the other hand, is characterized by a dispersed fabric, for which reason the increase in $e_{c,0}$ from 1.1. to 1.7 approximately equals the increase in total void ratio, caused by steric stabilization due to non-ionic polymer adsorption. In case of Ca^{++}-bentonite, the initial intra-cluster void ratio remains approximately constant due to polymer adsorption leading to the conclusion that clay mineral layer surface orientations remain unaffected by the overall state of the clay fabric, i.e., dispersed in case of pure Ca^{++}-bentonite as well as its PAA^{o} composite and aggregated in case of Ca^{++}-bentonite-PAA^{+} composite. This is in accordance to the microscopic observations in terms of clay mineral layer/stack orientation in bentonites as well as its PAA^{+} and PAA^{o} composites (see section 4.3).

It is noteworthy that the N-value obtained by fitting amounts 80 in case of Ca^{++}-bentonite as well as its PAA^{o} composite. Thus, the value of 5 stacked montmorillonite layers derived from PAA^{+} adsorption tests is exceeded significantly indicating that in spite of clay fabric dispersion preferential fluid flow paths develop between small assemblages of stacks.

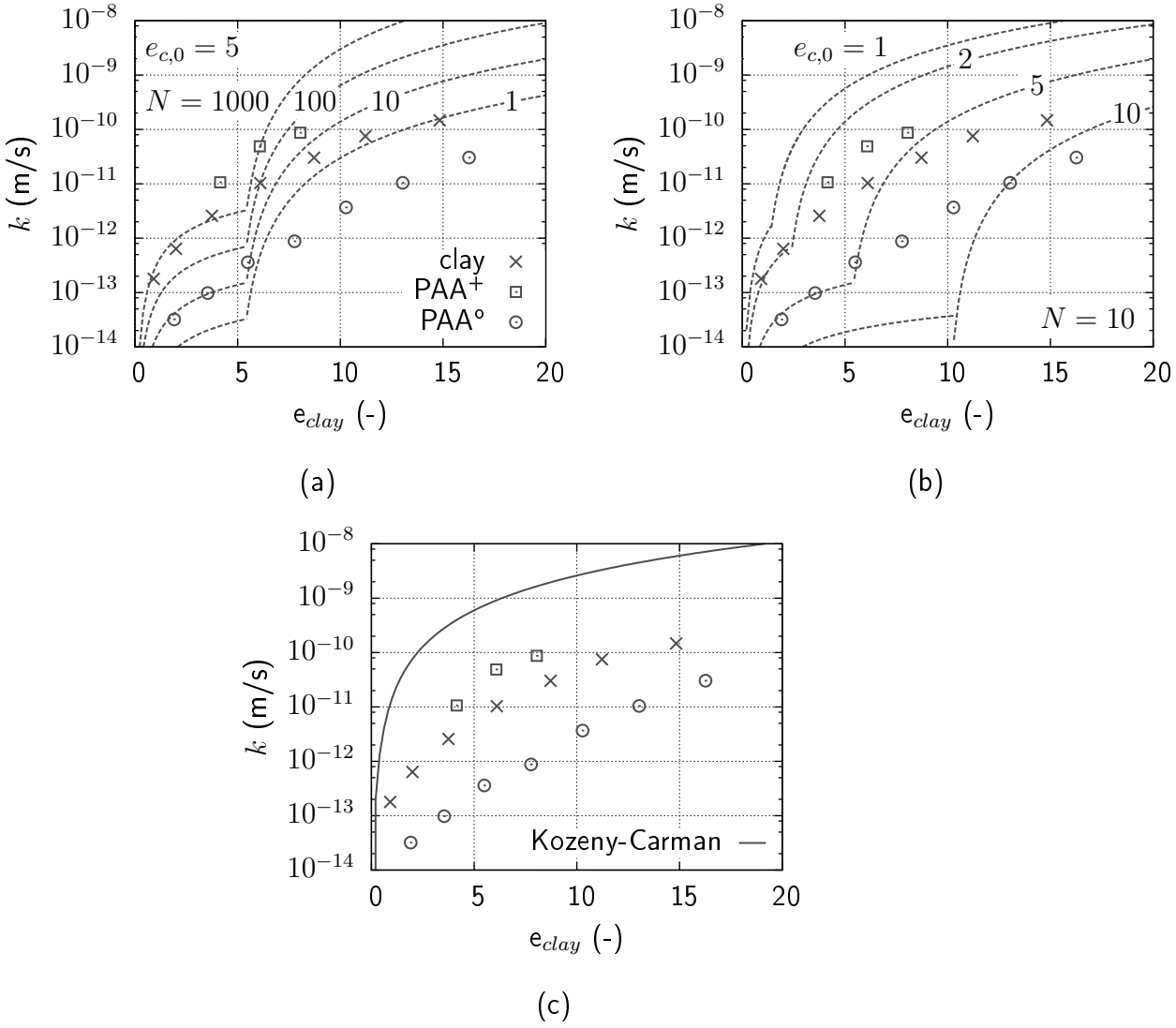

Figure 6.5: Hydraulic permeability versus void ratio plots of Na^+-bentonite and Na^+-bentonite-PAA^+- and -PAA° composites prepared with a polymer-to-clay ratio of q_{max} based on (i) experimental oedometer time-compression test results and (ii) theoretical analysis with $k = k_{CM}$ and $k = k_{KC}$: Influence of N according to cluster model approach (a); Influenece of $e_{c,0}$ according to cluster model approach (b); theoretical relationship according to Kozeny-Carman approach (c).

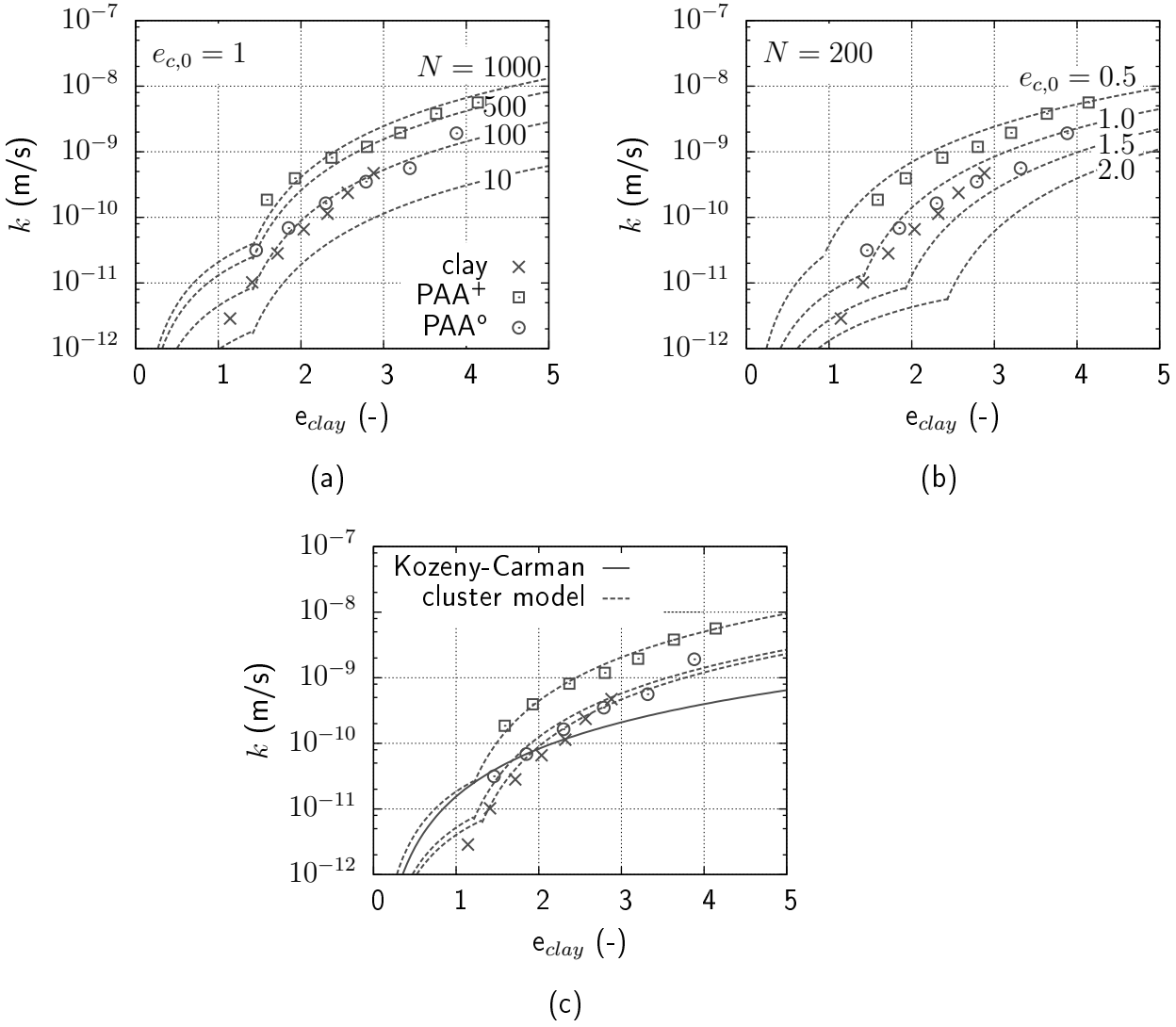

Figure 6.6: Hydraulic permeability versus void ratio plots of Ca^{++}-bentonite and Ca^{++}-bentonite-PAA^{+}- and -PAA° composites prepared with a polymer-to-clay ratio of q_{max} based on (i) experimental oedometer time-compression test results and (ii) theoretical analysis with $k = k_{CM}$ and $k = k_{KC}$: Influence of N according to cluster model approach (a); Influence of $e_{c,0}$ according to cluster model approach (b); best fit of experimental results by varying N and $e_{c,0}$, theoretical relationship according to Kozeny-Carman approach (c).

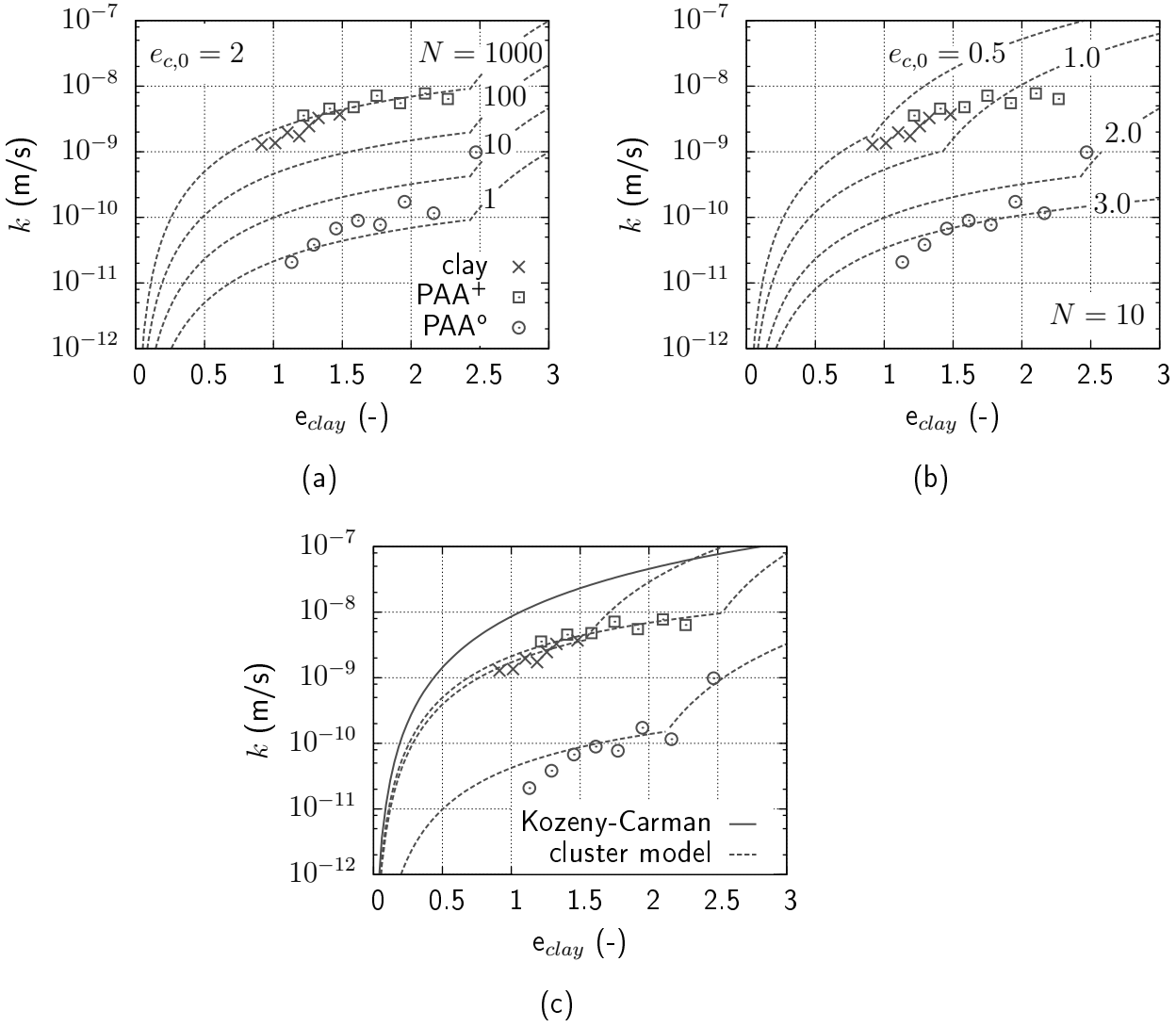

Figure 6.7: Hydraulic permeability versus void ratio plots of kaolin clay and kaolin-PAA$^+$- and -PAA° composites prepared with a polymer-to-clay ratio of q_{max} based on (i) experimental oedometer time-compression test results and (ii) theoretical analysis with $k = k_{CM}$ and $k = k_{KC}$: Influence of N according to cluster model approach (a); Influence of $e_{c,0}$ according to cluster model approach (b); best fit of experimental results by varying N and $e_{c,0}$, theoretical relationship according to Kozeny-Carman approach (c).

6.4 Summary

Clay and composite behaviour was analyzed based on classical theoretical multiscale approaches reproducing the micro- and macro-scale coupling in clays, i.e., diffuse double-layer theory and cluster model. Thereby, a set of equations was derived by solving the fundamental nonlinear differential equation of the diffuse double layer taking into account adsorbed layers of non-ionic polymers as proposed by Brooks (1973). Finally, by use of the novelly developed equations as well as the well known equations of classical DDL theory and cluster model the experimental macro-scale behaviour in terms of the volumetric behaviour of bentonite(-PAA^{o} composite)s as well as the hydraulic permeability of clay(-PAA^{+} and -PAA^{o} composite)s was analyzed with respect to the micro- and macro-scale coupling phenomena. The main findings are as follows:

The volumetric behaviour of bentonite-PAA^{o} composites has been reproduced quite accurately by use of the novelly developed equations when taking into account the well-known limitations of DDL theory, especially in terms of the deviations from perfectly parallel clay mineral layer surface orientation in the low pressure range. Thereby, a key finding concerns the rearrangement of polymer shape in the adsorbed state during compression, i.e., the extent of loop and tail segments decreases with increasing clay mineral layer surface approaching and thus, pressure, which is expressed by the thickness of the adsorbed non-ionic polymer layer, d_p. Consequently, the polymer-electrolyte interaction parameter, β, increases with increasing pressure. This behaviour accounts for the tendency in experimental bentonite-PAA^{o} composite behaviour to approach to the respective pure bentonite e-log (p') relationship with increasing pressure. An additional finding concerns the micro-scale observation in terms of layer stacking, which is macroscopically manifested in significantly reduced interlayer distances, $2d$, in case of predominantly divalent exchangeable cations. Thus, taking into account the presence of 5 stacked layers in case of Ca^{++}-bentonite as well as its composite with DDLs acting at the outer surfaces only, theoretical $2d$-log (p) relationships agree well with the experimental results.

With respect to clay and composite hydraulic permeability, theoretical analysis by use of cluster model approach confirmed the experimental findings on micro-scale fabric. Thus, aggregated (bentonite) and flocculated (kaolin) fabrics due to PAA^{+} adsorption as well as dispersed and deflocculated fabrics due to PAA^{o} adsorption were confirmed by the individual value of the fitting parameter N, i.e., the number of particles per cluster, which

was increased in case of aggregated and flocculated fabrics, whereas it was decreased in case of dispersed and deflocculated fabrics. Further, considerable agreement between the individual value of the fitting parameter, $e_{c,0}$, and the type of intra-cluster fabric deduced by microscopic investigation was found, i.e., intra-cluster E-E and E-F flocculation in case of the kaolin-PAA^{+} composite was confirmed by an increase in $e_{c,0}$, whereas constant clay mineral layer surface orientations in bentonites and its respective composites were indicated by an unchanged value of $e_{c,0}$ independently on the underlying fabric. However, in case of bentonites, the cluster model approach was successfully adopted in case of predominantly exchangeable Ca^{++} cations only. Thus, the exclusive dominance of clay fabric in governing the process of fluid flow, i.e., the cluster model approach, was found to be invalid in case of distinct DDL formation at clay mineral layer surfaces, i.e., in case of predominantly exchangeable Na^{+} cations.

7 Bentonite-polymer composites for geoenvironmental applications

7.1 General

In the following chapter, the influence of polymer addition on the hydraulic performance of Na^+-bentonite is investigated and discussed with respect to its application as barrier material in landfill lining. Therefore, cationic and anionic polymers are added with a polymer-to-clay ratio of 1% by weight. Further, with respect to the practical demands, composite preparation method is varied, i.e, dry powder mixing and solution intercalation, and its influence on hydraulic performance is investigated. Experimental investigation includes the determination of pure bentonite and composite hydraulic permeabilities, k_{H_2O} and k_{CaCl_2}, i.e., when permeated with deionized water and 0.5 M $CaCl_2$ solution, respectively. In addition, the relevance of index properties for estimating hydraulic permeability is veryfied. Therefore, pure bentonite and composite liquid limits and swelling pressures are determined and related to the respective values of hydraulic permeability. Thereby, the swelling pressure is determined instead of the classical swell index, although it is no index property. However, the general swelling behaviour can be derived from both, swelling pressure and swell index. Interpretation of the effect of polymer addition on macro-scale behaviour is based on the outcome of multiscale approach.

7.2 Liquid limits

Table 7.1 summarizes the values of liquid limits obtained on Na^+-bentonite-PAA^+ and -PAA^- composites prepared by (i) dry powder mixing (DP) and (ii) solution intercalation

(SI), respectively. Obviously, due to polymer addition an increase in w_l can be observed, which is most significant in case of PAA^- composites. Further, the effect of anionic polymer addition results in similar w_l-values for both types of preparation method. In case of PAA^+ addition, on the other hand, a moderate increase in w_l occurs in case of SI only, whereas the composite prepared by DP has a nearly unchanged liquid limit as compared to pure Na^+-bentonite. Taking into account the results obtained from multiscale approach, composite formation in case of Na^+-bentonite was found to be restricted to the cationic and non-ionic PAA, whereas PAA^- adsorption was not detected (see section 4.2). Thus, the insignificance of preparation method in case of PAA^- composites is plausible since polymer chains are located at similar positions within the clay matrix, i.e., in the pore system acting as individual solids. Thereby, the significant increase in liquid limits can be attributed to the high affinity of polymer chains to adsorb water, which is in accordance to the results of water retention tests on Ca^{++}-bentonite- and kaolin-PAA^- composites (section 5.5). It has to be noted that the procedure of SI adopted within the application-oriented approach differs from the procedure adopted within the multiscale approach in order to keep the non-adsorbed PAA^- within the Na^+-bentonite, i.e., the bentonite-polymer dispersion was dried to w_{opt} without preceding centrifugation. PAA^+ polymer chains, on the other hand, adsorb on clay mineral layer basal surfaces and the individual composite characteristics obviously differ with the variation in preparation method. In case of SI, the resulting fabric was found to be aggregated from multiscale approach, which accounts for the moderate increase in liquid limit. However, in consequence of DP, the dominance of clay fabric aggregation in micro- and macro-scale coupling behaviour cannot be confirmed from liquid limit test results.

Table 7.1: Liquid limits, w_l (%), of Na^+-bentonite and Na^+-bentonite-PAA composites prepared with a polymer-to-clay ratio of 1% by weight as well as by (i) dry powder mixing (DP) and (ii) solution intercalation (SI).

Na^+-bentonite	PAA^+ composite		PAA^- composite	
	DP	SI	DP	SI
588	602	750	941	971

7.3 Swelling pressure

In Figure 7.1 & Table 7.2 the results of swelling pressure tests are summarized. In the following, the great discrepancies observed in terms of the individual p_s-log($time$) relationships will not be considered since their interpretation is beyond the scope of the present research. However, with respect to the individual swelling pressure values reached in equilibrium, significant deviations from pure Na^+-bentonite behaviour can be observed in case of the PAA^+ composite prepared by DP as well as the PAA^- composite prepared by SI, i.e., the swelling pressures, p_s, are decreased. The PAA^+ composite prepared by SI as well as the PAA^- composite prepared by DP, on the other hand, have nearly unchanged values of p_s, i.e., they are slightly increased. Taking into account classical relations between the properties liquid limit and swelling behaviour in the context of estimating bentonite hydraulic barrier performance these results are not in agreement with consistently increased w_l-values. However, it has to be considered that the respective testing boundary conditions differ from each other: (i) liquid limit testing conditions imply a 'closed system' with a constant polymer-to-clay ratio, whereas swelling pressure testing conditions allow for a reduction in polymer-to-clay ratio by leaching of non adsorbed polymer chains during the water saturation process, which is of great importance in case of PAA^- composites; (ii) in case of composites prepared by DP, liquid limit testing conditions include polymer adsorption in the state of clay fabric dispersion since the water contents allow for complete clay mineral layer separation, whereas swelling pressure testing conditions include polymer adsorption within an existing clay fabric corresponding to the initial state of sample preparation, i.e., to optimum proctor conditions. The latter boundary condition during swelling pressure testing accounts for the decrease in p_s in case of the PAA^+ composite prepared by DP since initially aggregated and flocculated clay units are stabilized by a 'coat of paint' due to polymer adsorption (Greenland 1963) preventing clay mineral interlayer expansion

Table 7.2: Swelling pressures, p_s (kPa), of Na^+-bentonite and Na^+-bentonite-PAA composites prepared with a polymer-to-clay ratio of 1% by weight as well as by (i) dry powder mixing (DP) and (ii) solution intercalation (SI).

Na^+-bentonite	PAA^+ composite		PAA^- composite	
	DP	SI	DP	SI
430	365	450	450	325

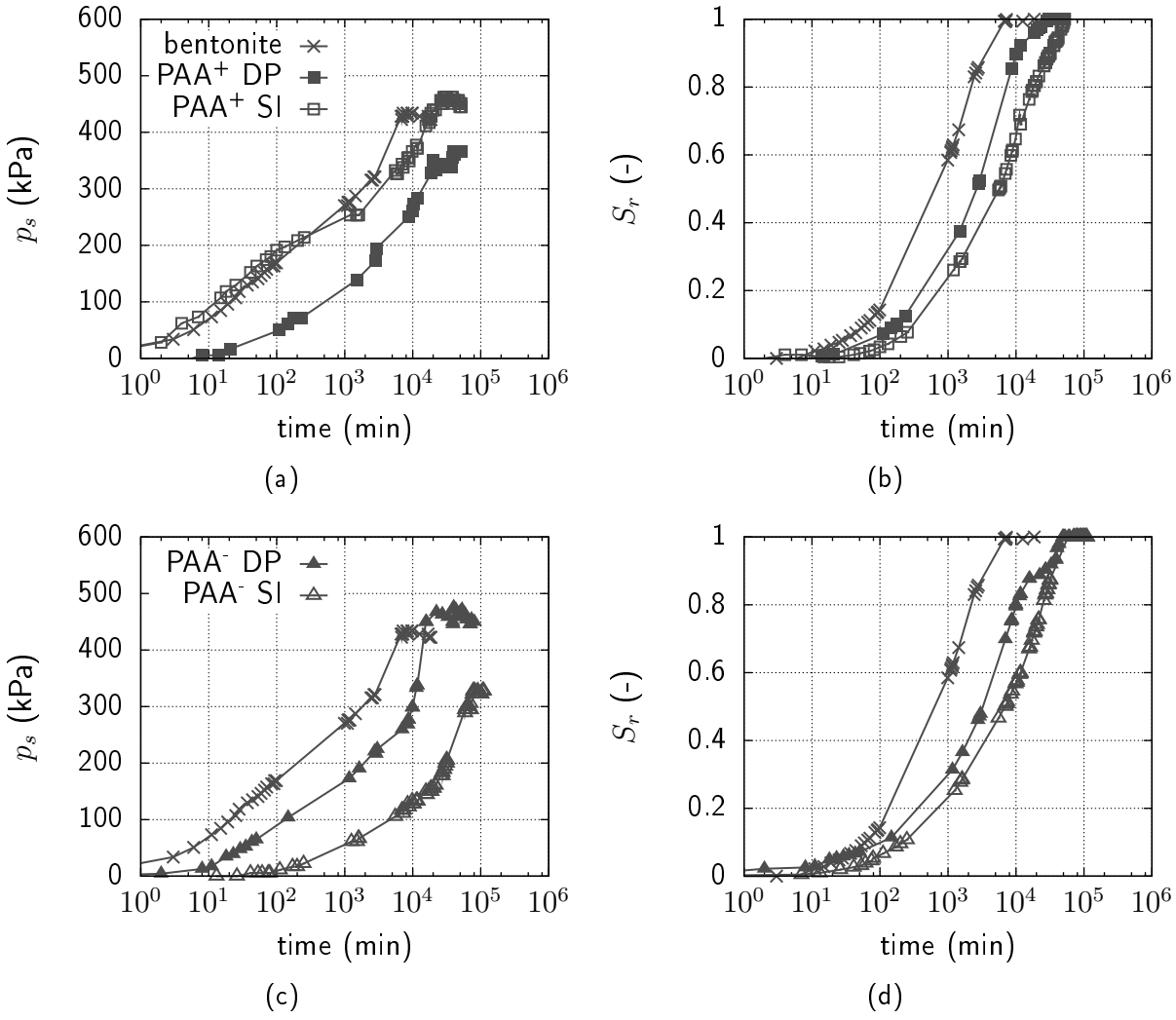

Figure 7.1: Swelling pressure and degree of saturation versus time plots of Na^+-bentonite and Na^+-bentonite-PAA composites prepared with a polymer-to-clay ratio of 1% by weight as well as by (i) dry powder mixing (DP) and (ii) solution intercalation (SI): PAA^+ composites (a) & (b); PAA^- composites (c) & (d).

within units and thus, swelling. However, the slight increase in p_s in case of SI preparation is in good agreement with the corresponding increase in w_l and thus, the dominance of clay fabric aggregation in composite micro- and macro-scale coupling behaviour. Taking into account the former boundary condition during swelling pressure testing, the slight increase in p_s as against the significant increase in w_l detected in case of the PAA^- composite prepared by DP is plausible. Thereby, the high affinity of anionic polymer chains to adsorb water as indicated by the w_l-value is macroscopically insignificant in terms of composite swelling pressure since polymer chains are leached during the saturation process. In case of SI preparation, on the other hand, additional effects obviously dominate PAA^- composite swelling behaviour accounting for the corresponding decrease in p_s. One possible explanation refers to an increase in clay fabric dispersion during SI preparation since repulsive forces between negatively charged solids, i.e., moderately charged clay mineral layers and highly charged polymer chains, are increased. Finally, due to polymer chain leaching during swelling pressure testing the alteration in clay fabric remains the only acting mechanism.

7.4 Hydraulic permeability

In Figure 7.2 & Table 7.3 the results of hydraulic permeability tests on pure Na^+-bentonite as well as its PAA^+ and PAA^- composites prepared by (i) DP and (ii) SI as well as permeated with (i) H_2O and (ii) 0.5 molar $CaCl_2$ solution are summarized. The hydraulic performance can be summarized as follows:

Pure Na^+-bentonite hydraulic permeability amounts $7.2 \cdot 10^{-13}$ m/s when permeated with deionized water. This value is in good agreement with the test results obtained from

Table 7.3: Hydraulic permeabilities, k (m/s), of Na^+-bentonite and Na^+-bentonite-PAA composites prepared with a polymer-to-clay ratio of 1% by weight as well as by (i) dry powder mixing (DP) and (ii) solution intercalation (SI).

	Na^+-bentonite	PAA^+ composite		PAA^- composite	
		DP	SI	DP	SI
k_{H_2O}	$7.2 \cdot 10^{-13}$	$1.3 \cdot 10^{-12}$	$4.5 \cdot 10^{-13}$	$5.8 \cdot 10^{-13}$	$2.6 \cdot 10^{-13}$
k_{CaCl_2}	$1.5 \cdot 10^{-12}$	$2.5 \cdot 10^{-12}$	$6.0 \cdot 10^{-13}$	$1.3 \cdot 10^{-12}$	$2.0 \cdot 10^{-13}$

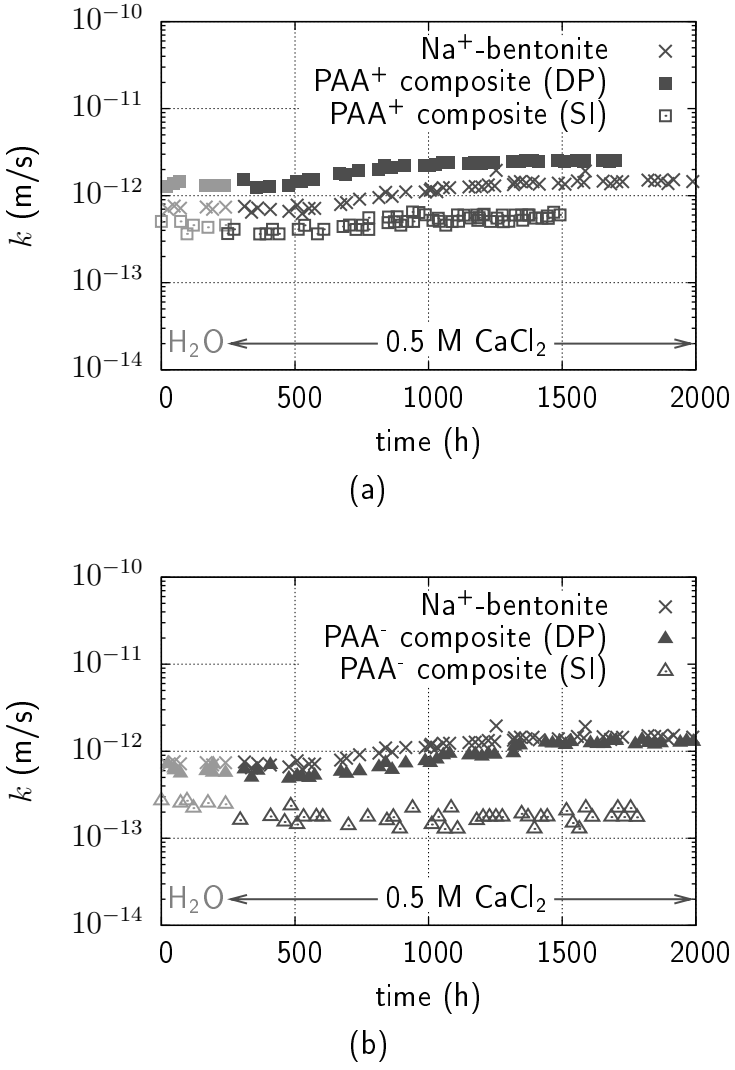

Figure 7.2: Hydraulic permeability versus time plots of Na^+-bentonite and Na^+-bentonite-PAA composites prepared with a polymer-to-clay ratio of 1% by weight as well as by (i) dry powder mixing (DP) and (ii) solution intercalation (SI): PAA^+ composites (a); PAA^- composites (b).

multiscale approach, i.e., the hydraulic permeabilities determined from oedometer time-compression curves (Figure 7.3). Thereby, the compacted bentonite is characterized by a slightly increased hydraulic permeability as compared to the $\log(k)$-e relationship established for bentonite slurries indicating that complete clay fabric dispersion and deflocculation cannot be reached from its initial state. This finding is in agreement with several studies on this topic referred to in section 2.3.

With respect to composites hydraulic permeability, considerable deviations from pure Na^+-bentonite can be observed in case of the PAA^+ composite prepared by DP, i.e., k_{H_2O} is increased by the factor 2, as well as the PAA^- composite prepared by SI, i.e., k_{H_2O} is decreased by the factor 3. This observation is in accordance to the respective effects of polymer addition concluded from swelling pressure test results, i.e., clay unit stabilization by a 'coat of paint' in case of the PAA^+ composite prepared by DP as well as an increase in clay fabric dispersion in case of the PAA^- composite prepared by SI. With respect to the former mechanism, interlayer expansion is prevented, which is manifested in a decreased value of p_s. Consequently clay fabric homogenization in terms of dispersion and deflocculation including the disappearance of preferential fluid flow paths through inter-aggregate pores is prevented, which is manifested in an increase in k_{H_2O}. The latter mechanism, i.e., an increase in clay fabric dispersion in case of the PAA^- composite prepared by SI, on the other hand, results in a decrease in both, p_s and k_{H_2O}, since non-adsorbed anionic polymer chains are leached during swelling pressure testing and thus, the alteration in clay fabric remains the only acting mechanism. The proposed mechanism can be confirmed when comparing the PAA^- composite hydraulic permeability with the results obtained on bentonite slurries, which are characterized by complete clay fabric dispersion and deflocculation, i.e., considerable agreement between the compacted composite hydraulic permeability and bentonite $\log(k)$-e_{clay} relationship obtained on slurries can be observed (Figure 7.3).

In case of the PAA^+ composite prepared by SI as well as the PAA^- composite prepared by DP, on the other hand, k_{H_2O}-values are very similar to the pure bentonite value, which is in agreement with previous findings from multiscale approach and swelling pressure tests, respectively. The effect of cationic polymer addition by SI, i.e., clay fabric aggregation, is insignificant with respect to k_{H_2O}, whereas it is obvious with respect to w_l and p_s. This is in accordance to the findings from multiscale approach on the influence of polymer-to-clay ratio on the liquid limit, the volumetric behaviour as well as the hydraulic permeability of composites prepared with a polymer-to-clay ratio of q_{max} as well as 10% of q_{max} (for

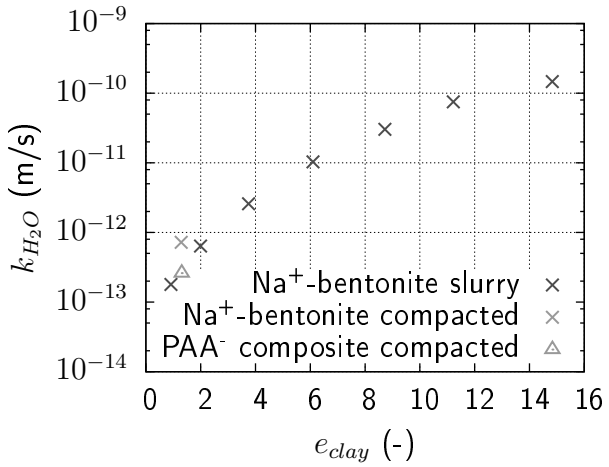

Figure 7.3: Hydraulic permeability versus void ratio plot of Na^+-bentonite (as well as Na^+-bentonite-PAA^- composite prepared with a polymer-to-clay ratio of 1% by weight as well as by SI) obtained by (i) oedometer time-compression test results of bentonite slurries and (ii) hydraulic permeability test results of compacted bentonite/composite (w_{opt}, ρ_{opt}) under isochoric and constant head conditions.

details see chapter 5). Anionic polymer addition by DP, on the other hand, is negligible with respect to both, p_s and k_{H_2O}, since polymer chains are leached during saturation process, whereas the difference in boundary conditions during liquid limit testing allow for a significant increase in w_l.

The hydraulic permeability obtained by permeating Na^+-bentonite with a 0.5 molar $CaCl_2$ solution, k_{CaCl_2}, is characterized by an increased value as compared to k_{H_2O}, approximately by the factor 2. The same finding applies for the PAA^+ composites as well as the PAA^- composite prepared by DP. However, in case of the PAA^- composite prepared by SI, the hydraulic permeability remains approximately constant. Thus, the hydraulic performance of this type of composite with respect to its application as hydraulic barrier material in geoenvironmental practice is significantly enhanced as compared to the pure Na^+-bentonite. Thereby, based on the foregoing conclusions on the effect of PAA^- addition by SI, the mechanism during $CaCl_2$ leaching is very similar to the well known effect of prehydration, i.e., the more dispersed and deflocculated the initial clay fabric, the lower the aggregating effect of divalent cation exchange. The enhancement of hydraulic barrier performance due to polymer addition amounts about one order of magnitude, whereas the enhancement reached by prehydration is characterized by the factor 5, which is illustrated in Figure 7.4.

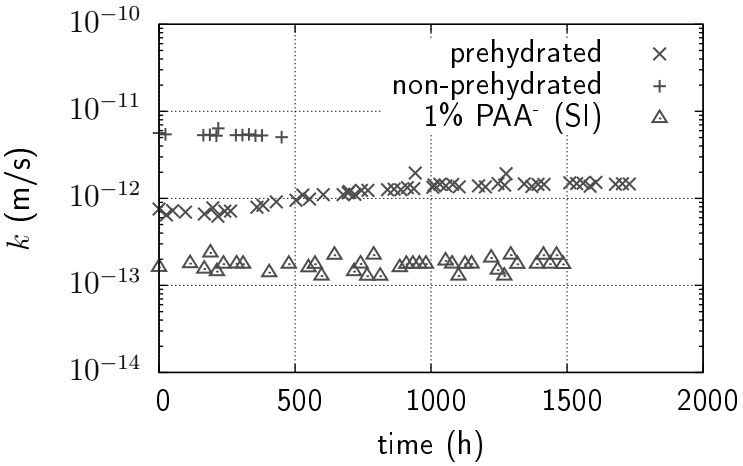

Figure 7.4: Enhancement of Na^+-bentonite hydraulic barrier performance due to (i) prehydration and (ii) polymer modification when permeated with a 0.5 molar $CaCl_2$ solution.

Taking into account previous studies on polymer enhancement of bentonite barriers, the preferred type of anionic polymers can be confirmed by the results obtained. However, the underlying mechanisms of barrier enhancement are related to alterations in the clay fabric rather than pore clogging by polymers as proposed by, e.g., Scalia et al. (2014). On this basis, the irregularity of classical relations between material hydraulic permeability and the liquid limit as well as the swelling behaviour, reported, e.g., by Scalia et al. (2014) and Ashmawy et al. (2002) and confirmed in the present study, is plausible. Further, the importance of composite preparation method has been demonstrated accounting for the limited hydraulic barrier performance using dry powder mixing.

7.5 Summary

Na^+-bentonite-polymer composites prepared with a polymer-to-clay ratio of 1% by weight and compacted to optimum proctor conditions have been experimentally investigated with respect to their application as barrier materials in geoenvironmental engineering. Thereby, the polymer charge (cationic and anionic) as well as the preparation method (dry powder mixing, DP, and solution intercalation, SI) have been varied in order to identify the governing mechanisms determining the macro-scale hydraulic permeability, k, by use of the permeants H_2O and 0.5 M $CaCl_2$ solution, respectively. The macro-scale results have

been interpreted by taking into account the outcome of the multiscale approach given in chapter 4 & 5. Further, (index) properties, i.e., the liquid limit, w_l, as well as the swelling behaviour indicated by the swelling pressure, p_s, have been investigated with respect to their significance in estimating hydraulic barrier performance. The results can be summarized as follows:

The addition of cationic polymer (PAA^+) using SI was found to result in a slight increase in w_l and p_s, whereas the hydraulic permeabilities, k_{H_2O} and k_{CaCl_2}, remain unaffected. This macro-scale behaviour is in accordance to the results of the multiscale approach and can be attributed to the tendency of clay fabric aggregation due to cationic polymer addition using SI. In case of DP, on the other hand, adsorption of polymer chains occurs within an existing clay fabric rather than a colloidal dispersion resulting in its stabilization. In consequence, p_s is decreased and k_{H_2O} as well as k_{CaCl_2} are increased. This can be attributed to the stabilization of the initially aggregated clay fabric, i.e., the restriction of interlayer expansion within aggregated clay units, and thus, the prevailing of preferential fluid flow paths through inter-aggregate pores. However, the value of w_l was found to be nearly unaffected by PAA^+ addition using DP.

Anionic polymer (PAA^-) addition was found to result in a significant enhancement of bentonite barrier performance in case of SI preparation, i.e., k_{H_2O} is decreased by the factor 3 as compared to pure Na^+-bentonite and remains constant in case of permeation using 0.5 M $CaCl_2$ solution. Thereby, an increase in clay fabric dispersion during SI preparation was concluded to be the governing mechanism accounting for the decrease in p_s, k_{H_2O} and k_{CaCl_2}. This conclusion assumes that anionic polymer chains are leached during saturation, which is based on the findings from multiscale approach, i.e., anionic polymer chains were found to be not adsorbed by the Na^+-bentonite type. Thus, extensive water adsorption of anionic polymer chains as concluded from water retention test results (multiscale approach) and indicated by the corresponding w_l-value (application-oriented approach) is insignificant with respect to p_s as well as k_{H_2O} and k_{CaCl_2}. The concluded mechanism of enhancement due to PAA^- addition using SI is illustrated in Figure 7.5 highlighting its similarity to the effect of pure bentonite prehydration. However, in accordance to the assumption of anionic polymer chain leaching, DP preparation in case of PAA^- was found to be insignificant with respect to p_s as well as k_{H_2O} and k_{CaCl_2} since the dispersing effect during composite preparation is not available. The resulting w_l-value, on the other hand, is significantly increased indicating the extensive water adsorption of anionic polymer chains.

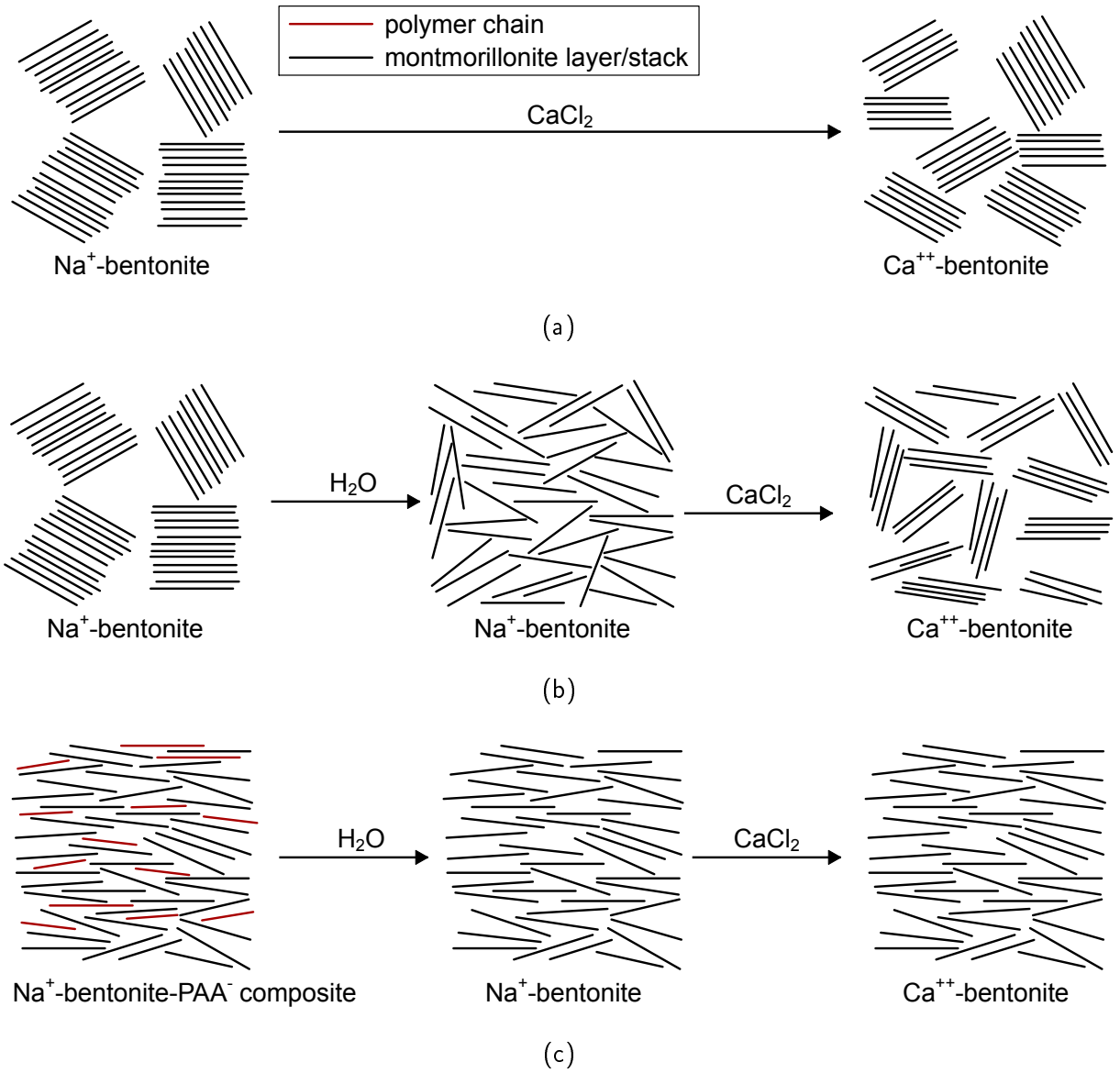

Figure 7.5: Illustration of Na^+-bentonite fabric when permeated with $CaCl_2$ solution: Non-prehydrated bentonite (a); enhancement due to prehydration (b); enhancement due to PAA^- addition using SI (c).

Finally, with respect to classical relations between bentonite hydraulic barrier performance and its index properties, great discrepancies have been observed in case of bentonite-polymer composites. Thereby, the following factors have been identified accounting for the discrepancies: (i) liquid limit testing conditions imply a fixed polymer-to-clay ratio, whereas hydraulic permeability testing conditions allow for a decreased value by non-adsorbed polymer chain leaching. The influence of polymer physico-chemical characteristics in terms of its water adsorbing capacity is therefore diminished in case of hydraulic permeability testing; (ii) polymer addition alters clay micro-scale properties with respect to the physico-chemical characteristics as well as the fabric, whereas classical relations between bentonite hydraulic barrier performance and its index properties are based on the physico-chemical characteristics, only. Alterations in clay fabric can therefore not be reproduced by the classical approach. Thus, index properties were found to be insignificant in terms of evaluating composite hydraulic barrier performance.

8 Summary and conclusions

8.1 General

In the present work, the topic of clay-polymer composites for application in geotechnical and geoenvironmental engineering was examined. Thereby, the concept of the research was developed based on the following situation discovered from the current literature on this topic: With respect to various geotechnical and geoenvironmental applications, such as landfill lining, tunnelling and expansive soil stabilization, clay-polymer composites were introduced in the literature. Their great potential to enhance pure clay hydro-mechanical properties was demonstrated. However, in many cases limitations in their gained properties were found. Thereby, the governing mechanisms with respect to both, success and failing in enhancing clay hydro-mechanical properties, have been examined rudimentary in scientific literature, for which reason the benefits of their high potential performance are strongly limited to single specific compositions and applications that have been developed to date. In addition to their presence in the geotechnical and geoenvironmental literature, clay-polymer composites have faced considerable attention in fields of colloid chemistry. Thereby, several mechanisms evoked by the respective constitutive characteristics of clay minerals and polymer chains as well as the environmental conditions during complex formation have been discovered. Thus, due to the significance of micro- and macro-scale coupling established in soil mechanics, especially when dealing with clays, the present work aims on the identification of multiscale coupling phenomena determining clay-polymer composite macro-scale hydro-mechanical behaviour in dependence on the constitutive characteristics of clay minerals and polymers and the related micro-scale properties of composites.

The study was conducted on the basis of two approaches, i.e., the multiscale approach and the application-oriented approach. Thereby, the former approach aimed on deriving fundamental information on the micro- and macro-scale coupling phenomena in clay-polymer

composites. Thus, clay and polymer constitutive characteristics in terms of the clay mineralogy, polymer charge and polymer-to-clay ratio were varied systematically and composites were analyzed experimentally in terms of their micro-scale characteristics, i.e., the adsorption behaviour by means of adsorption isotherms and the composite fabric using ESEM, as well as their macro-scale hydro-mechanical behaviour, i.e., the plastic properties by means of Atterberg limits, the volumetric behaviour and hydraulic permeability by means of oedometer (time-)compression and rebound test results and the water retention by means of unconfined drying and wetting test results. In addition to the experimental investigation and phenomenological identification of composite micro- and macro-scale coupling phenomena, theoretical multiscale approaches were adopted and advanced, i.e., (modified) DDL theory and cluster model. With respect to the application-oriented approach, one promising field of application, i.e., bentonite-polymer composites as hydraulic barrier materials for geoenvironmental applications, was explicitly addressed. Thereby, material modifications in accordance to the current literature as well as initial preparation and environmental boundary conditions relevant in this field of application were considered. The hydraulic barrier performance under these conditions was experimentally investigated by means of the hydraulic permeability as well as the (index) properties, liquid limit and swelling behaviour. Finally, interpretation was based on the outcome of the multiscale approach as well as established relationships of micro- and macro-scale coupling in clays. The main findings of the present work are summarized in the following.

8.2 Multiscale approach

The phenomenological multiscale behaviour of clay-polymer composites was found to depend significantly on the constitutive properties clay mineralogy and polymer charge. The general relationships derived are as follows:

Experimental multiscale analysis of clay-cationic polymer composites
Cationic polymer adsorption was found to promote clay fabric aggregation in case of montmorillonite being the predominant clay mineral due to the corresponding reduction in DDL extent at clay mineral surfaces, whereas in case of kaolinite being the predominant clay mineral, clay fabric flocculation was promoted due to long-distance interparticle and interaggregate bridging. Thereby, polymer shape in the adsorbed state is characterized by a flat stretched polymer chain in case of montmorillonite, whereas large loops and tails develop

in case of the kaolinite, which is caused by the corresponding differences in clay mineral layer charges. With respect to composite macro-scale behaviour, clay fabric aggregation in case of bentonite was found to result in an increase in liquid and shrinkage limits as well as compressibility and hydraulic permeability, which is in agreement with established relations on the multiscale coupling behaviour in pure clays governed by their fabric. Similarly, agreement between micro- and macro-scale findings was found in case of kaolin, i.e., liquid and shrinkage limits as well as the compressibility are increased, whereas the hydraulic permeability remains unaffected in consequence of clay fabric flocculation. With respect to composite water retention, water molecule replacement by the polymer chain in case of tightly adsorbed polymers on montmorillonite surfaces was reflected by decreased water contents in the high suction range. Large loop and tail segments in case of kaolinite, on the other hand, allowed for an increase in water adsorption in the medium suction range due to additional solid surfaces to be hydrated. However, with respect to the resulting degree of saturation versus suction relationships of clay-polymer composites, the various factors of clay fabric, solid surface hydration as well as some special features related to the presence of polymer chains within the clay matrix, i.e., its flexibility and bridging capacity, were found to affect composite (de)saturation behaviour with varying significance depending on clay mineralogy as well as the type of predominant exchangeable cations in case of bentonite.

Experimental multiscale analysis of clay-non-ionic polymer composites

Due to the adsorption of non-ionic polymers on clay mineral surfaces clay fabric dispersion and deflocculation is promoted, which is originated by an increase in DDL repulsion between polymer layered montmorillonite surfaces as well as steric stabilization between polymer layered kaolinite surfaces. Thereby, polymer shape in the adsorbed state is characterized by large loops and tails and tends to rearrange with increasing stress condition, i.e., the extent of loops and tails decreases and train segments increase. Macroscopically, the micro-scale alteration in clay fabric is reflected by an increase in liquid limit and compressibility as well as a decrease in hydraulic permeability caused by the reduction of maximum pore radii. In addition, shrinkage limits are decreased in case of DDL repulsion being the governing effect and increased in case of steric stabilization being the governing effect. Thus, clay fabric dispersion and deflocculation in consequence of steric stabilization is in parts in contrast to established relations on micro- and macro-scale coupling phenomena in clays. With respect to composite water retention, similar effects as observed for the cationic polymer were found, i.e., water molecule replacement by the polymer chain result-

ing in a decreased water content in the high suction range in case of bentonites as well as additional polymer chain surface hydration resulting in an increased water content in the medium suction range in case of kaolin. Finally, composite (de)saturation behaviour is governed by various factors depending on clay mineralogy as well as the type of predominant exchangeable cations in case of bentonite.

Experimental multiscale analysis of clay-anionic polymer composites
Anionic polymer adsorption was found to promote flocculated clay fabrics due to long-distance interparticle bridging. Thereby, multivalent cation bridging was concluded to be the governing mechanism in adsorption process since in case of predominant monovalent exchangeable cations no adsorption of polymers has been detected. In bentonites flocculation occurs between stacks of few montmorillonite layers, whereas in case of kaolin small F-F associated aggregates are flocculated. However, anionic polymer induced flocculation is highly sensitive to the stress level and becomes rearranged at vertical loadings of about 100 kPa in case of bentonite, whereas flocculation of aggregates in case of kaolin persists up to isotropic suction loadings of about 10 MPa. With respect to the macro-scale behaviour, liquid and shrinkage limits as well as the compressibility are increased, whereas the hydraulic permeability remains unaffected, which is in agreement with established relations on the multiscale coupling behaviour in pure clays. Finally, composite water retention behaviour is dominated by the interaction of non-adsorbed parts of the polymer chain with water resulting in slightly increased water contents over the whole suction range tested.

Polymer-to-clay ratio
With respect to the influence of the polymer-to-clay ratio, identical tendencies in terms of the composite macro-scale behaviour were detected for various ratios. Thereby, the effect of polymer adsorption is generally more pronounced for the higher polymer-to-clay ratio.

Theoretical multiscale analysis of clay-polymer composites
By theoretical analysis of clay-polymer composite multiscale behaviour good agreement was observed between theory and the actual micro- and macro-scale properties obtained by experiments. Based on a modified form of the Gouy-Chapman diffuse double-layer theory considering layers of non-ionic polymers on charged surfaces new equations were developed obtained by semi-analytical solution of the proposed nonlinear differential equation within the boundary conditions relevant in clay systems. As a result, the volumetric behaviour of bentonite-non-ionic polymer composites was found to be reproduceable quite accurately when taking into account the rearrangement of polymer shape during compression. Further,

cluster model was found to reproduce clay-cationic/non-ionic polymer composite hydraulic permeability when taking into account the micro-scale characteristics of composite fabric in terms of aggregation and dispersion.

8.3 Application oriented approach

The hydraulic barrier performance of Na^+-bentonite-polymer composites for application in geoenvironmental engineering was found to depend significantly on polymer charge as well as the composite preparation method. Thereby, the preference of anionic polymers suggested from literature in this field of application was confirmed by the results obtained. Based on the outcome of multiscale approach, i.e., no adsorption of anionic polymers on montorillonite surfaces having predominantly monovalent exchangeable cations was detected, the effect of barrier enhancement due to anionic polymer adsorption was concluded to be related to an increase in fabric dispersion during preparation, i.e., by solution intercalation. Thus, the underlying effect is quite similar to the effect of bentonite pre-treatment in terms of prehydration. Consequently, the effect of bentonite barrier enhancement is independent on the long-term polymer performance, which is an important finding regarding geoenvironmental practice. Finally, with respect to classical relations between bentonite hydraulic barrier performance and its (index) properties, liquid limit and swelling behaviour, it was found that index properties are insignificant in terms of evaluating composite hydraulic barrier performance.

8.4 Recommendations for further studies

Based on the outcome of the present study one important field of interest concerns the development of composite fabric with varying stress condition. Since the fabric has been investigated in its initial state only and macro-scale composite behaviour from a certain stress level on was found to be inconsistent with these findings to some extent, the respective mechanisms of fabric rearrangement proposed in this study should be investigated in detail, e.g, microscopically subsequent to the loading. These include the sensitivity in case of honeycomb-fabrics observed in bentonite-non-ionic polymer composites and flocculated fabrics in bentonite/kaolin-anionic polymer composites as well as the dominance of polymer

chain flexibility in case of very high polymer-to-clay ratios.

In addition, one important macro-scale composite property has been neglected in the present work, i.e., the shear strength. With respect to various geotechnical fields, e.g., embankment and dam construction, clay-polymer composites may offer beneficial performance due to, e.g., interparticle bridging as well as fabric flocculation.

Since from colloid chemical point of view, the polymer chain length was found to represent one of its constitutive properties determining clay-polymer composite micro-scale characteristics, i.e., clay-polymer complex morphology as well as the resulting fabric, the general influence of polymer molecular weight on composite multiscale behaviour should be investigated. Thereby, entropy effects leading to an increase in polymer adsorption with increasing chain length as well as limitations in clay mineral surface accessibility leading to a decrease in polymer adsorption with increasing chain length should be analyzed in terms of their influence on composite multiscale behaviour.

With respect to the application oriented approach, promising hydraulic barrier performance was found in case of anionic polymer addition using solution intercalation. However, the experimental research program on this type of composite should be extended in order to (i) identify the optimum polymer-to-bentonite ratio as well as (ii) to evaluate hydraulic barrier performance by means of further governing mechanisms, such as the development and self-healing of cracks during drying and wetting cycles as well as (de)protonation of clay mineral edges and mineral dissolution in consequence of the pH conditions.

Bibliography

Achari, G., Joshi, R. C., Bentley, L. R. & Chatterji, S. (1999), 'Prediction of the hydraulic conductivity of clays using the electric double layer theory', *Canadian Geotechnical Journal* **36**, 783–792.

Agus, S. S. (2005), An Experimental Study on Hydro-Mechanical Characteristics of Compacted Bentonite-Sand Mixtures, PhD thesis, Bauhaus-Universität Weimar.

Ahn, H.-S. & Jo, H. Y. (2009), 'Influence of exchangeable cations on hydraulic conductivity of compacted bentonite', *Applied Clay Science* **44**(1-2), 144–150.

Albrecht, B. A. & Benson, C. H. (2001), 'Effect of Desiccation on Compacted Natural Clays', *Journal of Geotechnical and Geoenvironmental Engineering* **127**(1), 67–75.

Ashmawy, A. K., El-Hajji, D., Sotelo, N. & Muhammad, N. (2002), 'Hydraulic Performance of Untreated and Polymer-treated Bentonite in Inorganic Landfill Leachates', *Clays and Clay Minerals* **50**(5), 546–552.

ASTM D4318-10e1 (2010), *Standard Test Methods for Liquid Limit, Plastic Limit, and Plasticity Index of Soils*, ASTM International, West Conshohocken, PA.

ASTM D4943-08 (2008), *Standard Test Method for Shrinkage Factors of Soils by the Wax Method*, ASTM International, West Conshohocken, PA.

ASTM D5084-03 (2003), *Standard Test Method for Measurement of Hydraulic Conductivity of Saturated Porous Materials Using a Flexible Wall Permeameter*, ASTM International, West Conshohocken, PA.

ASTM D5890-11 (2011), *Standard Test Method for Swell Index of Clay Mineral Component of Geosynthetic Clay Liners*, ASTM International, West Conshohocken, PA.

ASTM D854-14 (2014), *Standard Test Methods for Specific Gravity of Soil Solids by Water Pycnometer*, ASTM International, West Conshohocken, PA.

Baille, W. (2014), Hydro-mechanical behaviour of clays - significance of mineralogy, PhD thesis, Ruhr-Universität Bochum.

Baille, W., Tripathy, S. & Schanz, T. (2010), 'Swelling pressures and one-dimensional compressibility behaviour of bentonite at large pressures', *Applied Clay Science* **48**(3), 324–333.

Bergaya, F. & Lagaly, G., eds (2013), *Handbook of Clay Science*, 2. edn, Elsevier, Amsterdam.

Bharat, T. V., Sivapullaiah, P. V. & Allam, M. M. (2013), 'Novel procedure for the estimation of swelling pressures of compacted bentonites based on diffuse double layer theory', *Environmental Earth Sciences* **70**(1), 303–314.

Blackmore, A. V. & Warkentin, B. P. (1960), 'Swelling of Calcium Montmorillonite', *Nature* **186**(4727), 823–824.

Bohnhoff, G. L. & Shackelford, C. D. (2014), 'Hydraulic Conductivity of Polymerized Bentonite-Amended Backfills', *Journal of Geotechnical and Geoenvironmental Engineering* **140**(3).

Bolt, G. H. (1956), 'Physico-chemical analysis of the compressibility of pure clays', *Géotechnique* **6**(2), 86–93.

Breen, C. (1999), 'The characterisation and use of polycation-exchanged bentonites', *Applied Clay Science* (15), 187–219.

Brooks, D. E. (1973), 'The Effect of Neutral Polymers on the Electrokinetic Potential of Cells and Other Charged Particles Part II. A Model for the Effect of Adsorbed Polymer on the Diffuse Double Layer', *Journal of Colloid and Interface Science* **43**(3), 687–699.

Burton, G. J., Sheng, D. & Campbell, C. (2014), 'Bimodal pore size distribution of a high-plasticity compacted clay', *Géotechnique Letters* **4**, 88–93.

Carman, P. C. (1937), 'Fluid flow through granular beds', *Transactions of the Institution of Chemical Engineers* (15), 32–48.

Chapman, D. L. (1913), 'A contribution to the theory of electrocapillarity', *Philosophical Magazine* **25**, 475–481.

Cohen Stuart, M. A. (1991), 'Adsorbed Polymers in Colloidal Systems: from Statics to Dynamics', *Polymer Journal* **23**(5), 669–682.

Darcy, H. P. G. (1856), *Les Fontaines Publiques de la Ville de Dijon*, Victor Dalmont, Paris.

Delage, P., Howat, M. D. & Cui, Y. J. (1998), 'The relationship between suction and swelling properties in a heavily compacted unsaturated clay', *Engineering Geology* **50**, 31–48.

Delage, P. & Lefebvre, G. (1984), 'Study on the structure of a sensitive Champlain clay and of its evolution during consolidation', *Canadian Geotechnical Journal* **21**, 21–35.

Deng, Y., Dixon, J. B., White, G. N., Loeppert, R. H. & Juo, A. S. R. (2006), 'Bonding between polyacrylamide and smectite', *Colloids and Surfaces* **281**, 82–91.

Denoyel, R., Durand, G., Lafuma, F. & Audebert, R. (1990), 'Adsorption of Cationic Polyelectrolytes onto Montmorillonite and Silica: Microcalorimetric Study of Their Conformation', *Journal of Colloid and Interface Science* **139**(1), 281–290.

Di Emidio, G., Van Impe, W. & Flores, R. (2011), 'Advances in Geosynthetic Clay Liners: Polymer Enhanced Clays', *Geo-Frontiers 2011* pp. 1931–1940.

Di Maio, C., Santoli, L. & Schiavone, P. (2004), 'Volume change behaviour of clays: the influence of mineral composition, pore fluid composition and stress state', *Mechanics of Materials* **36**, 435–451.

Eggloffstein, T. (2000), *Der Einfluss des Ionenaustausches auf die Dichtwirkung von Bentonitmatten in Oberflächenabdichtungen von Deponien*, ICP Eigenverlag Bauen und Umwelt, Karlsruhe.

Espinasse, P. & Siffert, B. (1979), 'Acetamide and polyacrylamide adsorption onto clays: Influence of the exchangeable cation and the salinity of the medium', *Clays and Clay Minerals* **27**(4), 279–284.

Fleureau, J.-M., Verbrugge, J.-C., Huergo, P. J., Correia, A. G. & Kheirbek-Saoud, S.

(2001), 'Aspects of the behaviour of compacted clayey soils on drying and wetting paths', *Canadian Geotechnical Journal* **39**, 1341–1357.

Fredlund, D. G. & Rahardjo, H. (1993), *Soil mechanics for unsaturated soils*, John Wiley & Sons, Inc., New York.

Fredlund, D. G. & Xing, A. (1994), 'Equations for the soil-water characteristic curve', *Canadian Geotechnical Journal* **31**, 521–532.

Gens, A. & Alonso, E. E. (1992), 'A framework for the behaviour of unsaturated expansive clays', *Canadian Geotechnical Journal* **29**, 1013–1032.

Güngör, N. & Karaoglan, S. (2001), 'Interactions of polyacrylamide polymer with bentonite in aqueous systems', *Materials Letters* **48**, 168–175.

Gouy, G. (1910), 'Electric charge on the surface of an electrolyte', *Journal of Physics* **4**(9), 457.

Greenland, D. J. (1963), 'Adsorption of polyvinyl alcohols by montmorillonite', *Journal of Colloid Science* **18**(7), 647–667.

Haase, H. & Schanz, T. (2015), 'Hydro-mechanical properties of Calcigel-polyacrylamide composites', *Clay Minerals* **50**, 377–389.

Haase, H. & Schanz, T. (2016), 'Compressibility and saturated hydraulic permeability of clay-polymer composites - experimental and theoretical analysis', *Applied Clay Science* **130**, 62–75.

Head, K. H. (2006), *Manual of Soil Laboratory Testing*, Vol. 3, 3. edn, Whittles Publishing, Dunbeath.

Heller, H. & Keren, R. (2003), 'Anionic Polyactylamide Polymer Adsorption by Pyrophyllite and Montmorillonite', *Clays and Clay Minerals* **51**(3), 334–339.

Inyang, H. I. & Bae, S. (2005), 'Polyacrylamide sorption opportunity on interlayer and external pore surfaces of contaminant barrier clays', *Chemosphere* **58**, 19–31.

Inyang, H. I., Mbamalu, G. & Park, S.-W. (2007), 'Aqueos Polymer Effects on Volumetric Swelling of Na-Montmorillonite', *Journal of Materials in Civil Engineering* **19**(1), 84–90.

Jo, H. Y., Benson, C. H. & Edil, T. (2004), 'Hydraulic Conductivity and Cation Exchange in Non-Prehydrated and Prehydrated Bentonite Permeated with Weak Inorganic Salt Solutions', *Clays and Clay Minerals* **52**(6), 661–679.

Jo, H. Y., Benson, C. H., Shackelford, C. D., Lee, J.-M. & Edil, T. (2005), 'Long-Term Hydraulic Conductivity of a Geosynthetic Clay Liner Permeated with Inorganic Salt Solutions', *Journal of Geotechnical and Geoenvironmental Engineering* **131**(4), 405–417.

Kassiff, G. & Ben Shalom, A. (1971), 'Experimental Relationship Between Swell Pressure and Suction', *Géotechnique* **21**, 245–255.

Katsumi, T., Ishimori, H., Onikata, M. & Fukagawa, R. (2007), 'Long-term barrier performance of modified bentonite materials against sodium and calcium permeant solutions', *Geotextiles and Geomembranes* **26**, 14–30.

Kavanagh, B. V., Posner, A. M. & Qurik, J. P. (1975), 'Effect of Polymer Adsorption on the Properties of the Electrical Double Layer', *Faraday Discussions of the Chemical Society* **59**, 242–249.

Khan, M. I. (2012), Hydraulic Conductivity of Moderate and Highly Dense Expansive Clays, PhD thesis, Ruhr-Universität Bochum.

Kondo, M. (1996), 'Method of activation of clay and activated clay', US patent 5573583 A13.

Kozeny, J. (1927), Über kapillare Leitung des Wassers im Boden, *in* 'Sitzungsbericht Akademie der Wissenschaften', Wien, pp. 271–306.

Laird, D. A. (1997), 'Bonding between Polyacrylamide and Clay Mineral Surfaces', *Soil Science* **162**(11), 826–832.

Leong, E. C. & Rahardjo, H. (1997), 'Review of Soil-Water Characteristic Curve Equations', *Journal of Geotechnical and Geoenvironmental Engineering* **123**(12), 1106–1117.

Ma, C. & Eggleton, R. A. (1999), 'Cation exchange capacity of kaolinite', *Clays and Clay Minerals* **47**(2), 174–180.

Madsen, F. T. (1998), 'Clay mineralogical investigations related to nuclear waste disposal', *Clay Minerals* **33**, 109–129.

Madsen, F. T. & Müller-Vonmoos, M. (1985), 'Swelling Pressure Calculated from Mineralogical Properties of a Jrassic Opalinum Shale, Switzerland', *Clays and Clay Minerals* **33**(6), 501–509.

Madsen, F. T. & Müller-Vonmoos, M. (1989), 'The Swelling Behaviour of Clays', *Applied Clay Science* **4**, 143–156.

Marcial, D., Delage, P. & Cui, Y. J. (2002), 'On the high stress compression of bentonites', *Canadian Geotechnical Journal* **39**, 812–820.

Martin, R. T. (1960), 'Adsorbed Water on Clay: A Review', *Clays and Clay Minerals* **9**(1), 28–70.

Meier, L. & Kahr, G. (1999), 'Determination of the cation exchange capacity (CEC) of clay minerals using the complexes of copper(ii) ion with triethylenetetramine and tetraethylenepentamine', *Clays and Clay Minerals* **47**(3), 386–388.

Mesri, G. & Olson, R. E. (1971), 'Consolidation Characteristics of Montmorillonite', *Géotechnique* **21**(4), 341–352.

Mitchell, J. K. & Soga, K. (2005), *Fundamentals of Soil Behavior*, 3. edn, John Wiley & Sons, Hoboken.

Mpofu, P., Addai-Mensah, J. & Ralston, J. (2003), 'Investigation of the effect of polymer structure type on flocculation, rheology and dewatering behaviour of kaolinite dispersions', *International Journal of Mineral Processing* **71**(1-4), 247–268.

Nagaraj, T. S. & Miura, N. (2001), *Soft Clay Behaviour Analysis and Assessment*, Taylor & Francis.

Nagaraj, T. S. & Srinivasa Murthy, B. R. (1983), 'Rationalization of Skempton's compressibility equation', *Géotechnique* **33**, 433–443.

Norrish, K. (1954), 'Manner of Swelling of Montmorillonite', *Nature* **173**(4397), 256–257.

Norrish, K. & Quirk, J. P. (1954), 'Use of Electrolytes to control Swelling', *Nature* **173**(4397), 255–256.

Olsen, H. W. (1962), Hydraulic flow through saturated clays, *in* 'Proceedings of the 9th National Conference on Clays and Clay Minerals', pp. 131–160.

Onikata, M., Kondo, M., Hayashi, N. & Yamanaka, S. (1999), 'Complex formation of cation-exchanged montmorillonites with propylene carbonate: osmotic swelling in aqueous electrolyte solutions', *Clays and Clay Minerals* **47**(5), 672–677.

Ören, A. H., Durukan, S. & Kayalar, A. S. (2014), 'Influence of compaction water content on the hydraulic conductivity of sand-bentonite and zeolite-bentonite mixtures', *Clay Minerals* **49**, 109–121.

Parfitt, R. L. & Greenland, D. L. (1970), 'The Adsorption of Poly(Ethylene Glycols) on Clay Minerals', *Clay Minerals* **8**, 305–315.

Péron, H., Hueckel, T. & Laloui, L. (2007), 'An Improved Volume Measurement for Determining Soil Water Retention Curves', *Geotechnical Testing Journal* **30**(1), 1–8.

Pusch, R. (1982), 'Mineral-water interactions and their influence on the physical behavior of highly compacted Na bentonite', *Canadian Geotechnical Journal* **19**(3), 381–387.

Rad, N. S., Jacobson, B. D. & Bachus, R. C. (1994), Compatibility of geosynthetic clay liners with organic and inorganic permeants, *in* 'Proceedings Fifth International Conference on Geotextiles, Geomembranes and Related Products', pp. 1165–1168.

Rao, S. M. & Sridharan, A. (1985), 'Mechanisms Controlling the Volume Change Bhevaiour of Kaolinite', *Clays and Clay Minerals* **36**, 323–328.

Rao, S. N. & Mathew, P. K. (1995), 'Effects of Exchangeable Cations on Hydraulic Conductivity of a Marine Clay', *Clays and Clay Minerals* **43**(4), 433–437.

Razakamanantsoa, A. R., Barast, G. & Djeran-maigre, I. (2012), 'Hydraulic performance of activated calcium bentonite treated by polyionic charged polymer', *Applied Clay Science* **59-60**, 103–114.

Romero, E. (2013), 'A microstructural insight into compacted clayey soils and their hydraulic properties', *Engineering Geology* **165**, 3–19.

Romero, E., della Vecchia, G. & Jommi, C. (2011), 'An insight into the water retention properties of compacted clayey soils', *Géotechnique* **61**, 313–328.

Rouquerol, J., Avnir, D., Fairbridge, C. W., Everett, D. H., Haynes, J. H., Pernicone, N., Ramsay, J. D. F., Sing, K. S. W. & Unger, K. K. (1994), 'Recommendations for the Characterization of Porous Solids', *Pure and Applied Chemistry* **66**(8), 1739–1758.

Santamarina, J. C., Klein, K. A., Palomino, A. & Guimaraes, M. S. (2002), Micro-scale aspects of chemical-mechanical coupling: Interparticle forces and fabric, *in* C. D. Maio, T. Hueckel & B. Loret, eds, 'Chemo-Mechanical Coupling in Clays: From Nano-scale to Engineering Applications', Swets & Zeitlinger B. V., Lisse, Netherlands, pp. 47–64.

Scalia, J., Benson, C., Bohnhoff, G., Edil, T. & Shackelford, C. (2014), 'Long-Term Hydraulic Conductivity of a Bentonite-Polymer Composite Permeated with Aggressive Inorganic Solutions', *Journal of Geotechnical and Geoenvironmental Engineering* **140**(3).

Schamp, N. & Huylebroeck, J. (1973), 'Adsorption of polymers on clays', *Journal of Polymer Science* **42**, 553–562.

Schanz, T., Khan, M. I. & Al-Badran, Y. (2013), 'An alternative approach for the use of DDL theory to estimate the swelling pressure of bentonites', *Applied Clay Science* **83-84**, 383–390.

Schanz, T. & Tripathy, S. (2009), 'Swelling pressure of a divalent-rich bentonite: Diffuse double-layer theory revisited', *Water Resources Research* **45**(W00C12). doi:10.1029/2007WR006495.

Scheutjens, J. M. H. M. & Fleer, G. J. (1990), 'Statistical Theory of the Adsorption of Interacting Chain Molecules. 2. Train, Loop and Tail Size Distribution', *Journal of Physical Chemistry* **84**, 178–190.

Schofield, R. K. (1946), 'Ionic Forces in Thick Films of Liquid between Charged Surfaces', *Transactions of the Faraday Society* **42**, B219–B225.

Shackelford, C. D., Benson, C. H., Katsumi, T., Edil, T. B. & Lin, L. (2000), 'Evaluating the hydraulic conductivity of GCLs permeated with non-standard liquids', *Geotextiles and Geomembranes* **18**, 133–161.

Sridharan, A. (2002), Engineering behaviour of clays: Influence of mineralogy, *in* C. D. Maio, T. Hueckel & B. Loret, eds, 'Chemo-Mechanical Coupling in Clays: From

Nano-scale to Engineering Applications', Swets & Zeitlinger B. V., Lisse, Netherlands, pp. 3–28.

Sridharan, A. & Jayadeva, M. S. (1982), 'Double layer theory and compressibility of clays', *Géotechnique* **32**(2), 133–144.

Sridharan, A. & Prakash, K. (1998), 'Mechanisms Controlling the Shrinkage Limit of Soils', *Geotechnical Testing Journal* **21**(3), 240–250.

Sridharan, A. & Rao, G. V. (1973), 'Mechanisms controlling volume change of saturated clays and the role of the effective stress concept', *Géotechnique* **23**, 359–382.

Sridharan, A., Rao, S. M. & Murthy, N. S. (1986), 'Liquid Limit of Montmorillonite Soils', *Geotechnical Testing Journal* **9**(3), 156–159.

Sridharan, A., Rao, S. M. & Murthy, N. S. (1988), 'Liquid limit of kaolinitic soils', *Géotechnique* **38**(2), 191–198.

Sridharan, A. & Satyamurty, P. V. (1996), 'Potential-Distance Relationships of Clay-Water Systems Considering the Stern Theory', *Clays and Clay Minerals* **44**(4), 479–484.

Stern, O. (1924), 'Zur Theorie der elektrolytischen Doppelschicht', *Zeitschrift für Elektrochemie und angewandte physikalische Chemie* **30**(21-22), 508–516.

Stutzmann, T. & Siffert, B. (1977), 'Contribution to the Adsorption Mechanism of Acetamide and Polyacrylamide on to Clays', *Clays and Clay Minerals* **25**, 392–406.

Theng, B. K. G. (1982), 'Clay-Polymer Interactions: Summary and Perspectives', *Clays and Clay Minerals* **30**(1), 1–10.

Theng, B. K. G. (2012), *Formation and Properties of Clay-Polymer Complexes*, 2. edn, Elsevier, Amsterdam.

Thom, R., Sivakumar, R., Sivakumar, V., Murray, E. J. & Mackinnon, P. (2007), 'Pore size distribution of unsaturated compacted kaolin: the initial states and final states following saturation', *Géotechnique* **57**, 469–474.

Tripathy, S., Bag, R. & Thomas, H. R. (2010), Desorption and consolidation behaviour of initially saturated clays, *in* E. A. . A. Gens, ed., 'Proceedings of the 5th International Conference on Unsaturated Soils', Taylor & Francis Group, Barcelona, Spain, pp. 381–

386.

Tripathy, S., Bag, R. & Thomas, H. R. (2013), 'Effect of Stern-layer on the compressibility behaviour of bentonites', *Acta Geotechnica* **9**(6), 1097–1109.

Tripathy, S., Kessler, W. & Schanz, T. (2006), Determination of interparticle repulsive pressures in clays, *in* G. A. Miller, C. E. Zapata, S. L. Houston & D. G. Fredlund, eds, 'Proceedings of the Fourth International Conference on Unsaturated Soils', pp. 2198–2209.

Tripathy, S., Sridharan, A. & Schanz, T. (2004), 'Swelling pressures of compacted bentonites from diffuse double layer theory', *Canadian Geotechnical Journal* **41**(3), 437–450.

Tripathy, S., Tadza, M. Y. M. & Thomas, H. R. (2014), 'Soil-water characteristic curves of clays', *Canadian Geotechnical Journal* **51**, 869–883.

Ueda, T. & Harada, S. (1968), 'Adsorption of Cationic Polysulfone on Bentonite', *Journal of Applied Polymer Science* **12**, 2395–2401.

van Olphen, H. (1963), *An Introduction to Clay Colloid Chemistry*, Interscience Publishers.

Xiang, W. & Czurda, K. (1995), 'Einfluss des Kationenaustausches auf die Hydratation und Dehydratation von Tonmineralen', *Geologisch Paläontologische Mitteilungen* **20**, 107–119.

Ye, W. M., Zhang, F., Chen, B., Chen, Y. G., Wang, Q. & Cui, Y. J. (2014), 'Effects of salt solutions on the hydro-mechanical behavior of compacted GMZ01 Bentonite', *Environmental Earth Science* **72**(7), 2621–2630.

Yu, J., Wang, D., Ge, X., Yan, M. & Yang, M. (2006), 'Flocculation of kaolin particles by two typical polyelectrolytes: A comparative study on the kinetics and floc structures', *Colloids and Surfaces A: Physicochemial and Engineering Aspects* **290**, 288–294.

Zhu, C.-M., Ye, W.-M., Chen, Y.-G., Chen, B. & Cui, Y.-J. (2013), 'Influence of salt solutions on the swelling pressure and hydraulic conductivity of compacted GMZ01 bentonite', *Engineering Geology* **166**, 74–80.

Zumsteg, R., Plötze, M. & Puzrin, A. (2013*a*), 'Effect of dispersing foams and polymers

on the mechanical behaviour of clay pastes', *Géotechnique* **63**(11), 920–933.

Zumsteg, R., Plötze, M. & Puzrin, A. (2013*b*), 'Reduction of the clogging potential of clays: new chemical applications and novel quantification approaches', *Géotechnique* **63**(4), 276–286.

Schriftenreihe des Lehrstuhls für Grundbau, Boden- und Felsmechanik der Ruhr-Universität Bochum

Herausgeber: H.L. Jessberger

1 (1979) **Hans Ludwig Jessberger**
Grundbau und Bodenmechanik an der Ruhr-Universität Bochum

2 (1978) **Joachim Klein**
Nichtlineares Kriechen von künstlich gefrorenem Emschermergel

3 (1979) **Heinz-Joachim Gödecke**
Die Dynamische Intensivverdichtung wenig wasserdurchlässiger Böden

4 (1979) **Poul V. Lade**
Three Dimensional Stress-Strain Behaviour and Modeling of Soils

5 (1979) **Roland Pusch**
Creep of soils

6 (1979) **Norbert Diekmann**
Zeitabhängiges, nichtlineares Spannungs-Verformungsverhalten von gefrorenem Schluff unter triaxialer Belastung

7 (1979) **Rudolf Dörr**
Zeitabhängiges Setzungsverhalten von Gründungen in Schnee, Firn und Eis der Antarktis am Beispiel der deutschen Georg-von-Neumayer- und Filchner-Station

8 (1984) **Ulrich Güttler**
Beurteilung des Steifigkeits- und Nachverdichtungsverhaltens von ungebundenen Mineralstoffen

9 (1986) **Peter Jordan**
Einfluss der Belastungsfrequenz und der partiellen Entwässerungs-möglichkeiten auf die Verflüssigung von Feinsand

10 (1986) **Eugen Makowski**
Modellierung der künstlichen Bodenvereisung im grundwasserdurchströmten Untergrund mit der Methode der finiten Elemente

11 (1986) **Reinhard A. Beine**
Verdichtungswirkung der Fallmasse auf Lastausbreitung in nichtbindigem Boden bei der Dynamischen Intensivverdichtung

12 (1986) **Wolfgang Ebel**
Einfluss des Spannungspfades auf das Spannungs-Verformungsverhalten von gefrorenem Schluff im Hinblick auf die Berechnung von Gefrierschächten

13 (1987) **Uwe Stoffers**
Berechnungen und Zentrifugen-Modellversuche zur Verformungsabhängigkeit der Ausbaubeanspruchung von Tunnelausbauten in Lockergestein

14 (1988) **Gerhard Thiel**
Steifigkeit und Dämpfung von wassergesättigtem Feinsand unter Erdbebenbelastung

15 (1991) **Mahmud Thaher**
Tragverhalten von Pfahl-Platten-Gründungen im bindigen Baugrund, Berechnungsmodelle und Zentrifugen-Modellversuche

16 (1992) **Rainer Scherbeck**
Geotechnisches Verhalten mineralischer Deponieabdichtungsschichten bei ungleichförmiger Verformungswirkung

17 (1992) **Martin M. Bizialiele**
Torsional Cyclic Loading Response of a Single Pile in Sand

18 (1993) **Michael Kotthaus**
Zum Tragverhalten von horizontal belasteten Pfahlreihen aus langen Pfählen in Sand

19 (1993) **Ulrich Mann**
Stofftransport durch mineralische Deponieabdichtungen: Versuchsmethodik und Berechnungsverfahren

20 (1992) **Festschrift anlässlich des 60. Geburtstages von Prof. Dr.-Ing. H. L. Jessberger**
20 Jahre Grundbau und Bodenmechanik an der Ruhr-Universität Bochum

21 (1993) **Stephan Demmert**
Analyse des Emissionsverhaltens einer Kombinationsabdichtung im Rahmen der Risikobetrachtung von Abfalldeponien

22 (1994) **Diethard König**
Beanspruchung von Tunnel- und Schachtausbauten in kohäsionslosem Lockergestein unter Berücksichtigung der Verformung im Boden

23 (1995) **Thomas Neteler**
Bewertungsmodell für die nutzungsbezogene Auswahl von Verfahren zur Altlastensanierung

24 (1995) **Ralph Kockel**
Scherfestigkeit von Mischabfall im Hinblick auf die Standsicherheit von Deponien

25 (1996) **Jan Laue**
Zur Setzung von Flachfundamenten auf Sand unter wiederholten Lastereignissen

26 (1996) **Gunnar Heibrock**
Zur Rissbildung durch Austrocknung in mineralischen Abdichtungsschichten an der Basis von Deponien

27 (1996) **Thomas Siemer**
Zentrifugen-Modellversuche zur dynamischen Wechselwirkung zwischen Bauwerken und Baugrund infolge stoßartiger Belastung

28 (1996) **Viswanadham V. S. Bhamidipati**
Geosynthetic Reinforced Mineral Sealing Layers of Landfills

29 (1997) **Frank Trappmann**
Abschätzung von technischem Risiko und Energiebedarf bei Sanierungsmaßnahmen für Altlasten

30 (1997) **André Schürmann**
Zum Erddruck auf unverankerte flexible Verbauwände

31 (1997) **Jessberger, H. L. (Herausgeber)**
Environment Geotechnics, Report of ISSMGE Technical Committee TC 5 on Environmental Geotechnics

Herausgeber: Th. Triantafyllidis

32 (2000) **Triantafyllidis, Th. (Herausgeber)**
Boden unter fast zyklischer Belastung: Erfahrung und Forschungsergebnisse (Workshop)

33 (2002) **Christof Gehle**
Bruch- und Scherverhalten von Gesteinstrennflächen mit dazwischenliegenden Materialbrücken

34 (2003) **Andrzej Niemunis**
Extended hypoplastic models for soils

35 (2004) **Christiane Hof**
Über das Verpressankertragverhalten unter kalklösendem Kohlensäureangriff

36 (2004) **René Schäfer**
Einfluss der Herstellungsmethode auf das Verformungsverhalten von Schlitzwänden in weichen bindigen Böden

37 (2005) **Henning Wolf**
Zur Scherfugenbänderung granularer Materialien unter Extensionsbeanspruchung

38 (2005) **Torsten Wichtmann**
Explicit accumulation model for non-cohesive soils under cyclic loading

39 (2008) **Christoph M. Loreck**
Die Entwicklung des Frischbetondruckes bei der Herstellung von Schlitzwänden

40 (2008) **Igor Arsic**
Über die Bettung von Rohrleitungen in Flüssigböden

41 (2009) **Anna Arwanitaki**
Über das Kontaktverhalten zwischen einer Zweiphasenschlitzwand und nichtbindigen Böden

Herausgeber: T. Schanz

42 (2009) **Yvonne Lins**
Hydro-Mechanical Properties of Partially Saturated Sand

43 (2010) **Tom Schanz (Herausgeber)**
Geotechnische Herausforderungen beim Umbau des Emscher-Systems
Beiträge zum RuhrGeo Tag 2010

44 (2010) **Jamal Alabdullah**
Testing Unsaturated Soil for Plane Strain Conditions: A New Double-Wall Biaxial Device

45 (2011) **Lars Röchter**
Systeme paralleler Scherbänder unter Extension im ebenen Verformungszustand

46 (2011) **Yasir Al-Badran**
Volumetric Yielding Behavior of Unsaturated Fine-Grained Soils

47 (2011) **Usque ad finem**
Selected research papers

48 (2012) **Muhammad Ibrar Khan**
Hydraulic Conductivity of Moderate and Highly Dense Expansive Clays

49 (2014) **Long Nguyen-Tuan**
Coupled Thermo-Hydro-Mechanical Analysis: Experimental and Back Analysis

50 (2014) **Tom Schanz (Herausgeber)**
Ende des Steinkohlenbergbaus im Ruhrrevier: Realität und Perspektiven für die Geotechnik
Beiträge zum RuhrGeo Tag 2014

51 (2014) **Usque ad finem**
Selected research papers

52 (2014) **Houman Soleimani Fard**
Study on the Hydro-Mechanical Behavior of Fiber Reinforced Fine Grained Soils,
with Application to the Preservation of Historical Monuments

53 (2014) **Wiebke Baille**
Hydro-Mechanical Behaviour of Clays - Significance of Mineralogy

54 (2014) **Qasim Abdulkarem Jassim Al-Obaidi**
Hydro-Mechanical Behavior of Collapsible Soils

55 (2015) **Veselin Zarev**
Model Identification for the Adaption of Numerical Simulation Models -
Application to Mechanized Shield Tunneling

56 (2015) **Meisam Goudarzy**
Micro and Macro Mechanical Assessment of Small and Intermediate Strain
Properties of Granular Material

57 (2016) **Oliver Detert**
Analyse einer selbstregulierenden interaktiven Membrangründung für Schüttkörper
auf geringtragfähigen Böden

58 (2016) **Yang Yang**
Analyses of Heat Transfer and Temperature-induced Behaviour in Geotechnics

59 (2016) **Alborz Pourzargar**
Comparison of Measured and Predicted Suction Stress in Partially Saturated Compacted Soils

60 (2017) **Hanna Haase**
Multiscale Analysis of Clay-Polymer Composites for Geoenvironmental Applications